The role of the *Canonical transient receptor potential 6* (TRPC6) channel and the *C-terminal LIM domain protein of 36 kDa* (CLP36) for platelet function

***

Die Rolle des *Canonical transient receptor potential 6* (TRPC6) Kanals und des *36 kDa C-terminalen LIM Domänenproteins* (CLP36) in der Thrombozytenfunktion

Doctoral thesis for a doctoral degree

at the Graduate School of Life Sciences,

Julius-Maximilians-Universität Würzburg,

Section Biomedicine

submitted by

Shuchi Gupta

from

New Delhi, India

Würzburg, 2012

Submitted on:

Members of the *Promotionskomitee*:

Chairperson:	**Prof. Dr. Manfred Gessler**
Primary Supervisor:	**Prof. Dr. Bernhard Nieswandt**
Supervisor (Second):	**Prof. Dr. Georg Krohne**
Supervisor (Third):	**Prof. Dr. Johan W. M. Heemskerk**

Date of Public Defense:

Date of Receipt of Certificate:

एक विचार बना लो. उस एक विचार को अपना जीवन बना लो. उसके बारे में सोचो, उसका सपना दखो, और उस विचार पर जीवित रहो. मस्तिष्क, मांसपेशियों, नसों, और शरीर के हर भाग को उस विचार से परिपूण कर लो, और हर दूसरे विचार को छोड़ दो. वही सफलता का रास्ता है.

स्वामी विवेकानंद

Take up one idea. Make that one idea your life - think of it, dream of it, and live on that idea. Let the brain, muscles, nerves, every part of your body, be full of that idea, and just leave every other idea alone. This is the way to success.

Swami Vivekananda

Table of contents

SUMMARY

Platelet activation and aggregation are essential to limit posttraumatic blood loss at sites of vascular injury, but also contribute to arterial thrombosis, leading to myocardial infarction and stroke. Thrombus formation is the result of well-defined molecular events, including agonist-induced elevation of intracellular calcium ($[Ca^{2+}]_i$) and series of cytoskeletal rearrangements. With the help of genetically modified mice, the work presented in this thesis identified novel mechanisms underlying the process of platelet activation in hemostasis and thrombosis.

Store-operated calcium entry (SOCE) through Orai1 was previously shown to be the main Ca^{2+} influx pathway in murine platelets. The residual Ca^{2+} entry in the Orai1-deficient platelets suggested a role for additional *non-store-operated* Ca^{2+} (non-SOC) and *receptor operated* Ca^{2+} *entry* (ROCE) in maintaining platelet calcium homeostasis. *Canonical transient receptor potential channel 6* (TRPC6), which is expressed in both human and murine platelets, has been attributed to be involved in SOCE as well as in *diacylglycerol* (DAG)-triggered ROCE. In the first part of the study, the function of TRPC6 in platelet Ca^{2+} signaling and activation was analyzed by using the TRPC6 knockout mice. *In vitro* agonist-induced Ca^{2+} responses and *in vivo* platelet function were unaltered in *Trpc6*$^{-/-}$ mice. However, *Trpc6*$^{-/-}$ mice displayed a completely abolished DAG-mediated Ca^{2+}-influx but a normal SOCE. These findings identified TRPC6 as the major DAG-operated ROC channel in murine platelets, but DAG-mediated ROCE has no major functional relevance for hemostasis and thrombosis.

In the second part of the thesis, the involvement of the PDLIM family member CLP36 in the signaling pathway of the major platelet collagen receptor *glycoprotein* (GP) VI was investigated. The GPVI/FcRγ-chain complex initiates platelet activation through a series of tyrosine phosphorylation events downstream of the FcRγ-chain-associated *immunoreceptor tyrosine-based activation motif* (ITAM). GPVI signaling has to be tightly regulated to prevent uncontrolled intravascular platelet activation, but the underlying mechanisms are not fully understood. The present study reports the adaptor protein CLP36 as a major inhibitor of GPVI-ITAM signaling in platelets. Platelets from mice expressing a truncated form of CLP36, (*Clp36*$^{\Delta LIM}$) and platelets from mice lacking the entire protein (*Clp36*$^{-/-}$) displayed profound hyper-activation in response to GPVI-specific agonists, whereas GPCR signaling pathways remained unaffected. These alterations translated into accelerated thrombus formation and enhanced pro-coagulant activity of *Clp36*$^{\Delta LIM}$ platelets and a pro-thrombotic phenotype *in vivo*. These studies revealed an unexpected inhibitory function of CLP36 in GPVI-ITAM signaling and established it as a key regulator of arterial thrombosis.

Zusammenfassung

Die Aktivierung und die Aggregation von Thrombozyten (Blutplättchen) sind essentielle Prozesse, um Blutverluste nach Verletzungen zu begrenzen, sie spielen jedoch auch eine Rolle bei der arteriellen Thrombose, die zu Herzinfarkt und Schlaganfall führen kann. Die Thrombusbildung ist das Ergebnis wohldefinierter molekularer Vorgänge, die die Agonisten-induzierte Konzentrationserhöhung von intrazellulärem Kalzium ($[Ca^{2+}]_i$) und eine Reihe von Umlagerungen des Zytoskeletts mit einschließen. Die Ergebnisse dieser Arbeit, die mit Hilfe genetisch veränderter Mauslinien erzielt wurden, decken neue Mechanismen der Thrombozytenaktivierung in Thrombose und Hämostase auf.

Es wurde bereits gezeigt, dass der durch Orai1 vermittelte *Store-operated calcium entry* (SOCE) den Haupteintrittsweg für Ca^{2+} in Mausthrombozyten darstellt. Der verbleibende Ca^{2+} Einstrom führte zur Annahme, dass zusätzlich *non-store-operated* Ca^{2+} (non-SOC) und *receptor operated* Ca^{2+} *entry* (ROCE) eine Rolle in der Aufrechterhaltung der Ca^{2+} Homöostase spielen. Dem *Canonical transient receptor potential channel* 6 (TRPC6), der in Thrombozyten des Menschen als auch der Maus exprimiert wird, wurde eine Rolle in dem SOCE und *diacylglycerol* (DAG)-vermitteltem ROCE zugeschrieben. Im ersten Teil dieser Arbeit wurde die Funktion von TRPC6 im Ca^{2+} *Signaling* und der Aktivierung von Thrombozyten mit Hilfe der TRPC6 defizienten Mauslinie untersucht. Die Funktion der *Trpc6*$^{-/-}$ Thrombozyten waren *in vitro* (z.B. Agonisten-induzierte Ca^{2+}-Antworten) als auch *in vivo* unverändert. Jedoch zeigten Thrombozyten von *Trpc6*$^{-/-}$ Mäusen einen komplett fehlenden DAG-vermittelten Kalziumeinstrom, aber normalen SOCE. Diese Ergebnisse identifizierten TRPC6 als den Haupt-DAG-aktivierten ROC Kanal in Mausthrombozyten. Jedoch hatte diese DAG-vermittelte ROCE keine größere funktionelle Relevanz für Thrombose und Hämostase.

Im zweiten Teil dieser Arbeit wurde die Rolle von CLP36, einem Mitglied der PDLIM Proteinfamilie, im Signalweg des Haupt-Kollagenrezeptors, Glykoprotein (GP) VI, auf Thrombozyten untersucht. Der GPVI/FcRγ–Kette Komplex initiiert die Thrombozytenaktivierung durch eine Reihe von Tyrosinphosphorylierungen, die dem FcRγ-Kette-assoziiertem *immunoreceptor tyrosine based activation motif* (ITAM) nachgeschaltet sind. GPVI-vermittelte Signale müssen sorgfältig reguliert sein, um eine unkontrollierte intravaskuläre Thrombozytenaktivierung zu verhindern. Jedoch sind die zugrunde liegenden Mechanismen nicht komplett verstanden. Die vorliegende Arbeit zeigt, dass das Adapterprotein CLP36 als ein wichtiger Inhibitor des GPVI-ITAM Signalwegs wirkt. Thrombozyten von Mäusen, welche eine trunkierte Form von CLP36 exprimieren, der die LIM-Domäne fehlt (*Clp36*$^{\Delta LIM}$*),* als auch von Mäusen, denen das komplette Protein fehlt (*Clp36*$^{-/-}$), zeigten eine deutlich verstärkte Aktivierung als Antwort auf GPVI-spezifische Agonisten. Andere Signalwege aber waren nicht beeinflusst.

Diese Veränderungen resultierten in einer schnelleren Thrombusbildung und erhöhten prokoagulatorischen Aktivität von *Clp36*$^{\Delta LIM}$ Thrombozyten, welche sich letztendlich als prothrombotischer Phänotyp *in vivo* bemerkbar machten. Diese Ergebnisse deckten eine unerwartete inhibitorische Funktion von CLP36 im GPVI-ITAM Signalweg auf und etablierten CLP36 als einen wichtigen Regulator der arteriellen Thrombose.

1 INTRODUCTION

1.1 Platelets

Anucleated and discoid-shaped platelets represent the smallest cells of the blood system with a diameter of 2-4 μm in humans and 1-2 μm in mice. Platelets are released into the circulation by fragmentation of their precursor cells, the megakaryocytes. According to a current hypothesis, the mature megakaryocytes in the bone marrow expand pseudopodial protrusions, called proplatelets. The tips of these proplatelets become continuously shed and fragmented into platelets by the shear forces in the blood circulation.[1,2] Platelets circulate in a resting state at a concentration of 150,000-300,000/mL in humans for 8-10 days and approximately 1,000,000/mL in mice for approximately 5 days, before they are cleared by the reticulo-endothelial system in the spleen and liver. Platelets have the ability to rapidly respond upon disruption of the vessel wall. Under these conditions, exposed components of the *extracellular matrix* (ECM) trigger initial platelet adhesion and activation. This event is further reinforced by soluble mediators released from activated platelets together with locally produced thrombin which results in recruitment of further platelets from the circulation, thus resulting in aggregation and finally leading to thrombus formation. The process of platelet activation and final aggregate formation is important for normal hemostasis after vascular injury and thus prevents posttraumatic blood loss. However, under pathological conditions, such as after the rupture of an atherosclerotic plaque in stenosed vessels, platelet aggregation may also lead to uncontrolled thrombus formation causing vessel occlusion. This arterial occlusion results in tissue ischemia[3] if occurring in the brain or myocardial infarction if occuring in coronary arteries. These two diseases are among the most common causes of mortality in the developed nations.[4] Therefore, a selective inhibition of platelet activation has emerged as a major antithrombotic treatment to prevent or treat ischemia and cardiovascular diseases.

This two-faced function of platelets indicates that their activation requires a well-defined and tightly regulated signaling machinery to allow efficient sealing of a wound. At the same time uncontrolled platelet adhesion and excessive platelet activation has to be limited to prevent undesired vessel occlusion. To achieve this equilibrium under physiological conditions, platelets express different activation/adhesion and inhibitory receptors combined with complex signaling machinery.

Apart from the major well defined function of platelets in hemostasis and thrombosis, platelets also play important roles in wound healing, inflammatory processes, tumor metastasis and embryonic development.[5,6]

1.2 Platelet Activation and Thrombus Formation

Platelet activation and thrombus formation at sites of vascular wall injury is a multistep process which can be divided into three major steps: (1) Platelet tethering, (2) activation and (3) firm adhesion and aggregation. The first step of platelet adhesion involves interactions of platelet surface receptors with the exposed sub-endothelial matrix which comprises adhesive macromolecules such as fibronectin, collagens, laminins and *von Willebrand Factor* (vWF). Platelet adhesion mechanisms are largely governed by the rheological conditions prevailing in the vasculature. Blood flows with a higher velocity in the center of the vessel than near the wall, thus generating shear forces between the adjacent layers. Platelets experience maximal opposing shear forces at the vessel wall.[7] Under high shear flow conditions, found in arterioles or stenosed arteries, the initial platelet tethering with the ECM is mediated by the platelet receptor *glycoprotein* (GP)Ib-V-IX and vWF immobilized on exposed collagen.[8] However, this interaction is not stable enough to mediate stable adhesion of the platelets to the injury site, but rather induces platelet deceleration and their rolling on the vessel wall.[9] The deceleration facilitates interaction of the platelet specific immunoglobulin superfamily receptor GPVI with collagen fibers of the ECM. While GPVI binds to collagen with low affinity and by itself is unable to mediate firm adhesion, it triggers an intracellular signaling cascade that induces an inside-out activation of integrin αIIbβ3 and α2β1, which change from a low- to high affinity binding state and induce the release of the "second wave" mediators *adenosine diphosphate* (ADP), *thromboxane A₂* (TxA_2) and epinephrine. These agonists, together with the locally produced thrombin, contribute to platelet activation by stimulating receptors that couple to heterotrimeric G proteins (G_q, $G_{12/G13}$, G_i) to further activate downstream signaling cascades and this subsequently results in full platelet activation[3,10,11] (Figure 1).

Activated integrins, in turn, bind their ligands; α2β1 binds to collagen, α6β1 to laminin and α5β1 to fibronectin. Integrin αIIbβ3, the major platelet integrin involved in the adhesion process binds to collagen-bound vWF immobilized on the ECM and it is a critical mediator of platelet aggregation by linking platelets via fibrinogen and vWF. Finally, thrombus growth is reinforced by recruitment and activation of additional platelets from the blood stream by the released mediators ADP and TxA_2 and subsequent clustering of platelets via plasma fibrinogen and vWF bound to αIIbβ3.

The platelet activating machinery can be divided into two major receptor classes: *G protein coupled-receptors* (GPCRs) and *immunoreceptor tyrosine-based activation motif* (ITAM) signaling receptors. Soluble agonists like thrombin, ADP, TxA_2 or serotonin all lead to the activation of *phospholipase C*β (PLCβ) downstream of G_q-induced signaling. $G_{12/13}$ stimulation results in a Rho/Rho kinase-mediated regulation of *myosin light chain* (MLC) phosphorylation

and consequently induction of platelet shape change.[12] In contrast, $G_{i/z}$ proteins triggers subunit-specific *adenylyl cyclase* (AC) inhibition and *phosphatidylinositol 3-kinase* (PI3K) activation.[13]

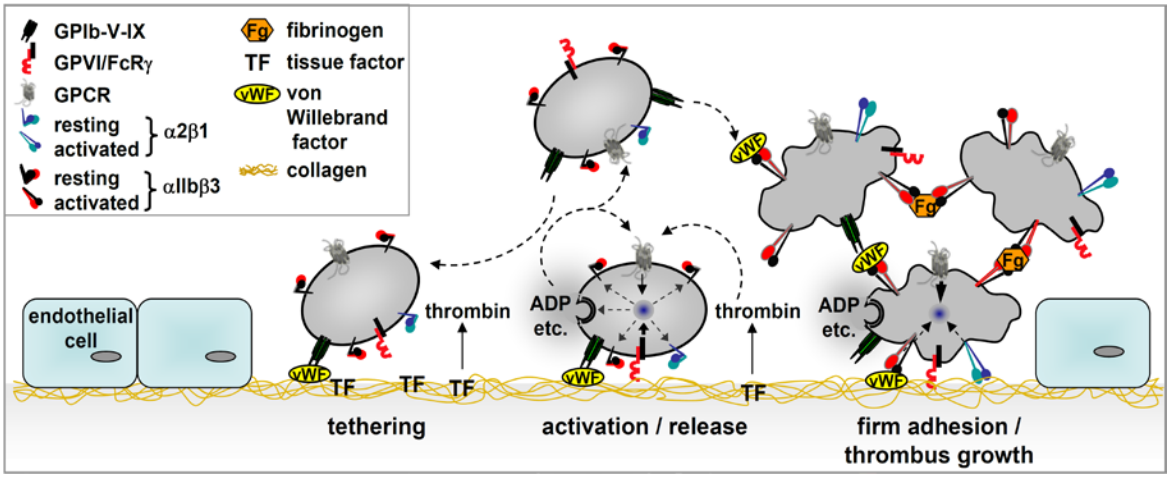

Figure 1: **Model of platelet activation, adhesion and aggregation at the site of vascular wall injury.** The GPIbα-vWF interaction mediates platelet deceleration and tethering on the exposed ECM thus allowing the interaction of GPVI with exposed collagen. This subsequently triggers the shift of integrins (notably αIIbβ3) from a low affinity state to a high affinity state and to the release of secondary mediators such as ADP and TXA_2. Together with the locally produced *tissue factor* (TF) -induced thrombin formation, soluble mediators enhance platelet activation and contribute to the recruitment of further platelets into a growing thrombus. (Taken from: [9]).

The second important pathway of platelet activation involves GPVI and *C-type lectin-like receptor 2* (CLEC-2) and results in the activation of the other PLC isoform, PLCγ2. Upon activation, both PLC isoforms hydrolyze *phosphatidylinositol-4, 5-bisphosphate* (PIP_2) to *inositol-1, 4, 5-trisphoshate* (IP_3) and *diacylglycerol* (DAG). IP_3 in turn activates IP_3 receptors on the *endoplasmatic reticulum* (ER) and triggers Ca^{2+} mobilization from the ER and subsequently results in opening of Ca^{2+} channels in the plasma membrane, leading to a process called *store operated* Ca^{2+} *entry* (SOCE).[9,14] Apart from that, DAG activates *protein kinase C* (PKC) and contributes to Ca^{2+} influx by non-SOCE mechanisms.[15] The elevations in the $[Ca^{2+}]_I$ are indispensable for platelet activation and essential for granule release, firm adhesion, stable aggregate formation,[16] cytoskeletal remodeling and externalization of *phosphatidylserine* (PS) on the platelet surface, which is necessary for the local generation of thrombin[17] (Figure 2).

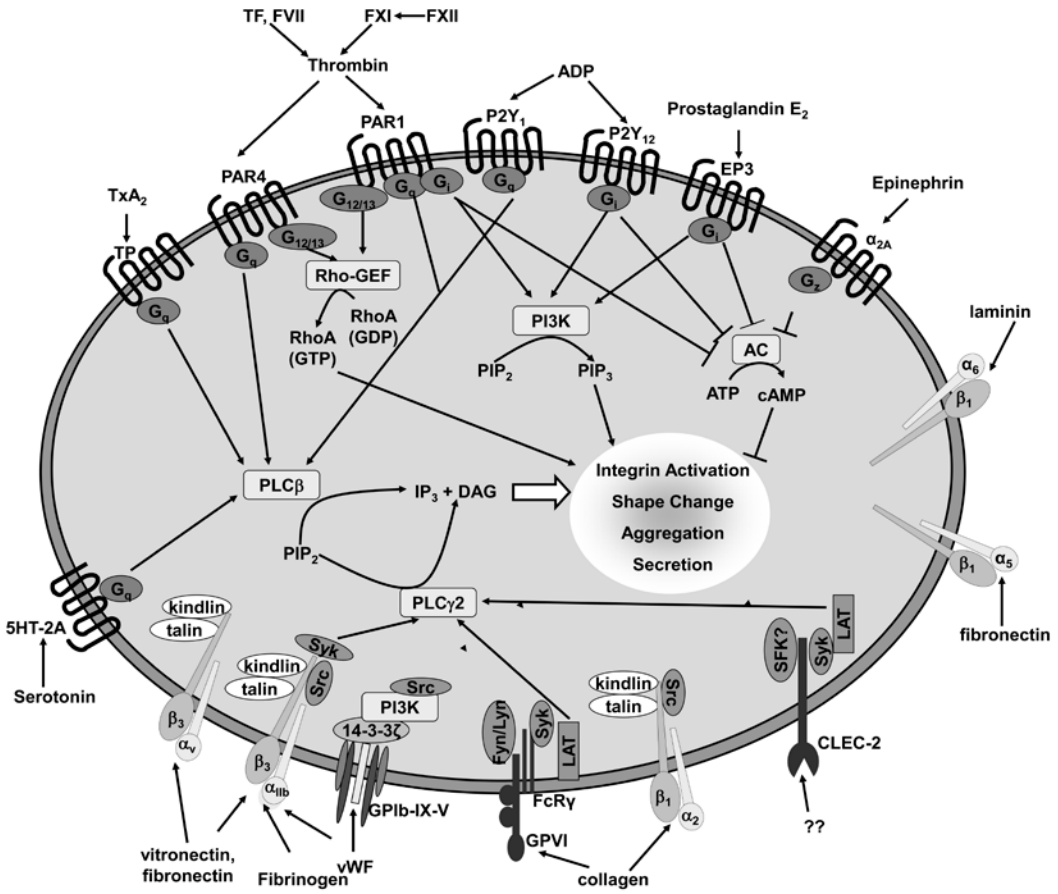

Figure 2: **Scheme of platelet receptors and main signaling pathways.** Receptor activation leads to stimulation of different intracellular signaling molecules. Signaling via *G protein-coupled receptors* (GPCRs) involves the corresponding G proteins. Soluble agonists such as ADP, TXA_2, thrombin, serotonin and epinephrine act via specific GPCRs involving $G_{12/13}$, G_q and $G_{i/z}$ stimulation. $G_{12/13}$ leads to Rho/Rho kinase-mediated cytoskeleton rearrangements, G_q activates phospholipase (PL) Cβ and $G_{i/z}$ induces inhibition of the *adenylyl cyclase* (AC). Adhesion receptor signaling induced by GPVI, CLEC-2 and integrins results in PLCγ2 activation. PLCs generate *inositol-1,4,5-trisphosphate* (IP_3) and *diacylglycer*ol (DAG) from *phosphatidylinositol-4,5-bisphosphate* (PIP_2). IP_3 then mediates elevation of the *intracellular* Ca^{2+} *concentration* $[Ca^{2+}]_I$, a process crucial for full platelet activation. TXA_2, *thromboxane A2*; PAR, *protease activated receptor*; Rho-GEF*, Rho-specific guanine nucleotide exchange factor*; PI-3-K, *phosphatidylinositol 3-kinase*; PIP_3, *phosphatidylinositol-3,4,5-trisphosphate*; Fg, *fibrinogen* (Taken from: [18]).

1.2.1 The GPVI/FcRγ-chain complex

GPVI is a type I transmembrane receptor of 62 kDa composed of two immunoglobulin (Ig)-like domains in its extracellular region, a mucin-like stalk, a transmembrane region and a short 51-amino acid long cytoplasmic tail (Figure 3). GPVI is expressed exclusively in platelets and megakaryocytes.[19] The positively charged arginine residue in the transmembrane region of GPVI is non-covalently associated with the FcRγ-chain.[20] The association of GPVI with the γ-chain is essential for expression of GPVI on the platelet surface and also critical for signaling.[21-23]

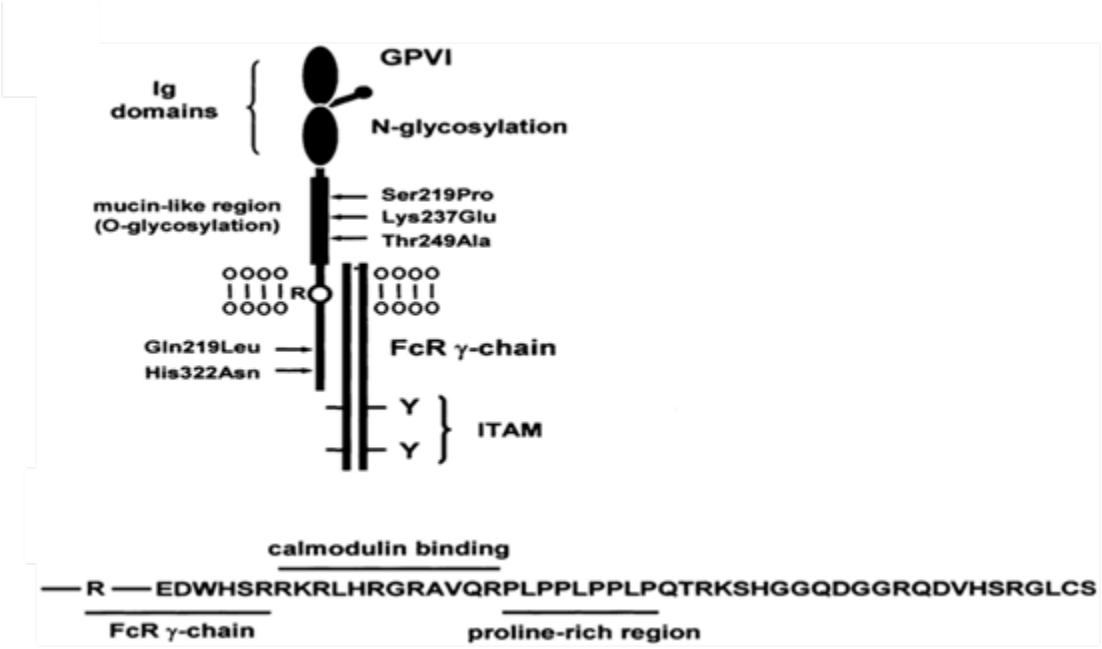

Figure 3: Structure of the GPVI/FcRγ-chain complex. Upper panel: GPVI contains two extracellular immunoglobulin domains that are coupled to a mucin-like stalk rich in O-glycosylation sites. The transmembrane domain has an arginine group (R) which mediates the association with the disulphide-linker homodomain FcRγ-chain through a salt bridge. Tyrosine residues (Y) in the ITAMs are indicated. Lower panel: amino acid sequence of the cytosolic tail of GPVI with the indicated regions of interaction with the FcRγ-chain, calmodulin and SH3 recognition domain (proline-rich region). (Taken from: [24])

The FcRγ-chain contains an ITAM sequence which represents the signaling subunit of the receptor complex. GPVI exists as a dimer on resting platelets[25] and is shed from the surface of the activated platelets as a way of regulating the signaling.[26-28] GPVI triggers signaling by ligand mediated clustering[29,30] of the receptor which is induced by physiological ligands like collagen and laminin[31] and non-physiological ligands like the collagen-derived synthetic peptide *collagen related peptide* (CRP)[32] and the snake venom toxin convulxin.[33] Apart from these agonists, *in vivo* administration of rat monoclonal anti-GPVI antibodies (JAQ1, 2, 3), which bind to the extracellular domain of GPVI, has been shown to induce a transient thrombocytopenia and downregulation of the receptor in circulating platelets leading to a "knock-out like" phenotype in mice.[34] This GPVI deficiency resulted in long term protection from mortality in a model of collagen-dependent lethal pulmonary thromboembolism.[34] JAQ1 treated mice were also protected in models of arterial thrombosis and ischemic stroke, but displayed mildly prolonged tail bleeding times.[34-37] Due to all of these intriguing findings, GPVI is considered as a potential anti-thrombotic target.[26,34,35,38] It was shown that JAQ1 induced GPVI down-regulation can occur via two different ways, either through receptor internalization[38] or metalloproteinase-dependent ectodomain shedding.[27,39,40] Furthermore, it was demonstrated that GPVI cleavage *in vitro* is mediated by two different sheddases, *a disintegrin and metalloproteinase* (ADAM) 10 and

ADAM 17, depending on the shedding-stimulating experimental conditions. However, the study suggested that either both or a not yet identified third sheddase in platelets may be responsible for GPVI-cleavage under *in vivo* conditions.[26]

1.2.1.1 The GPVI Signaling Pathway

Upon ligand binding to the extracellular domain of GPVI, the conserved ITAM tyrosine residues defined by the consensus motif Yxx(L/I)x_{6-12}Yxx(L/I) on the FcRγ-chain are phosphorylated by *Src family kinases* (SFKs). Studies using mutant mice have identified Fyn and Lyn as the two major Src kinases inducing the FcRγ-chain phosphorylation.[41,42] However, a residual level of activation was also found in mice deficient in the two Src kinases indicating the involvement of one or more other SFKs.[42] Fyn and Lyn associate by their SH3 domains with the proline rich region of the cytoplasmic tail of GPVI placing them proximal to their substrate. Mutations in these regions resulted in inhibition of GPVI mediated signaling.[43-45] The phosphorylated ITAM tyrosine residues on GPVI serve as a docking site for the tandem SH2 domains of Syk tyrosine kinase. Platelets from Syk-deficient mice are unresponsive to GPVI agonists, confirming the essential role of Syk kinase in platelet activation.[21] In addition, mutagenesis studies have shown that both ITAM tyrosine residues and also both SH2 domains of the Syk kinase are required for signaling; hence indicating that Syk binds to the dually phosphorylated ITAM.[46,47]

GPVI mediated activation of Syk leads to phosphorylation of a number of downstream proteins including *linker for activation of T-cells* (LAT). Upon phosphorylation on the nine conserved tyrosine residues, LAT serves as a docking site for a range of SH2 domain-containing proteins like *growth factor receptor bound protein 2* (Grb2), *Grb2 related adaptor protein downstream of Shc* (Gads) and most importantly PLCγ2.[48] Other adaptor proteins like *SH2 domain containing leucocytes protein of 76 kDa* (SLP-76) are further recruited by its interaction with Gads and PLCγ2[49] and these associations have been shown to be critical for PLCγ2 activity.[50-52] SLP-76 binds to Tec family kinase, *Bruton's tyrosine kinase* (Btk) and Tec, which phosphorylate and activate PLCγ2.[50] Platelets from mice deficient in both Btk and Tec exhibit a loss in signaling through GPVI.[53] Nevertheless, due to the complexity of the LAT signalosome it is unclear whether additional protein kinases also mediate phosphorylation of PLCγ2 (Figure 4). Upon activation, PLCγ2 hydrolyzes its substrate PIP_2 into secondary messengers, IP_3 and DAG, which release Ca^{2+} from the intracellular stores and activate protein kinase C (PKC), respectively. Mice deficient in PLCγ2 display defective GPVI signaling[54] whereas, the gain of function mutation in PLCγ2 leads to platelet hyperactivity and a pro-thrombotic phenotype.[55]

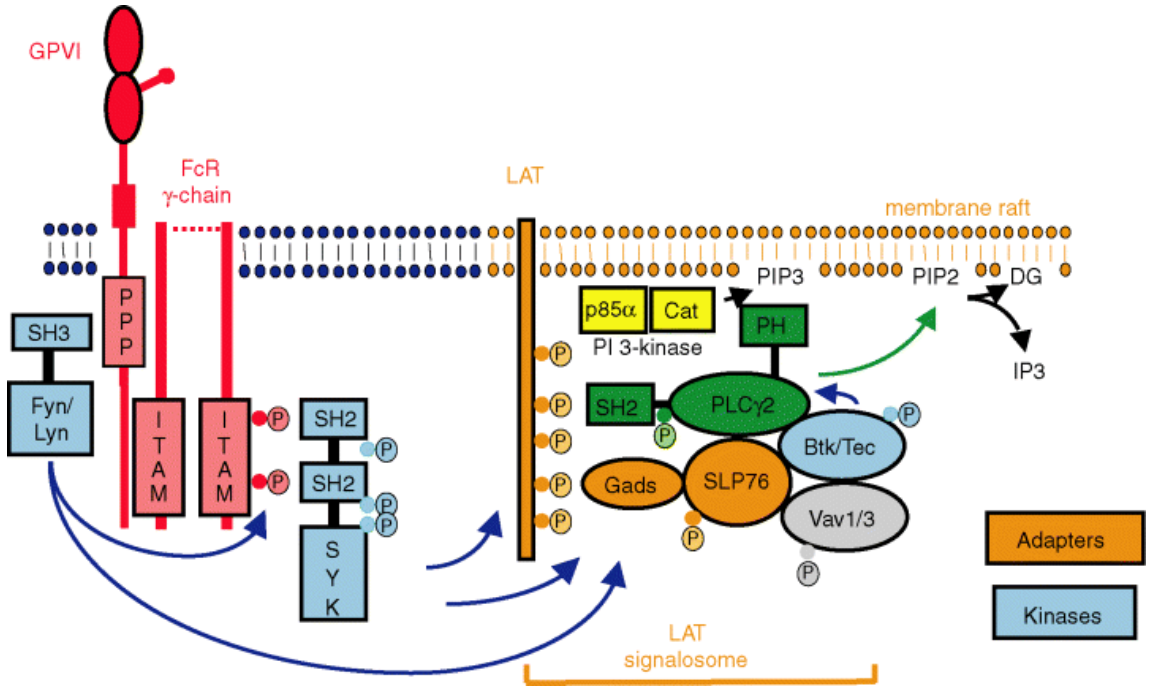

Figure 4: The GPVI signaling cascade. Upon ligand binding, crosslinking of GPVI initiates tyrosine phosphorylation of the FcR γ-chain by the Src family kinases Fyn and Lyn, followed by a Syk-dependent signaling cascade in which various adapter proteins and kinases are involved. This pathway culminates in activation of PLCγ2 and the release of DAG and IP3. DAG/ DG, *1,2-diacylglycerol*; IP3, *inositol-3,4,5-trisphosphate*; PIP_2, *phosphatidylinositol-4,5-bisphosphate*; PIP_3, *phosphatidylinositol-3,4,5-trisphosphate*; SH, *Src homology domain*; Syk, *spleen tyrosine kinase*; LAT, *linker for activation of T cells*; Gads, *Grb2-related adapter downstream of Shc*; SLP76, *SH2-domain containing leukocyte protein of 76 kDa*; Btk, *Bruton's tyrosine kinase* (Modified from: [20]).

1.3 Calcium Signaling in Platelets

A central event in agonist induced platelet activation involves an increase in the cytosolic Ca^{2+} concentration. The increase in intracellular Ca^{2+} induced a number of structural and functional changes including reorganization of the actin cytoskeleton which is necessary for shape change,[56] granule secretion and inside-out activation of αIIbβ3 integrins, leading to platelet activation and aggregation.[57] Elevations in the intracellular Ca^{2+} concentration ($[Ca^{2+}]_i$) can originate from two major sources: the release of compartmentalized Ca^{2+} and the entry of extracellular Ca^{2+} through the *plasma membrane* (PM). Although the process of Ca^{2+} release from the intracellular stores has been well described for several years, the mechanisms underlying Ca^{2+} entry remained largely unknown, until recently.

The Ca^{2+} channels expressed on the platelet plasma membrane include:

1. Store-operated Ca^{2+} (SOC) channels: these channels are regulated by the filling state of the intracellular stores.

2. Receptor-operated Ca^{2+} (ROC) channels: these channels are activated upon ligand binding including the non-SOC channels activated by DAG (Figure 5).

SOCE has been established as the major Ca^{2+} entry pathway in platelets. Receptor activation results in release of Ca^{2+} from the intracellular stores which in turn leads to an opening of plasma membrane SOC channels and entry of extracellular Ca^{2+} into the cytoplasm. *Stromal interaction molecule 1* (STIM1) has been shown to be the major Ca^{2+} sensor in the ER membrane, which upon store release activates Orai1, the major SOC channel in the plasma membrane. Mice lacking either STIM1 or Orai1 show severely reduced – though not completely abolished – Ca^{2+} influx in response to all major platelet agonists resulting in the formation of unstable thrombi *in vivo*. Interestingly, these platelets were still able to perform many of their functions *in vitro,* suggesting that Ca^{2+} from the intracellular stores and Ca^{2+} influx through ROC and non-SOC channels provide a sufficient increase in $[Ca^{2+}]_i$.[58,59] In human platelets, the non-selective *Canonical transient receptor potential* (TRPC) channels, TRPC1 and TRPC6 have been proposed to mediate SOCE and non-SOCE, respectively. Rosado *et al*. used an anti-human TRPC1 blocking antibody to propose reduced SOCE in human platelets upon store depletion. They further proposed a conformational coupling model where Ca^{2+} store release upon thrombin or thapsigargin stimulation resulted in a *de novo* coupling of IP_3–R2 with TRPC1, thus activating TRPC1 as a SOC channel in the PM.[60,61] However, platelets from *Trpc1*$^{-/-}$ mice exhibited normal functional responses, Ca^{2+} store release and SOCE.[62] Moreover, low expression levels of TRPC1 in platelets and megakaryocytes underscore the importance of Orai1 mediated SOCE in platelet physiology. Another interesting study performed by Bousquet *et al*. demonstrated PKC mediated phosphorylation of TRPC6 lead to downregulation of the channel activity. They further showed an increased TRPC6 mediated Ca^{2+} entry in the presence of a PKC inhibitor, thus proposing a negative feedback mechanism operated by PKC to regulate TRCP6 activity.[63] Although it is widely accepted that TRPC6 is expressed in human and murine platelets and contributes to store-independent Ca^{2+} entry, the physiological significance of this calcium flux for platelet biology is not known.

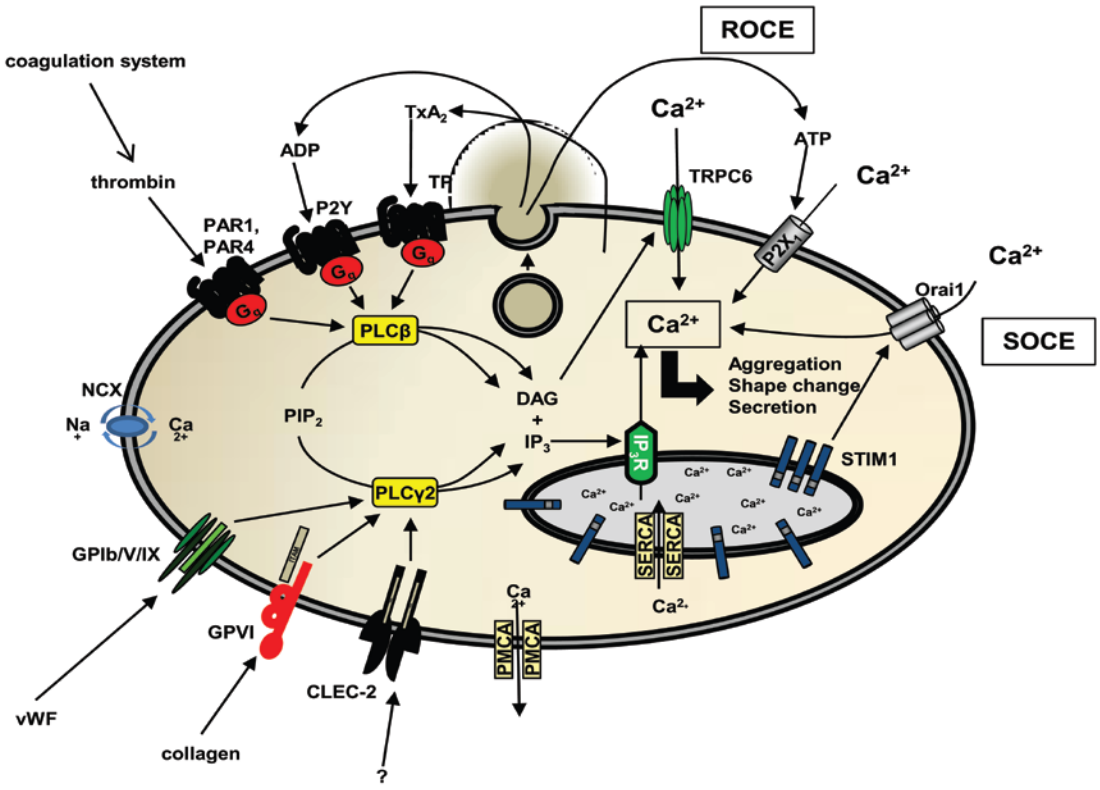

Figure 5: Platelet calcium signaling mechanisms. Agonist-receptor interaction activates phospholipase isoforms to hydrolyze *phosphatidylinositol-4,5-bisphosphate* (PIP_2) to *inositol-1,4,5-trisphosphate* (IP_3) and *diacylglycerol* (DAG). IP_3 releases Ca^{2+} from intracellular stores and STIM1 opens the Orai1 channels in the plasma membrane, resulting in *store-operated calcium entry* (SOCE). DAG mediates non-SOCE through *canonical transient receptor potential channel* 6 (TRPC6). Additionally, a direct *receptor-operated calcium* (ROC) channel, P2X1, and a *Na^+/ Ca^{2+} exchanger* (NCX) contribute to the elevation in $[Ca^{2+}]_i$. *Sarcoplasmic/endoplasmic reticulum Ca^{2+} ATPases* (SERCAs) and *plasma membrane Ca^{2+} ATPases* (PMCAs) pump Ca^{2+} back into the stores or out of the cell, respectively. IP_3R, $InsP_3$-receptor; ATP, adenosine triphosphate; ADP, adenosine diphosphate; GPVI, glycoprotein VI; FcRγ, Fc receptor γ chain; FcRIIa, Fc receptor IIa; CLEC-2, *C-type lectin-like receptor 2*; PI3-K, *phosphatidylinositol 3-kinase*; Syk, *spleen tyrosine kinase*. (Modified from: [17])

1.3.1 The TRPC6 Channel

TRPC6 has been characterized as a receptor-operated but not store-regulated cation channel though recent findings suggested the sensitivity of TRPC6 to store-depletion. Agonist induced TRPC6 activation can be blocked by the PLC inhibitor, U73122, indicating a PLC-dependent activation mechanism. TRPC6 activity was found to be increased by *1-oleoyl-1-acetyl-sn-glycerol* (OAG), a membrane-permeable analogue of DAG and *1-stearoyl-2-arachidonyl-sn-glycerol* (SAG).[64] Regulation of TRPC6 channel activity was suggested to occur through many ways; tyrosine phosphorylation by the Src kinase, Fyn and Ca^{2+}/calmodulin acting from the intracellular side were found to increase channel activity,[65] while PKC-dependent Ser^{448} and PKG-dependent Thr^{69} phosphorylation contributed to channel inactivation.[63,66]. In cultured neurons, TRPC6 was shown to be involved in *brain-derived neurotrophic factor* (BDNF) induced

neuronal outgrowth and transferrin-independent iron uptake.[67,68] TRPC6 expression was observed in synaptosomes and excitatory postsynaptic sites indicating a role in synaptic and behavioural plasticity. Overstimulation of TRPC6 in cardiac myocytes led to pathological cardiac remodeling.[69] Other functions of TRPC6 include regulation of myogenic tone of cerebral arteries, where knockdown of the channel resulted in attenuated depolarization and constriction of cerebral arteries induced by intraluminal pressure.[70] Paradoxically, the myogenic response in *Trpc6*$^{-/-}$ mice was increased but a compensatory upregulation of TRPC3 was also observed.[71] Transgenic mice over-expressing TRPC6 were more sensitive to pressure overload and agonist induced cardiac hypertrophy accompanied by decreased systolic function.[72] The TRPC6 transgenic mice developed cardiomegaly, interstitial fibrosis, and ventricular dilatation with congestive heart failure.[72]

1.4 The PDZ and LIM Domain Protein Family

PDZ/LIM genes encode a group of proteins that play diverse biological roles like cytoskeletal organization, neuronal signaling, organ development and oncogenesis. All PDZ/LIM family members exhibit at least one PDZ and one LIM domain. Originally, PDZ domains were recognized in the postsynaptic density protein PSD-95,[73] the septate junction protein Discs-large of *Drosophila melanogaster*,[74] and the epithelial tight junction protein ZO-1.[75] PDZ domains play an important role in organizing cell signaling assemblies[76] and are found in plants, yeast, bacteria, and a variety of metazoans.[77,78] PDZ domains interact with short C-terminal peptide motifs, internal sequences resembling a C-terminus, and have further been shown to bind to phospholipids.[76,79] The LIM domains consist of 50-60 amino acids and are defined by a cysteine rich consensus, which forms the basis for two closely associated zinc fingers. The term ‘LIM’ is the abbreviation of three homeodomain proteins in which LIM domains were originally identified, namely Linl-1, Isl-1, and Mec-3.[80,81] The two zinc fingers that constitute a LIM domain contain eight conserved residues, mostly cysteines and histidines, which coordinately bind to two zinc atoms. Despite zinc fingers being typical DNA binding structures, there is little evidence supporting the observation that LIM domains can bind DNA directly. The LIM domain proteins are established as protein adaptors in the cytoplasm. They associate with cytoskeleton-associated structures, such as actin filaments, focal adhesions, growth cones, intercalated discs and Z-lines of muscle cells. Through these interactions, LIM domain proteins are involved in many cellular physiological activities, such as cell shape modulation, cell motility and integrin-dependent adhesion and signaling. PDLIM proteins have been suggested to act as adaptors between kinases and the cytoskeleton,[82,83] which is based on studies showing that on the one hand PDZ-LIM proteins associate with the actin cytoskeleton via their PDZ domain[82-85] and on the other hand to the kinases via their LIM domains.[83,86-88]

PDZ as well as LIM domain proteins often contain multiple copies of these interaction domains. A combination of PDZ and LIM domains has been discovered in ten genes in the mammalian genome that share similar domain architecture. These ten genes are: *actinin-associated LIM protein* (ALP, PDLIM3), CLP36 (Elfin, CLIM1, PDLIM1), Enigma (LMP-1, PDLIM7), *Enigma homologue* (ENH, PDLIM5), *reversion-induced LIM protein* (RIL, PDLIM4), Mystique (PDLIM2, SLIM), *Z-band associated protein* (ZASP, cyper, Oracle, PDLIM6), the two LIM domain kinases (LIMK1, LIMK2), and *LIM-domain only* 7 (LMO7, FBXO20) that, despite its name, also contains a PDZ domain.

The PDZ/LIM genes can be divided into four different subgroups based on their gene structures and phylogenetic relationships:

1. The ALP subfamily – ALP, RIL, CLP36 and Mystique
2. The Enigma subfamily – Enigma, ENH and ZASP
3. The LIM kinases – LIMK1 and LIMK2
4. LMO7

1.4.1 The ALP subfamily

The four mammalian ALP subfamily proteins– ALP, CLP36, Mystique and RIL are characterized by the presence of a N-terminal PDZ domain followed by a C-terminal LIM domain, and are postulated to play a role in actin anchorage in muscle as well as nonmuscle cells.[85,89-93] All genes in the ALP subfamily encode a N-terminal PDZ and a single C-terminal LIM domain with the smallest member RIL encompassing 7 exons in humans, *Clp36 (Elfin)* contains 7 exons and *Mystique*, contains 11 exons. ALP subfamily members at exon 5 (8 for *Mystique*) have the coding sequence for a conserved ALP-like motif.[94] *Alp* and *Clp36* both encode two and one *ZASP-like motif* (ZM) protein domain, respectively.[76,78]

1.4.1.1 Physiological function of ALP subfamily proteins

All the ALP subfamily members are widely expressed in mammalian tissues. Ablation of ALP in mice leads to selective *right ventricle* (RV) cardiomyopathy without any obvious alterations in skeletal muscles.[95,96] ALP was found to play an important role in the development of RV as ALP-deficiency resulted in a decrease trabeculation, irreversible chamber dilation and dysmorphogenesis of the embryonic RV.[96] Studies with intact myocardium revealed the co-localization of ALP with both α-actinin and β-catenin at the intercalated disc. Moreover, these studies found that ALP enhanced the ability of α-actinin to crosslink actin filaments, suggesting ALP to serve as a genetic modifier of embryonic ventricular muscle to biomechanical stress that

accompanies exposure to normal workload *in utero*.[96] In response to hypoxic stress, ALP-deficient mice were shown to exhibit an altered regional RV function and abrogated hypertrophic remodeling.[97]

Gene Expression, Molecular Interactions, and Role of ALP Subfamily Proteins in Development and Disease

Protein	Domain	Interaction	Complex	Expression	Development / disease	Ref.
ALP	PDZ ZM LIM	α-actinin 2 α-actinin 2 --	Sarcomeres	Cardiac and skeletal muscle	Heart development, Cardiomyopathies	85,95,96,98-100
CLP36	PDZ ZM LIM	α-actinin 1 and 4, PMCA -- α-actinin 2, Clik1	Sarcomeres, cytoskeleton	Cardiac and skeletal muscle, lungs, liver and other epithelial cells		89,91,93,100-103
Mystique	PDZ LIM	α-actinin --	Nucleus, cytoskeleton	Heart, spleen, testis	Migration of breast cancer cells	100,104
RIL	PDZ LIM	α-actinin 2 AMPA receptor, PTP-BL	Cytoskeleton	Brain	Neuronal development, bone development, tumor progression	90,100,105-107

Mystique has shown to play a role in epithelial cell migration.[104] *Small interfering* (si)RNA-mediated silencing of Mystique resulted in loss of cell migration and adhesion.[104] Mystique mostly has a nuclear location where it is proposed to promote degradation of phosphorylated STAT1 and STAT4 transcription factors. Interestingly, cells from Mystique knockout mice showed increased expression of STAT proteins.[108] Mystique was also shown to promote nuclear degradation of the p65 subunit of the NF-kB family to *promyelocytic leukemia protein* (PML) nuclear bodies for ubiquitination and subsequent degradation.[109] RIL has been well studied for its role in tumor growth and neuronal signaling.[110,111]

CLP36 has been implicated in regulation of actin stress fibers in different cell types.[91,101] In situ hybridization in mouse embryos revealed expression of CLP36 during early heart development.[93] However, the function of CLP36 in the heart remains to be elucidated. Recently, CLP36 has been studied in the nervous system, where it was found to be expressed in sensory ganglia but not in the *central nervous system* (CNS) of adult rats. CLP36 was up-regulated in *dorsal root ganglion* (DRG) neurons and facial motor-neurons after nerve injury, thus suggesting CLP36 to serve as a scaffold forming a multi-protein complex that regulates actin cytoskeleton dynamics and plays a role in controlling neurite outgrowth.[112]

1.4.1.2 CLP36 function and its interactions

The human homolog of CLP36 (hCLP36) was initially shown to interact with α-actinin 2 by yeast two-hybrid screening similar to the other PDLIM family members. The initial studies done by Kotaka *et.al* [93] suggested that this interaction was mediated by the C-terminal LIM domain of hCLP36. To study the subcellular localization of CLP36 in cell lines of non-muscle origin, Myc epitope-tagged CLP36 was expressed into the U2OS osteosarcoma cell line. Double fluorescence analysis with anti–Myc and rhodamine-labeled phalloidin from transfected cells indicated co-localization of CLP36 with actin filaments resembling stress fibers. A significant amount of CLP36 was found to be associated with stress fibers even after treatment of cells with the microfilament formation inhibitor cytochalasin B.[89] Interestingly, CLP36-knock-down studies performed using *short hairpin* (sh) RNAs led to prominent morphological changes in transfected cells. The transfected cells developed a ruffled membrane and displayed a round shape, in contrast to the fibroblast-like shape of wild-type cells. The phalloidin staining revealed that actin stress fibers were absent in CLP36-knockdown cells. Furthermore, replenishment with exogenous CLP36 in these cells resulted in the restoration of stress fibers leading to reversion from ruffled to fibroblast-like cell morphology.[113] Interaction of CLP36 with palladin was studied using yeast two-hybrid screening.[114] Palladin is an important structural element of the actin cytoskeleton and associates with α-actinin. This interaction was dependent on the PDZ domain of CLP36 and the C-terminus of palladin.[114] Characterization of a novel, ubiquitously expressed kinase, Clik1 by yeast two hybrid screening indicated a highly specific interaction between Clik1 and CLP36. The association was mediated by the C-terminal LIM domain of CLP36 and was unique to CLP36. Furthermore, the association of CLP36 with Clik1 led to the relocalization of the otherwise nuclear Clik1 to actin stress fibers.[102]

1.4.1.3 CLP36 in platelets

The role of CLP36 in platelets was studied for the first time in the year 2000 by Bauer *et al.*[115] Double immunofluorescence microscopy on human platelets revealed the co-localization of

CLP36 and F-actin. CLP36 was found to be associated with actin filaments in long pseudopodia, short filopodia and lamellipodia. Furthermore, in spread platelets CLP36 concentrated along the radially outgrowing actin filaments without being present in the region where the secretory granules are concentrated. In the later stages of spreading, CLP36 was observed along actin stress fibers in a regular dotted pattern. CLP36 was found to be absent in focal adhesions that co-localized with the tips of actin stress fibers. The interaction between F-actin and CLP36 was also confirmed in endothelial cells, where in resting confluent endothelial cells CLP36 co-localized with the peripheral actin filaments beneath the plasma membrane. Upon thrombin stimulation, these cells exhibited a dramatic reorganization of their actin cytoskeleton; thereby CLP36 was translocated to the newly formed actin structures. The immunostaining performed on endothelial cells with anti-α-actinin and anti-CLP36 antibodies revealed co-localization of both proteins on actin stress fibers.[115] CLP36 could be co-immunoprecipitated with α-actinin, but not with vinculin in the platelet lysates. Furthermore, yeast two hybrid analysis indicated that the intervening region of CLP36, but not its PDZ or LIM domain, interacted with the spectrin-like repeats 2 and 3 within the rod domain of the α-actinin-1. Depolymerization of F-actin by treating platelets with cytochalasins did not change the amount of α-actinin-1 co-immunoprepitated with CLP36, indicating that the binding of CLP36 to α-actinin-1 is constitutive and independent of the α-actinin-1/F-actin interaction.[115] Using stoichiometric analysis, two molecules of CLP36 were found to be associated with an α-actinin dimer.[89] Another study performed by Bozulic *et al.* in 2007 showed that the PDZ domain of CLP36 associated with the plasma membrane Ca^{2+}-ATPase (PMCA) 4b isoform in human platelets.[103] CLP36, α-actinin and actin were immunoprecipitated with PMCA. Their study suggested that PMCA associated with small actin complexes comprising of CLP36, α-actinin, and monomeric G-actin, which remained unbound to the cytoskeleton in resting platelets. Upon platelet activation and cytoskeletal rearrangements, this small actin complex became associated with the cytoskeleton via polymerization of G-actin monomers into filamentous F-actin in structures such as filopods. They further speculated that interaction of PMCA to the actin cytoskeleton via CLP36 regulates intracellular Ca^{2+} levels. This process may play a role in regulation of clot retraction and maintenance of thrombus integrity on platelet activation.[103]

2 AIM OF THE STUDY

Platelet activation essentially involves an increase in the cytosolic Ca^{2+} concentration and the cytoskeletal rearrangements. These two events play a crucial role during platelet shape change, secretion and spreading. The major Ca^{2+} entry pathway in platelets involves the receptor mediated release of intracellular Ca^{2+} followed by subsequent influx from outside, mediated by different Ca^{2+} channels present on the platelet plasma membrane. These channels include Orai1 (CRACM1), the major Ca^{2+} SOC channel in platelets. Apart from this, other channels like TRPC6 are also thought to mediate the Ca^{2+} influx. However, the function of TRPC6 in platelet physiology was unknown. Thus, the first aim of this thesis was to analyze the function of Ca^{2+} channel TRPC6 in platelets. For this purpose, TRPC6-deficient platelets were analyzed using *in vitro* and *in vivo* models of platelet function, thrombosis and hemostasis.

Cytoskeletal rearrangements upon platelet activation result in the formation of a platelet plug. The process of actin reorganization involves the coordinated action of a large number of proteins and signaling pathways. The PDZ/LIM domain family member, CLP36, has been reported to play an important role in stress fiber assembly, but its exact role in platelet signaling and actin organization was not known. The second aim of the thesis was to investigate the function of CLP36 and role of its LIM domain in platelet signaling. For this purpose, *Clp36*$^{\Delta LIM}$ mice, lacking the C-terminal LIM domain and *Clp36*$^{-/-}$ mice, lacking the whole protein were generated and analyzed for CLP36 function in platelets.

3 MATERIALS AND METHODS

3.1 Materials

3.1.1 Kits and chemicals

Reagent	Company
Acetic acid	Roth (Karlsruhe, Germany)
ADP	Sigma (Deisenhofen, Germany)
Agarose	Roth (Karlsruhe, Germany)
Alexa Fluor 488	Invitrogen (Karlsruhe, Germany)
Ammonium peroxodisulphate (APS)	Roth (Karlsruhe, Germany)
Apyrase (grade III)	Sigma (Deisenhofen, Germany)
Atipamezole	Pfizer (Karlsruhe, Germany)
ATP release kit	Roche Diagnostics (Mannheim, Germany)
Avertin® (2,2,2-tribromoethanol)	Sigma (Deisenhofen, Germany)
β-mercaptoethanol	Roth (Karlsruhe, Germany)
Bovine serum albumin (BSA)	AppliChem (Darmstadt, Germany)
Calcium chloride	Roth (Karlsruhe, Germany)
Chrono-Lume® (d-luciferase/luciferin reagent + ATP standard)	Probe & go (Osburg, Germany)
Complete mini protease inhibitors (+EDTA)	Roche Diagnostics (Mannheim, Germany)
Convulxin	Alexis Biochemicals (San Diego, USA)
Disodiumhydrogenphosphate	Roth (Karlsruhe, Germany)
Dry milk, fat-free	AppliChem (Darmstadt, Germany)
dNTP mix	Fermantas (St. Leon-Rot, Germany)
Dylight-488	Pierce (Rockford, IL, USA)
EDTA	AppliChem (Darmstadt, Germany)
Enhanced chemoluminiscence (ECL)-detection substrate	PerkinElmer LAS (Boston, USA)
Ethanol	Roth (Karlsruhe, Germany)
Ethidium bromide	Roth (Karlsruhe, Germany)

Fentanyl	Janssen-Cilag GmbH (Neuss, Germany)
Fibrillar type I collagen (Horm)	Nycomed (Munich, Germany)
Flumazenil	Delta Select GmbH (Dreieich, Germany)
Fluorescein-isothiocyanate (FITC)	Molecular Probes (Oregon, USA)
Forene® (isoflurane)	Abott (Wiesbaden, Germany)
Fura-2/AM	Molecular Probes/Invitrogen (Germany)
GeneRuler 1kb DNA Ladder	Fermentas (St. Leon-Rot, Germany)
Glucose	Roth (Karlsruhe, Germany)
Glutaraldehyde	Roth (Karlsruhe, Germany)
Glycerol	Roth (Karlsruhe, Germany)
HEPES	Roth (Karlsruhe, Germany)
High molecular weight heparin	Sigma (Deisenhofen, Germany)
Human fibrinogen	Sigma (Deisenhofen, Germany)
Igepal CA-630	Sigma (Deisenhofen, Germany)
Indomethacin	Sigma (Deisenhofen, Germany)
IP_1 ELISA kit	Cisbio (Paris, France)
Iron-III-chloride hexahydrate ($FeCl_3$ $6H_2O$)	Roth (Karlsruhe, Germany)
Isopropanol	Roth (Karlsruhe, Germany)
Loading Dye solution, 6x	Fermentas (St. Leon-Rot, Germany)
Magnesium chloride	Roth (Karlsruhe, Germany)
Magnesium sulfate	Roth (Karlsruhe, Germany)
Medetomidine (Dormitor)	Pfizer (Karlsruhe, Germany)
Midazolam (Dormicum)	Roche (Grenzach-Wyhlen, Germany)
MOPS	AppliChem (Darmstadt, Germany)
Naloxon	Delta Select GmbH (Dreieich, Germany)
4-12% NuPage Bis-Tris gradient gels	Invitrogen (Karlsruhe, Germany)
Oleoyl-2-acetyl-sn-glycerol (OAG)	Sigma (Deisenhofen, Germany)
PageRuler Prestained Protein Ladder	Fermentas (St. Leon-Rot, Germany)
Paraformaldehyde (PFA)	Roth (Karlsruhe, Germany)

Phalloidin-rhodamine	Invitrogen (Karlsruhe, Germany)
Phalloidin-Atto647N	AttoTec GmbH (Siegen, Germany)
Phenol/chloroform/isoamylalcohol	AppliChem (Darmstadt, Germany)
Phorbol-12-myristate-13-acetate	Sigma (Deisenhofen, Germany)
PKC inhibitor Gö6983	Calbiochem (Bad Soden, Germany)
Pluronic F-127	Invitrogen (Karlsruhe, Germany)
Potassium acetate	Roth (Karlsruhe, Germany)
Potassium chloride	Roth (Karlsruhe, Germany)
Prostacyclin	Calbiochem (Bad Soden, Germany)
Protein G-Sepharose	GE Healthcare (Uppsala, Sweden)
QIAquick gel extraction kit	Qiagen (Hilden, Germany)
RNeasy Mini Kit	Qiagen (Hilden, Germany)
R-phycoerythrin (PE)	EUROPA (Cambridge, UK)
Rotiphorese Gel 30 (PAA)	Roth (Karlsruhe, Germany)
Sodium chloride	AppliChem (Darmstadt, Germany)
Sodium citrate	AppliChem (Darmstadt, Germany)
Sodiumdihydrogenphosphate	Roth (Karlsruhe, Germany)
Sodium hydroxide	AppliChem (Darmstadt, Germany)
TEMED	Roth (Karlsruhe, Germany)
Thrombin	Roche Diagnostics (Mannheim, Germany)
Titan One Tube RT-PCR-Kit	Roche (Ingelheim, Germany)
TRIS ultra	Roth (Karlsruhe, Germany)
Triton X-100	AppliChem (Darmstadt, Germany)
U46619	Alexis Biochemicals (San Diego, USA)
Vectashield hardset mounting medium	Vector Laboratories (Burlingame, USA)

Collagen-related peptide (CRP) was kindly provided by Paul Bray (Baylor College, USA). Rhodocytin was a generous gift from J. Eble (University Hospital Frankfurt, Germany). Annexin V- Dylight 488 was generously provided by Jonathan F. Tait, Medical Center, University of Washington. All enzymes were purchased from Fermentas (St. Leon-Rot, Germany) or

obtained from Invitrogen (Karlsruhe, Germany). Primers were purchased from Metabion (Planegg-Martinsried, Germany) or MWG-Eurofins (Ebersberg, Germany). All non-listed chemicals were obtained from AppliChem (Darmstadt, Germany), Sigma (Deisenhofen, Germany) or Roth (Karlsruhe, Germany).

3.1.2 Antibodies

3.1.2.1 Purchased primary and secondary antibodies

Antibodies	Source
Anti-phosphotyrosine 4G10	Millipore (CA, USA)
Rat anti-mouse IgG-HRP	DAKO (Hamburg, Germany)
Rabbit anti-CLP36 antibody (ab64971)	Abcam (Cambridge, UK)
Goat anti-CLP36 antibody (ab17022)	Abcam (Cambridge, UK)
Rabbit anti-rat IgG-FITC	DAKO (Hamburg, Germany)
Rabbit anti-TRPC6 antibody	Almone labs (Jerusalem, Israel)
Rat anti-tubulin IgG	Millipore (CA, USA)
Rabbit anti-α-actinin antibody (H-300)	Santa Cruz Biotechnology (Germany)
Goat anti-rabbit IgG-Alexa-488	Invitrogen (Karlsruhe, Germany)

3.1.2.2 Monoclonal antibodies (mAbs)

mAbs generated and modified in our laboratory

Antibody	Isotype	Antigen	Described in
DOM2	IgG1	GPV	[116]
INU1	IgG1κ	CLEC-2	[117]
JAQ1	IgG2a	GPVI	[34]
JON/A	IgG2b	GPIIb/IIIa	[118]
JON1	IgG2a	GPIIb/IIIa	[116]
p0p4	IgG2b	GPIbα	[116]
p0p6	IgG2b	GPIX	[116]
ULF1	IgG2a	CD9	[116]
WUG1.9	IgG1	P-selectin	unpublished
12C6	IgG2b	α2 integrin	unpublished

3.1.3 Buffers and media

All buffers were prepared and diluted in double-distilled water (ddH_2O).

Acid-citrate-dextrose (ACD) buffer, pH 4.5

Trisodium citrate dehydrate	85 mM
Anhydrous citric acid	65 mM
Anhydrous glucose	110 mM

Blocking solution for immunoblotting

BSA or fat-free dry milk in PBS or washing buffer	5%

Blotto B

BSA	1%
Fat-free dry milk	1%
Tween 20	0.05%

Blotting buffer A for immunoblotting

TRIS, pH 10.4	0.3 M
Methanol	20%

Blotting buffer B for immunoblotting

TRIS, pH 10.4	25 mM
Methanol	20%

Blotting buffer C for immunoblotting

ε-amino-n-caproic acid, pH 7.6	4 mM
Methanol	20%

Coomassie staining solution

Acetic acid	10%
Methanol	40%
Coomassie Brilliant blue	0.01%

Coomassie destaining solution

Acetic acid	10%
Methanol	40%

***Immunoprecitation* (IP) buffer, pH 8.0**

TRIS/HCl, pH 8.0	15 mM
NaCl	155 mM
EDTA	1 mM
NaN_3	0.005%

Laemmli buffer for SDS-PAGE

TRIS	40 mM
Glycine	0.95 M
SDS	0.5%

Lysis buffer (DNA isolation), pH 7.2

TRIS base	100 mM
EDTA	5 mM
NaCl	200 mM
SDS	0.2%
Proteinase K (20 mg/ mL)	100 µg/mL

Lysis buffer (tyrosine phosphorylation), pH 7.5

NaCl	300 mM
TRIS	20 mM
EGTA	2 mM
EDTA	2 mM
Na_3VO_4	2 mM
Igepal CA-630	2%
add complete mini protease inhibitors	

PHEM, pH 7.2

PIPES	60 mM
HEPES	25 mM
EGTA	10 mM
$MgSO_4$	2 mM

PHEM complete pH 7.2

PHEM buffer	
PFA	1%
NP-40	0.005%

Phosphate buffered saline (PBS), pH 7.14

NaCl	137 mM
KCl	2.7 mM
KH_2PO_4	1.5 mM
Na_2HPO_4	8 mM

SDS sample buffer, 2x

β-mercaptoethanol (for reduced conditions)	10%
TRIS buffer (1.25 M), pH 6.8	10%
Glycerine	20%
SDS	4%
Bromophenolblue	0.02%

Separating gel buffer (Western Blot), pH 8.8

TRIS/HCl	1.5 M

Stacking gel buffer (Western Blot), pH 6.8

TRIS/HCl	0.5 M

Stripping buffer (Western Blot), pH 6.8

TRIS/HCl	62.5 mM
SDS	2%
β-mercaptoethanol	100 mM

TAE buffer, 50x, pH 8.0

TRIS	0.2 M
Acetic acid	5.7%
EDTA (0.5 M, pH 8)	10%

TE buffer, pH 8

TRIS base	10 mM
EDTA	1 mM

Tris-buffered saline (TBS), pH 7.3

NaCl	137 mM (0.9%)
TRIS/HCl	20 mM

Tyrode´s buffer, pH 7.3

NaCl	137 mM (0.9%)
KCl	2.7 mM
$NaHCO_3$	12 mM
NaH_2PO_4	0.43 mM
$CaCl_2$	1 mM
$MgCl_2$	1 mM
HEPES	5 mM
BSA	0.35%
Glucose	0.1%

Washing buffer (western blot)

Tween 20	0.1%
in PBS, pH 7.2	

3.2 Methods

3.2.1 RNA isolation and Polymerase chain reaction

For platelet RNA isolation, 2 x 10^6 platelets/µL were washed in PBS/EDTA and the pellet was resuspended in 200 µL IP buffer with 1% NP-40. 800 µL of Trizol reagent was added and samples were incubated for 60 min at 4°C. After incubation, 200 µL of chloroform was added and samples were incubated again for 15 min at 4°C. Samples were then centrifuged at 10,000 rpm for 10 min and the upper phase was incubated with three volumes of 70% ethanol with 10% sodium acetate (pH 5.2) for 1 h at -20°C. After centrifugation at maximal speed for 15 min, the pellet was washed with 70% ethanol, then centrifuged again and dried at 37°C. The pellet was resuspended in 30-40 µL of RNase free water and concentration was determined by absorbance readings at 260 nm, whereas the ratio of absorbance at 260/280 and 260/230 was used to assess purity. Samples with 260/280 readings of >1.8 and 260/230 readings of >1.9 were subsequently used to prepare cDNA. 1-2 µg RNA were incubated with 1 µL Oligo dNTP (0.5 µg/µL) in a total volume of 11.9 µL at 70°C for 5 min and afterwards transferred on ice. 2 µL DTT (0.1 M), 1 µL dNTPs (10 mM), 0.5 U RNase inhibitor, 4 µL 5x first strand buffer and 200 U

Super Script Reverse Transcriptase were added. The total volume was adjusted to 40 µL by adding RNase-free water and the sample were incubated at 42°C for 1 h. A gradient PCR was performed with Taq polymerase to determine the correct annealing temperature. Following this, a *Polymerase chain reaction* (PCR) with the appropriate annealing temperature was performed.

The following primers were used to study TRPC family members:

Trpc1	**Trpc1for.:** 5´-catggagcatcgtatttcac-3´
	Trpc1rev.: 5´-gagtcgaaggtaactcagaa-3´
Trpc2	**Trpc2for.:** 5´-cctgccagaaggacctgtatg-3´
	Trpc2rev.: 5´-cacatgcccagcaactcgaag-3´
Trpc3	**Trpc3for.:** 5´-tgtctggtcgtgttggtcgtg-3´
	Trpc3rev.: 5´-tgaacgcggcgatgaagatgg-3´
Trpc4	**Trpc4for.:** 5´-gggctaagctgcaaaggcatc-3´
	Trpc4rev.: 5´-caccaggttcctcatcacctc-3´
Trpc5	**Trpc5for.:** 5´-tgtgggatggtggattcacgg-3´
	Trpc5rev.: 5´-gcagcactaccagggagatg-3´
Trpc6	**Trpc6for.:** 5´-acgcggttctcccatgatgtg-3´
	Trpc6rev.: 5´-cgagcagccccaggaaaatg-3´
Trpc7	**Trpc7for.:** 5´-gagggcgttaagactctgcc-3´
	Trpc7rev.: 5´-cgagatgacctcagacaagcc-3´
Actin	**Actinfor.:** 5´-gtgggccgctctaggcaccaa-3´
	Actinrev.: 5´-ctctttgatgtcacgcacgatttc-3´

To study the expression of different PDLIM family members in mouse platelets, following primer sequences were used as depicted below.

Alp	**ALP/For :** 5´-taaagcagegtcctaccagt-3´
	ALP/Rev : 5´-tgaggggcactgaagctgt-3´
Ril	**Ril/For :** 5´-taaaggctgccacgatcatc-3´
	Ril/Rev : 5´-caggtctaccctgcagtccc-3´
Clp36	**CLP36/For :** 5´-caagggctgcgcagacaaca-3´
	CLP36/Rev : 5´-cttgtcaatgataaggctgc-3´

Mystique	**Mystique/For :** 5´-ccgacagagcgcctcacccc-3´ **Mystique/Rev :** 5´-ttcctccagatccaaactgc-3`
Enh1	**Enh1/For :** 5´-cacttcatcacatgcttccc-3´ **Enh1/Rev :** 5´-aactccgtgttgcgctccac-3´
Enigma	**Enigma/For:** 5´-atattgacggtgagaacgcg-3´ **Enigma/Rev:** 5´-gcaactgtccattctgccgc-3´
Zasp	**Zasp/For :** 5´-agaggctctgcgaaggtcaa-3´ **Zasp/Rev :** 5´-ctcgctgtagctggtatggg-3´

3.2.2 Generation of mice

3.2.2.1 Generation of *Clp36$^{\Delta LIM}$* mice

Clp36$^{\Delta LIM}$ chimeric mice were generated by microinjection of embryonic stem (ES) cell clone XC 262 (*BayGenomics*) into C57Bl/6 blastocysts. After germ line transmission, heterozygous and knockin animals were genotyped by PCR using mouse tail DNA and Western blotting detecting different domains of CLP36.

3.2.2.2 Generation of *Clp36$^{-/-}$* mice

Clp36$^{-/-}$ chimeric mice were generated by microinjection of embryonic stem (ES) cell clone IST12013D3 (*TIGM*) into C57Bl/6 blastocysts. After germ line transmission, heterozygous and knockout animals were genotyped by PCR using mouse tail DNA and Western blotting detecting different domains of CLP36.

3.2.2.3 Bone marrow mice generation

For the generation of bone marrow chimeras, 5-6 week-old *Wt* and *Clp36$^{\Delta LIM}$* mice were irradiated with a single dose of 10 Gy, and bone marrow cells from 3 week-old *Wt* and *Clp36$^{\Delta LIM}$* mice from the same litter were injected intravenously into the irradiated *Clp36$^{\Delta LIM}$* and *Wt* mice (4×10^6 cells/mouse) for crisscross transplantation experiments. Water supplemented with 2 g/L neomycin was provided to the mice for 2 weeks. Bone marrow chimerism was confirmed by Western blot of platelet lysates from the chimeric mice using the antibody against the LIM domain of CLP36.

3.2.3 Mouse Genotyping

3.2.3.1 Mouse DNA isolation

5 mm^2 of ear tissue was digested in 500 µL DNA digestion buffer at 56°C overnight under shaking conditions. Samples were mixed (1:1 vol) with Phenol/chloroform, then vortexed for 5 min and centrifuged at 14,000 rpm for 10 min. The upper aqueous phase containing the DNA was transferred to a fresh tube containing isopropanol (1:1 vol) and was mixed well. After centrifugation at 14,000 rpm for 10 min, the DNA pellet was washed twice with ice cold 70% ethanol. The DNA pellet was left to dry at 37°C and finally resuspended in 50 µL of H_2O.

3.2.3.2 *Trpc6*$^{-/-}$ mice PCR genotyping

Two separated reactions with different primer pairs were performed to amplify the wild-type (*Trpc6 Wt* For and *Trpc6 Wt* Rev) or the knockout allele (*Trpc6 KO* For and *Trpc6 KO* Rev). The mice were termed heterozygous if a PCR band was amplified in both of the reactions.

PCR primers:

***Trpc6 Wt* For:**	5´-atcatctctgaaggtctttatgc-3´
***Trpc6 Wt* Rev:**	5´-gaatgcttcattctgttttgcgcc-3´
***Trpc6 KO* For:**	5´-agactagtgagacgtgctacttcc-3´
***Trpc6 KO* Rev:**	5´-tttaatgtctgtatcactaaagcctcc-3´

PCR program:

Wild-type allele: 1) 96°C 3 min; 2) 94°C 30 s; 3) 51.5°C 30 s; 4) 72°C 1 min; 5) repeat step 2.-4. 30 cycles; 6) 72°C 10 min; 7) 4°C hold.

Knockout allele: 1) 96°C 3 min; 2) 94°C 30 s; 3) 55°C 30 s; 4) 72°C 1 min; 5) repeat step 2.-4. 30 cycles; 6) 72°C 10 min; 7) 4°C hold.

3.2.3.3 Genetrap PCR genotyping for *Clp36*$^{\Delta LIM}$ and *Clp36*$^{-/-}$ mice

Genetrap PCR was performed to differentiate the *Wt* from the heterozygous or homozygous mice. A band of 680 bp was amplified in genetrap PCR.

PCR primers:

Genetrap For:	5´-ttatcgatgagcgtggtggttatg-3´
Genetrap Rev:	5´-gcgcgtacatcgggcaaataatat-3´

PCR program:

1) 96°C 3 min; 2) 94°C 30 sec; 3) 51.4°C 30 sec; 4) 72°C 1 min; 5) repeat step 2.-4. 35 cycles; 6) 72°C 10 min; 7) 4°C hold

3.2.4 Immunoprecipitation and immunoblotting

3.2.4.1 Immunoprecipitation

For co-immunoprecipitation of proteins, washed platelets ($0.5x10^6$ platelets/µL) were prepared and were solubilized in an equal volume of IP buffer containing protease inhibitors and Igepal added to 1% f.c. Cell debris was removed by centrifugation (15,000x *g*, 10 min). Following pre-cleaning (1 h) with 10 µL of protein G-Sepharose, 10 µg antibody were added and allowed to incubate with protein lysates for 2 h at 4°C. Precipitation was carried out o/n at 4°C by addition of 25 µL protein G-Sepharose to the above incubated lysates. Samples were separated on SDS-PAGE (10%) along with a molecular weight marker and transferred onto a *polyvinylidene difluoride* (PVDF) membrane. Western blotting was performed as described below.

3.2.4.2 Immunoblotting

For Western blot analysis, *platelet rich plasma* (prp) was prepared and centrifuged at 2,800 rpm for 5 min. Platelets were washed twice in PBS containing 5 mM EDTA. The platelet pellet was resuspended in IP buffer containing protease inhibitors to a final concentration of $0.5x10^6$ platelets/µL and Igepal was added to 1% f.c. After incubation for 10 min at 4°C and centrifugation at 14,000 rpm for 5 min, the supernatant was mixed with an equal amount of 2x SDS sample buffer and incubated at 95°C for 5 min. Samples were separated by 10% SDS-PAGE and transferred onto a PVDF membrane. To prevent non-specific antibody binding, membranes were blocked in specific blocking buffer for 2 h at RT depending on the primary antibody. Membranes were incubated with the required primary antibody (5 µg/mL) o/n with gentle shaking at 4°C. Afterwards, membranes were washed three times with washing buffer for 15 min at RT. Next, membranes were incubated with appropriate HRP-labeled secondary antibodies for 1 h at RT. After three washing steps, proteins were visualized by ECL.

3.2.4.3 Tyrosine phosphorylation assay

For tyrosine phosphorylation studies, $0.7x10^6$ platelets/µL were activated with 5 µg/mL CRP, 0.1 µg/mL CRP and 0.01 U/mL thrombin under constant stirring conditions (1,000 rpm) at 37°C. Stimulation was stopped by the addition of an equal volume of ice-cold lysis buffer after the indicated time points. For whole-cell tyrosine-phosphorylation, 4x NuPage sample buffer (Invitrogen) was added. Samples were incubated at 70°C for 10 min and separated by SDS-

PAGE on 4-12% NuPage Bis-Tris gradient gels under reducing conditions followed by transfer onto a PVDF membrane. Membranes were blocked for 1 h at RT in 5% BSA in PBS and then incubated with the primary α-phosphotyrosine antibody 4G10 o/n at 4°C. The membranes were then washed 4x 15 min in washing buffer before incubation with secondary α-mouse horseradish peroxidase-conjugated antibody in washing buffer (1:2,000). Following extensive washing, proteins were visualized by ECL.

3.2.5 Blood cell analysis by FACS

100 µL blood was collected from the retro-orbital plexus in 300 µL heparin from 10 mice of each group and centrifuged at 2,800 rpm for 5 min to remove plasma. The cells were resuspended in 1.5 mL of ACK buffer for 2 min followed by centrifugation at 2,800 rpm for 5 min. Finally cells were suspended in 250 µL of FACS buffer. 100 µL of the samples were aliquoted twice in 96 well plates and volume was made up to 200 µL with ACK buffer. Cells were again centrifuged at 1,500 rpm for 3 min. The supernatant was discarded and 25 µL of 2.4G2 blocking antibody (10 µg/mL f.c.) was added to the cells. Further, in one of the sets, Gr1 (1:500) and CD11b antibody (1:200) were added to stain granulocytes and the other set of cells were stained against TcRβ, CD4, CD8 and B220 to stain T and B lymphocytes. The cells were incubated for 15 min with the antibody followed by addition of 100 µL of FACS buffer and centrifuged at 1,500 rpm for 3 min. The cell pellet was finally resuspended in 300 µL of FACS buffer. The samples were then transferred to FACS tubes and cells were measured on FACSCalibur instrument (Becton Dickinson, Heidelberg, Germany)

3.3 *In vitro* analysis of platelet function

3.3.1 Platelet preparation and washing

Mice were bled under isofluran anesthesia from the retroorbital plexus. 700 µL blood were collected in a reaction tube containing either 300 µL heparin in TBS (20 U/mL, pH 7.3) or 300 µL *acid citrate dextrose* (ACD). Blood was centrifuged at 1,800 rpm for 5 min at RT. Supernatant and buffy coat were transferred into a new tube and centrifuged at 800 rpm for 6 min at RT to obtain *platelet rich plasma* (prp). To prepare washed platelets, prp was centrifuged at 2,500 rpm for 5 min at RT and the pellet was resuspended in 1 ml Ca^{2+}-free Tyrode's buffer containing apyrase (0.02 U/mL) and PGI_2 (0.1 µg/mL). After 10 min incubation at 37°C the sample was centrifuged at 2,500 rpm for 5 min. After a second washing step, the platelet pellet was resuspended in the appropriate volume of Tyrode's buffer containing apyrase (0.02 U/mL, $0.5x10^6$ platelets/µL) and left to incubate for at least 30 min at 37°C before analysis.

3.3.2 Platelet counting

For determination of platelet count and size, 50 µL blood were drawn from the retroorbital plexus of anesthetized mice using heparinized microcapillaries and collected into a reaction tube containing 300 µL heparin in TBS (20 U/mL, pH 7.3). Platelet count and size were determined using a Sysmex KX-21N automated hematology analyzer (Sysmex Corp., Kobe, Japan).

3.3.3 Aggregometry

To determine platelet aggregation, light transmission was measured using washed platelets in Tyrode's buffer without Ca^{2+} adjusted to a concentration of $0.5x10^6$ platelets/µL. Alternatively, heparinized prp was used and diluted 1:3 in Tyrode's buffer. For determination of aggregation, agonists or reagents (100-fold concentrated) were added and light transmission was recorded over 10 min on a Fibrintimer 4 channel aggregometer (Apact 4-channel optical aggregation system, APACT, Hamburg, Germany). For calibration, Tyrode's buffer (for washed platelets) or 1:3-diluted plasma (for prp) was set as 100% aggregation and washed platelet suspension or prp was set as 0% aggregation. For activation with thrombin, washed platelets were diluted in Tyrode's buffer containing 2 mM Ca^{2+}, for all other agonists platelets were diluted in the same buffer in presence of 70 µg/mL human fibrinogen.

3.3.4 Measurement of *inositol 1 phosphate* (IP_1)

Washed platelets were adjusted to the final concentration of $0.6x10^6$/µL in a modified phosphate-free Tyrode-HEPES buffer containing 50 mM $LiCl_2$ and 2 mM Ca^{2+}. Indomethacin (10 µM) and apyrase (2 U/mL) were also added. Platelets were activated with the indicated agonists for 5 min at 37°C with constant shaking at 450 rpm. After stimulation, platelets were lysed in the buffer supplied with the kit. 50 µL of lysed platelets were used for the IP_1 ELISA assay according to the manufacturer's protocol (Cisbio, Cedex, France).

3.3.5 Flow cytometry

For determination of basal glycoprotein expression levels, washed platelets ($1x10^6$) were stained for 10 min at RT with saturating amounts of fluorophore-conjugated antibodies. The reaction was stopped by addition of 500 µL PBS, and samples were analyzed directly on a FACSCalibur instrument (Becton Dickinson, Heidelberg, Germany). For activation studies, platelets were activated with the indicated agonists or reagents for 15 min at RT in the presence of saturating amounts of *phycoerythrin* (PE)-coupled JON/A and *fluorescein isothiocyanate*

(FITC)-coupled α-P-selectin antibody. The reaction was stopped by addition of 500 µl PBS and samples were analyzed. For a two-color staining, the following settings were used:

Detectors/Amps:

Parameter	Detector	Voltage
P1	FSC	E01
P2	SSC	380
P3	Fl1	650
P4	Fl2	580
P5	Fl3	150

Threshold:

Value	Parameter
253	FSC-H
52	SSC-H
52	Fl1-H
52	Fl2-H
52	Fl3-H

Compensation:

Detector	Setting
Fl1	2.4% of Fl2
Fl2	7.0% of Fl1
Fl2	0% of Fl3
Fl3	0% of Fl2

3.3.6 Measurement of ATP release

ATP secretion was measured using CHRONO-LUME reagent according to the manufacturer's protocol on a Chronolog aggregometer (Chrono-Log Corp. Philadelphia, PA, USA). 5µL of luciferase reagent was directly added to the platelets ($0.5x10^6$ platelets/µL) under constant stirring and indicated concentrations of various agonists were added to study ATP release. The luminescence intensity was measured at a setting of ×0.01.

3.3.7 Adhesion under flow conditions

Rectangular coverslips (24 x 60 mm) were coated with 0.2 mg/mL fibrillar type I collagen (Horm, Nycomed) o/n at 37°C and blocked for 1 h with 1% BSA in H_2O. Blood (700 µL) was collected into 300 µL heparin (20 U/mL in TBS, pH 7.3) or ACD-buffer (for studies under non-anticoagulated conditions). Platelets were labeled with a Dylight-488 conjugated α-GPIX Ig derivative (0.2 µg/mL) for 5 min at 37°C. Whole blood was diluted 2:1 in Tyrode's buffer containing Ca^{2+} and filled into a 1 mL syringe. Transparent flow chambers with a slit depth of 50 µm, equipped with the coated coverslips, were connected to the syringe filled with diluted whole blood. Perfusion was performed using a pulse-free pump under high shear stress equivalent to a wall shear rate of 1,000 s^{-1} or 1,700 s^{-1} (for 4 min). Thereafter, coverslips were washed for 1 min by perfusion with Tyrode's buffer at the same shear stress and phase-contrast and fluorescent images were recorded from at least five different microscopic fields (40x objective). Image analysis was performed off-line using MetaVue® software. Thrombus formation was expressed as the mean percentage of total area covered by thrombi and as the mean integrated fluorescence intensity per mm^2.

3.3.8 Determination of phosphatidylserine exposing platelets after perfusion

Adhesion experiments under flow conditions (1000 s^{-1}) were performed with heparinised whole blood. Rectangular coverslips were coated with type I collagen (Nycomed) overnight at 37°C, rinsed with PBS and blocked with 1% bovine serum albumin (BSA). To prevent coagulation, chamber and tubing were prewashed extensively with HEPES buffer supplemented with heparin (5 U/mL). The blood was perfused through the flow chamber with 1 mL syringe and a pulse-free pump at a shear rate of 1700 s^{-1} for 4 min. The flow chamber was perfused with HEPES buffer containing heparin (5 U/mL), 1 mM $CaCl_2$ and 250 ng/mL of Annexin V- Dylight 488 for 4 min followed by washing with HEPES buffer for 2 min to remove unbound Annexin V-Dylight 488. Phase-contrast and fluorescent images were obtained from at least 10 different collagen-containing microscopic fields, which were randomly chosen (40X/0.75 NA objective; Carl Zeiss, Heidelberg, Germany). Image analysis was performed off-line using Metavue software (Visitron, Munich, Germany).

3.3.9 Determination of phosphatidylserine-exposing platelets by flowcytometry

The washed platelets were incubated with Annexin V-Dylight 488 after activation with different agonists for 15 min at 37°C and the percentage of fluorescently labeled platelets were detected by flow cytometry.

3.3.10 Intracellular calcium measurements

Platelets isolated from blood were washed and suspended in Tyrode's buffer without Ca^{2+}. The washed platelets were loaded with fura-2/AM (5 µM) in the presence of Pluronic F-127 (0.2 µg/mL; Molecular Probes) for 30 min at 37°C. After 30 min platelets were washed and resuspended in Tyrode's buffer containing no (for measurement of store release) or 1 mM Ca^{2+} (for measurement of influx). Stirred platelets were activated with different agonists, and fluorescence was measured with a PerkinElmer LS 55 fluorimeter (Waltham, MA). Excitation was alternated between 340 and 380 nm, and emission was measured at 509 nm. Each measurement was calibrated using Triton X-100 and EDTA.

3.3.11 Spreading assay

Platelets were isolated from blood and washed as described above. Washed platelets were resuspended in Tyrode's buffer and adjusted to a concentration of 0.2 x 10^6 platelets/µL. 60 µL of the platelet suspension was stimulated with 0.01 U/mL thrombin and immediately placed on coverslips (24 x 60 mm) that had been coated overnight with 100 µg/mL human fibrinogen (Sigma, Germany) and blocked for 1 h with 1% BSA (Sigma, Germany). Coverslips were mounted on an inverted microscope Zeiss HBO 100 (Zeiss, Germany). Time-lapse images were recorded (every 5 seconds for 20 min) with a 40x objective and analyzed using MetaVue® software. Starting points and percentages of adhered and completely spread platelets were considered as indicators of platelet adhesion and spreading dynamics.

3.3.12 Immunofluorescence microscopy of platelets

Washed platelets were allowed to spread on fibrinogen after thrombin (0.01 U/mL) stimulation and were fixed in PHEM complete buffer for 20 min at 4°C, blocked with 5% BSA and 1% goat serum for 2 h at 37°C. Spread platelets were stained with rabbit anti-CLP36 antibody (ab64971, Abcam, Cambridge, UK) for 2 h followed by 4x washing with PBS and incubation of 1 h with secondary Alexa 488- labeled anti-rabbit antibody (Invitrogen) and phalloidin-Atto647N (Sigma-Aldrich, Deisenhofen, Germany). Then, samples were washed again with PBS, mounted using Vectashield mounting medium and finally left to dry o/n at 4°C. Samples were visualised on a Leica SP5 confocal microscope with a 100x oil objective (Leica Microsystem GmH, Wetzlar, Germany). Images were further processed using Image J software (National Institute of Health, USA)

3.3.13 Determination of platelet filamentous (F)-actin content

Washed platelets were prepared and the platelet count was adjusted to approximately $0.2x10^6$ platelets/µL in Tyrode's buffer without Ca^{2+}. Platelets were diluted 1:10 in Tyrode's buffer in a final volume of 50 µL per sample and incubated for 3 min at 37°C after addition of 5 µL Dylight 649-conjugated anti-GPIX Ig derivatives. Then, platelets were stimulated with different agonists for 2 min at 37°C (400 rpm) and fixed for 10 min by addition of 0.55% volume 10% PFA in PBS. Samples were finally centrifuged for 5 min at 2,500 rpm, the pellet was resuspended in 55 µL Tyrode's buffer containing 0.1 volume-percentage Triton-X 100 and phalloidin-FITC at a final concentration of 10 µM. Samples were incubated for 30 min at RT in the dark and the reaction was stopped by addition of 500 µL PBS. After centrifugation for 5 min at 2,500 rpm the supernatant was discarded and the pellet was resuspended again in 500 µL PBS. Samples were immediately analyzed on a FACSCalibur.

3.4 *In vivo* analysis of platelet function

3.4.1 Platelet life span

Circulating platelets were labeled *in vivo* by i.v. injection in the retro-orbital plexus of 5 µg Dylight-488-anti-GPIX Ig derivative in 200 µL PBS. 30 min after antibody injection (and every 24 hours for 5 days) 50 µL blood was taken from the retro-orbital plexus of the treated mice and as the percentage of the whole PE-Cy5 positive population was determined by flow cytometry.

3.4.2 Tail bleeding time assay

Mice were anesthetized by intraperitoneal injection of the substances dormitor, dormicum and fentanyl, and a 1 mm segment of the tail tip was ablated with a scalpel. Tail bleeding was monitored by gently absorbing the drop of blood with a filter paper in 20 s intervals without interfering with the wound site. When no blood was observed on the paper, bleeding was determined to have ceased. The experiment was manually stopped after 20 min by cauterization.

Alternatively, tail bleeding times were determined in 37°C warm saline (0.9% NaCl). Upon amputation, the tail was placed in a plastic tube containing 4 mL saline, bleeding was observed and determined to have ceased when stopped for >1 min. Lost blood volume was determined via weight against a saline filled reference tube and increased weight of the tube was multiplied by the density of blood.

3.4.3 Intravital microscopy of thrombus formation in $FeCl_3$-injured mesenteric arterioles

3- to 4-week old mice were anesthetized i.p. with ketamine/xylazine (100/5 mg/kg; Parke-Davis, Berlin, Germany and Bayer, Leverkusen, Germany) and the mesentery was exteriorized through a midline abdominal incision. Endothelial damage was induced by application of a 3 mm^2 filter paper saturated with 20% $FeCl_3$. Arterioles were visualized using a Zeiss Axiovert 200 inverted microscope equipped with a 100-W HBO fluorescent lamp source and a CoolSNAP-EZ camera (Visitron). Digital images were recorded and analyzed using the Metavue software. Adhesion and aggregation of fluorescently labeled platelets (Dylight-488 conjugated anti-GPIX antibody derivative) in arterioles was monitored for 40 min or until complete occlusion occurred (blood flow stopped for >1 min).

3.4.4 Intravital microscopy of thrombus formation in the abdominal aorta

Mice were anesthetized i.p. with ketamine/xylazine (100:5 mg/kg; Parke-Davis, Berlin, Germany and Bayer, Leverkusen, Germany). A longitudinal incision was used to open the abdominal cavity of the anesthetized mice and abdominal aorta was exposed. An ultrasonic flow probe was placed around the vessel and thrombus formation was induced by a single firm compression with a forceps. Blood flow was monitored until complete occlusion of vessel; or experiments were stopped manually after an observation period of 30 min.

3.4.5 Intravital microscopy of thrombus formation in $FeCl_3$-injured carotid artery

Mice were anesthetized i.p. with ketamine/xylazine (100:5 mg/kg; Parke-Davis, Berlin, Germany and Bayer, Leverkusen, Germany) and the right carotid artery was exposed through a vertical midline incision in the neck. An ultrasonic flow probe (0.5PSB699 Transonic System, Ithaca, NY) was placed around the vessel and thrombosis was induced by topical application of a 0.5 mm by 1 mm filter paper saturated with 10% $FeCl_3$ for 2 min and 30 s. Blood flow was monitored with an ultrasonic flow probe until full occlusion of the vessel occurred for 30 min. All the above mentioned thrombosis models were performed by Martina Morowski or Ina Thielmann in the group of Prof. Bernhard Nieswandt.

3.4.6 *Transient middle cerebral artery occlusion* (tMCAO) model

Experiments were conducted on 6-to 8-week old male mice according to published recommendations for research in mechanism-driven basic stroke studies.[119] Transient middle cerebral artery occlusion (tMCAO) was induced under inhalation anesthesia using the intraluminal filament (6021PK10; Doccol Company) technique.[36] After 60 min, the filament was

withdrawn to allow reperfusion. For measurements of ischemic brain (infarct) volume, animals were sacrificed 24 h after induction of tMCAO and brain sections were stained with 2% 2,3,5-triphenyltetrazolium chloride (TTC; Sigma-Aldrich, Germany). Brain infarct volumes were calculated and corrected for oedema as described.[36] Neurological function and motor function were assessed 24 h after tMCAO. This work was performed by and in collaboration with Dr. Peter Kraft in the group of Prof. Guido Stoll, Department of Neurology, University Hospital, Würzburg.

3.5 Data analysis

The results presented in this thesis are mean ± SD from at least three independent experiments per group, if not otherwise stated. Differences between the groups were statistically analyzed using the Mann-Whitney-U-test. *P*-values <0.05 were considered as statistically significant (*), *P* <0.01 = (**) and *P* <0.001 was taken as the level of highest significance (***).

4 RESULTS

4.1 Diacylglycerol-induced Ca^{2+} entry by TRPC6 is dispensable for murine platelet function

To investigate the role of canonical transient receptor potential channel 6 (TRPC6) in platelet physiology, TRPC6 deficient mice[71] kindly provided by Dr. Alexander Dietrich (Ludwig-Maximilians University, Munich, Germany) were analyzed. TRPC6 deficient mice were referred as *Trpc6*$^{-/-}$ and their littermate wildtype (referred as *Wt*) served as control animals. This part of the study was conducted together with Gajalakshmi Ramanathan (Medical University of Vienna, Austria).

4.1.1 Protein and mRNA expression of TRPC family members in *Trpc6*$^{-/-}$ platelets

Western blot analysis of *Wt* platelets showed a strong band at the expected protein size of TRPC6 of about 110 kDa, while the protein was absent in *Trpc6*$^{-/-}$ platelets (Figure 6A). Since an upregulation of *Trpc3* mRNA has been observed in the vascular smooth muscle cells of thoracic aortas and cerebral arteries of *Trpc6*$^{-/-}$ mice,[71] the mRNA expression of other TRPC family members known to be expressed in mouse platelets was analyzed using RT-PCR.[120] Interestingly, only *Trpc1* mRNA was detected in *Wt* and *Trpc6*$^{-/-}$ murine platelets, whereas other *Trpc* mRNAs isoforms, including *Trpc3* were absent (Figure 6B). These results indicated that the lack of TRPC6 cannot be compensated by other TRPC isoforms in murine platelets.

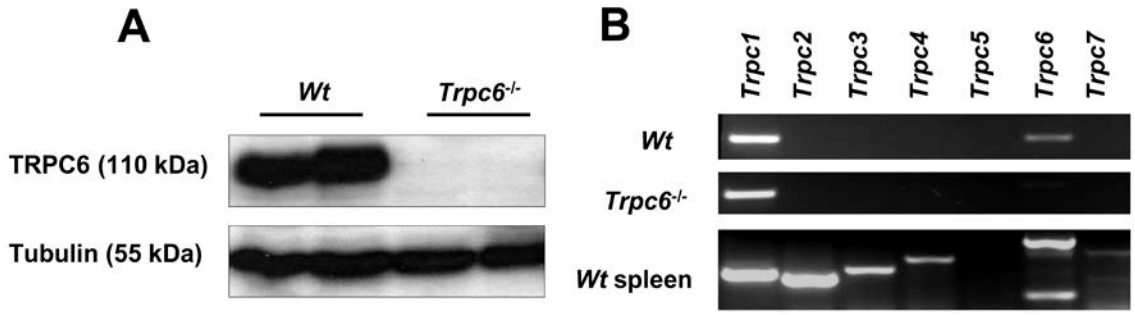

Figure 6: Western Blot analysis and mRNA expression profile of the TRPC family members of *Trpc6*$^{-/-}$ platelets. (A) Western blot analysis of *Wt* platelets shows the TRPC6 protein migrating at 110 kDa whereas no TRPC6 protein was detected in *Trpc6*$^{-/-}$ platelets. Tubulin (55 kDa) was used as loading control. (B) mRNA was isolated from *Wt* and *Trpc6*$^{-/-}$ platelets and RT-PCR was performed. mRNA isolated from spleen cells served as control.

4.1.2 TRPC6 is the major diacylglycerol activated Ca^{2+} channel in murine platelets

TRPC6 and its closest relative, TRPC3, have been shown to be receptor operated calcium (ROC) channels activated by the secondary messenger diacylglycerol (DAG). PLC activation in response to platelet activation leads to hydrolysis of PIP_2 to DAG and IP_3.[121] To determine the contribution of TRPC6 function in DAG-activated ROCE, *Wt* and *Trpc6*$^{-/-}$ platelets were stimulated with the 150 µM of membrane permeable DAG analogue, *1-oleoyl-2-acetyl-sn-glycerol* (OAG) and the change in *intracellular Ca*$^{2+}$ $[Ca^{2+}]_i$ was measured. *Wt* platelets exhibited a transient increase in $[Ca^{2+}]_i$ with a maximal change of 65 ± 7.6 nM in $[Ca^{2+}]_i$. In sharp contrast, virtually no Ca^{2+} influx was observed in *Trpc6*$^{-/-}$ platelets (Figure 7A). These findings established TRPC6 as the major DAG activated Ca^{2+} channel in murine platelets. Apart from that, studies performed by Bousquet *et al*. have shown that PKC mediated phosphorylation of TRPC6 regulates channel activity.[63] To study whether PKC phosphorylation regulates TRPC6 mediated Ca^{2+} influx, platelets were activated with 150 µM OAG in presence of protein kinase C (PKC) inhibitor, Gö6983 (300 nM). Interestingly, in presence of Gö6983, Ca^{2+} influx was further elevated in *Wt* platelets whereas, *Trpc6*$^{-/-}$ platelets did not display any effect on OAG-induced Ca^{2+} entry in (92 ± 9.4 nM for *Wt* and 18.5 ± 3.7 nM for *Trpc6*$^{-/-}$; $P < 0.001$, Figure 7B). These results revealed that PKC regulates TRPC6 activity in platelets.

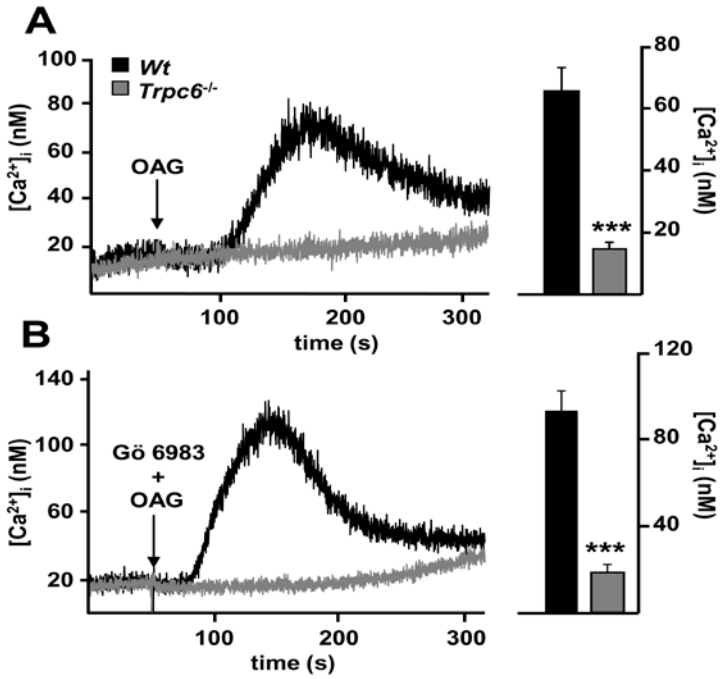

Figure 7: Abolished DAG activated ROCE in *Trpc6*$^{-/-}$ platelets. (A) DAG activated ROCE was measured in fura-2 loaded platelets using the DAG analogue, OAG (150 µM), in the presence of 1 mM $CaCl_2$. Statistical analysis of Ca^{2+} concentration upon stimulation with OAG. (B) DAG mediated ROCE was measured in fura-2 loaded platelets using OAG (150 µM) in the presence of the PKC inhibitor Gö6983 (300 nM) and 1 mM $CaCl_2$. Platelets were incubated with the inhibitor for 50 s followed by stimulation with OAG. ** $P<0.01$; *** $P<0.001$ as compared to *Wt* values.

4.1.3 TRPC6 is dispensable for store operated calcium entry and agonist induced Ca^{2+} mobilization in platelets

Earlier studies on human platelets have indicated a regulatory role of TRPC6 in the activation of SOCE[122] via functional coupling of the Ca^{2+} channel to the IP_3 receptor[123] and to the STIM1-Orai1 complex.[124] To investigate the role of TRPC6 in regulation of SOCE, *Wt* and *Trpc6*$^{-/-}$ platelets were incubated with *SR/ER* Ca^{2+} *ATPase* (SERCA) inhibitor *thapsigargin* (TG) for 5 min followed by addition of Ca^{2+} to extracellular medium. Store release and resulting SOCE were found to be comparable in *Wt* and *Trpc6*$^{-/-}$ platelets ($\Delta[Ca^{2+}]_i$ 868 ± 123 nM for *Wt* and 814 ± 127 nM for *Trpc6*$^{-/-}$; *P*=0.95, Figure 8), thus confirming that TRPC6 is dispensable for regulation of SOCE in murine platelets.

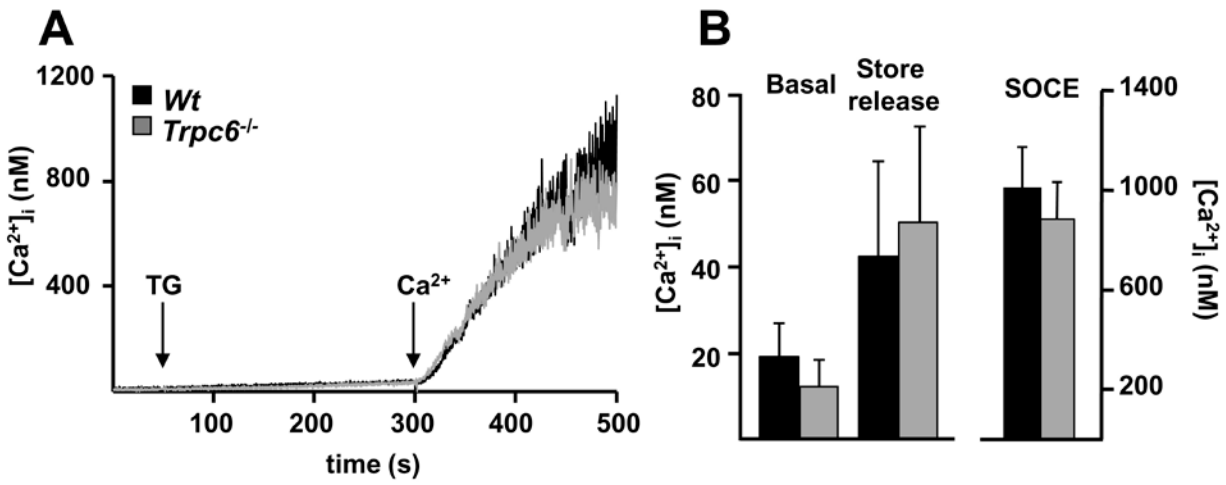

Figure 8: Normal SOCE in *Trpc6*$^{-/-}$ platelets. (A) SOCE was measured by incubating platelets with thapsigargin (TG) (5 µM) for 5 min followed by the addition of $CaCl_2$ (1 mM). (B) Statistical analysis of Ca^{2+} concentrations before TG addition, after TG mediated store depletion and SOCE upon addition of Ca^{2+} for *Wt* and *Trpc6*$^{-/-}$ mice.

Furthermore, to investigate the impact of deficiency of TRPC6 on agonist induced Ca^{2+} mobilization in platelets, $[Ca^{2+}]_i$ was measured in response to different agonists, like thrombin, ADP, CRP and the TxA_2 analogue U46619 in combination with ADP. Unexpectedly, *Trpc6*$^{-/-}$ platelets displayed normal Ca^{2+} influx indicating that loss of TRPC6 mediated ROCE could be compensated by other ROC channels or by SOCE (Figure 9A). Apart from that, Ca^{2+} release from the intracellular stores, measured in absence of Ca^{2+}, was also comparable between *Trpc6*$^{-/-}$ and *Wt* platelets (Figure 9B).

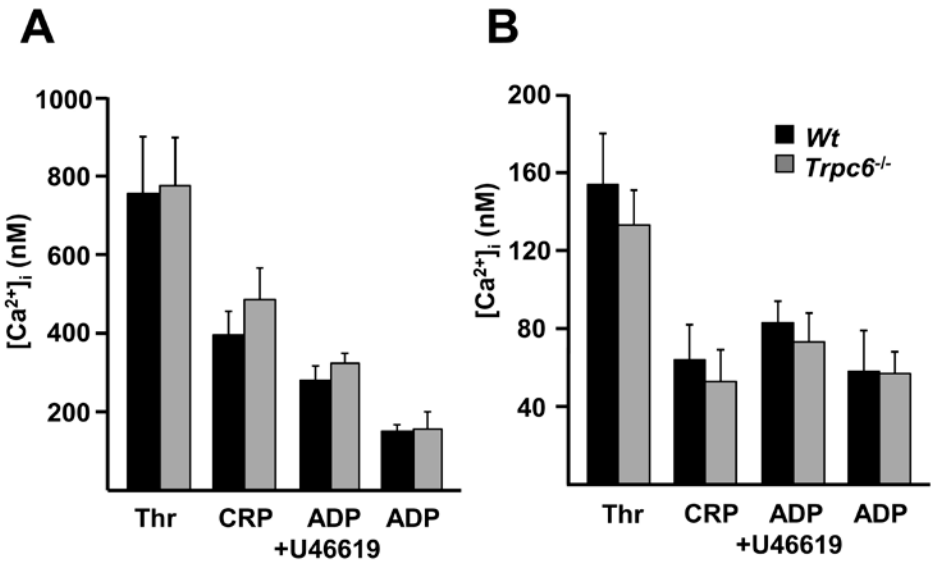

Figure 9: Normal calcium influx and store release in *Trpc6*$^{-/-}$ platelets. (A) Calcium influx measured upon stimulation with thrombin (0.1 U/mL), CRP (10 µg/mL), ADP (10 µM) and U46619 (3 µM) in the presence of extracellular Ca^{2+} (1 mM). (B) Calcium store release measured upon stimulation with the above agonists in calcium free buffer. The maximal change in $[Ca^{2+}]_i$ (mean ± SD, *n* = 4-6) of *Wt* and *Trpc6*$^{-/-}$ platelets are shown.

4.1.4 *Trpc6*$^{-/-}$ mice display a normal platelet life span

Mouse platelets exhibit a life span of approximately 5 days in the circulation which is internally controlled by the balance of their apoptotic machinery at steady state.[125,126] Activation of ion channels has been implicated in the regulation of platelet life span and apoptosis;[127] therefore the platelet life span in *Trpc6*$^{-/-}$ and *Wt* mice was analyzed *in vivo*. Circulating platelets were labeled with a fluorescent non-toxic anti-GPIX antibody derivative, injected i.v. and the percentage of labeled platelet population was monitored by flow cytometry over time. One hour after antibody treatment, >90% of circulating platelets were labeled in mice and this platelet population constantly declined over 5 days in both *Wt* and *Trpc6*$^{-/-}$ mice (Figure 10A). Additionally, platelet counts, platelet size and expression of major surface glycoproteins in *Trpc6*$^{-/-}$ platelets were also comparable to *Wt* (Figure 10B, C and D). These findings demonstrated that TRPC6 is dispensable for platelet production and for the regulation of platelet turnover *in vivo*.

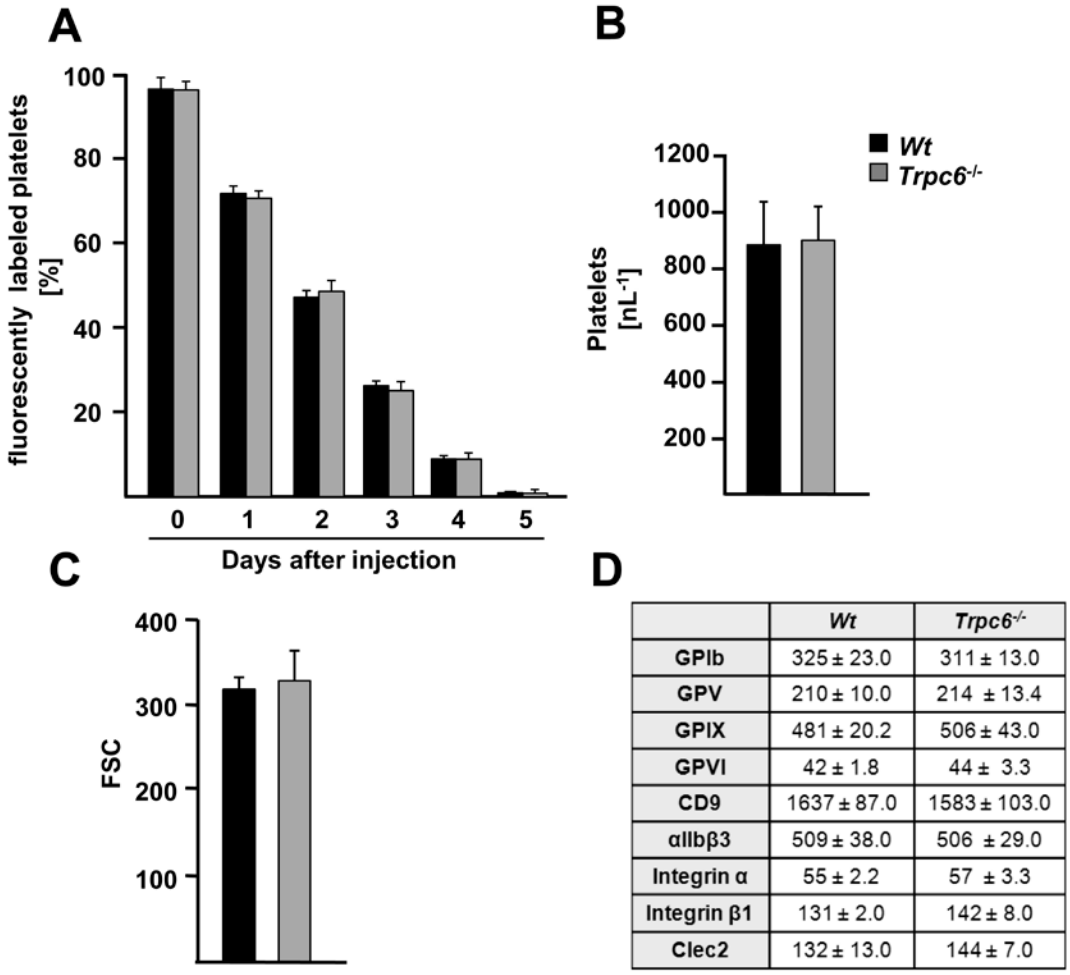

	Wt	*Trpc6*$^{-/-}$
GPIb	325 ± 23.0	311 ± 13.0
GPV	210 ± 10.0	214 ± 13.4
GPIX	481 ± 20.2	506 ± 43.0
GPVI	42 ± 1.8	44 ± 3.3
CD9	1637 ± 87.0	1583 ± 103.0
αIIbβ3	509 ± 38.0	506 ± 29.0
Integrin α	55 ± 2.2	57 ± 3.3
Integrin β1	131 ± 2.0	142 ± 8.0
Clec2	132 ± 13.0	144 ± 7.0

Figure 10: Unaltered platelet life span and platelet membrane glycoprotein expression in *Trpc6*$^{-/-}$ platelets. (A) Platelet life span was determined as the percentage of fluorescently labeled platelets in *Wt* and *Trpc6*$^{-/-}$ mice over a 5 day period after i.v. injection of a Dylight-488 anti-GPIX antibody derivative (0.5 mg/kg). (B and C) Platelet count (x10^3)/µL and size expressed as forward scatter (FSC) signal in flow cytometry of *Wt* and *Trpc6*$^{-/-}$ mice. (D) Diluted whole blood was incubated with saturating concentrations of FITC-labeled antibodies of the indicated specificity for 15 min and analyzed by flow cytometry. Results are shown as mean fluorescence intensity (MFI) ± SD of 4-6 mice per group.

4.1.5 Normal agonist-induced integrin activation and granule release in *Trpc6*$^{-/-}$ platelets

To study the effect of the TRPC6-deficiency on platelet activation, agonist–induced activation of the major platelet integrin αIIbβ3 and degranulation-dependent P-selectin exposure were analyzed by flow cytometry. In this experimental setting, the use of highly diluted platelet suspension excludes the accumulation of released secondary messengers and thus allows conclusions about the primary platelet signaling response. *Trpc6*$^{-/-}$ platelets displayed integrin activation and degranulation similar to that of *Wt* controls in response to all tested agonists at different concentrations (Figure 11).

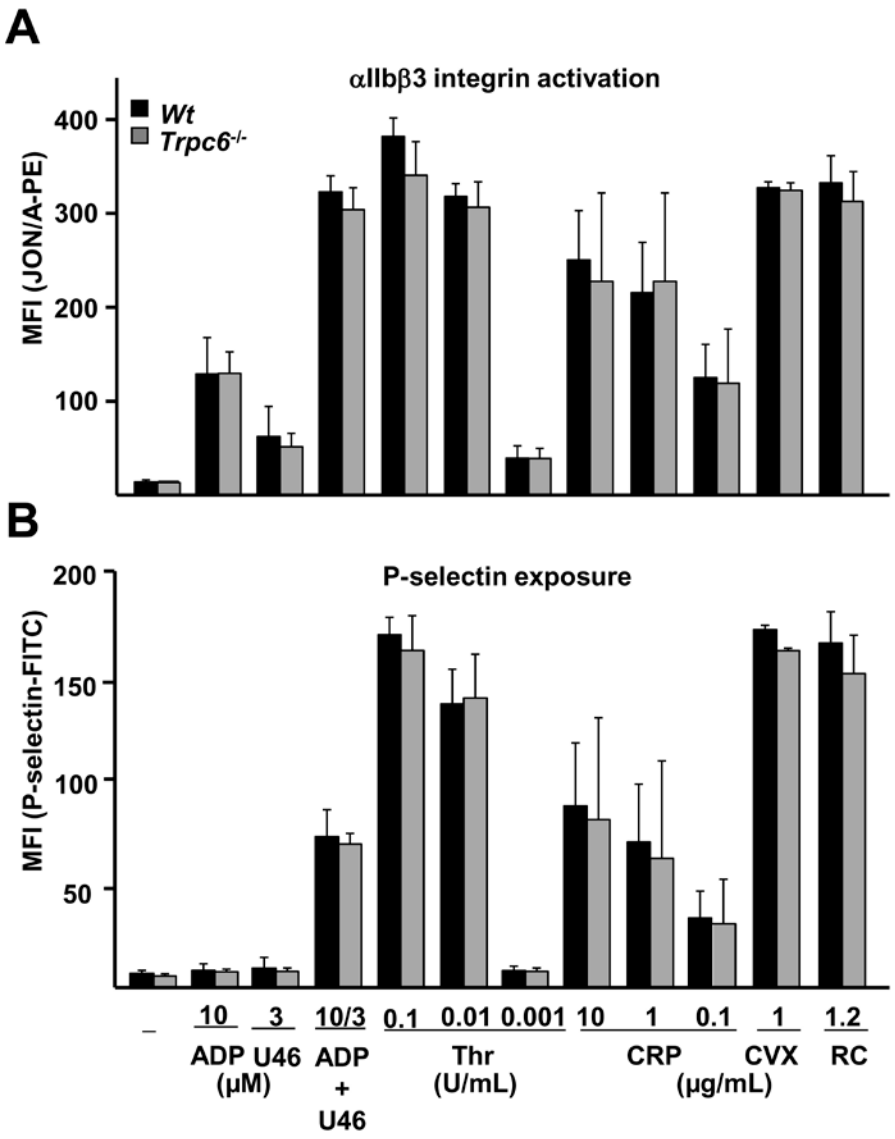

Figure 11: Agonist-induced integrin activation and degranulation of *Trpc6*$^{-/-}$ mice. (A, B) Flow cytometric analysis of integrin αIIbβ3 activation and P-selectin exposure in *Wt* and *Trpc6*$^{-/-}$ platelets (*n*=4). Diluted whole blood was incubated with saturating concentrations of FITC-labeled antibodies for 15 min after stimulation with indicated agonists and analyzed by flow cytometry for integrin activation and degranulation.

Apart from DAG mediated ROCE by TRPC6, DAG also activates PKC resulting in granule secretion and platelet activation. To test whether TRPC6 influences PKC mediated signaling, *phorbol-12-myristate-13-acetate* (PMA) was used to activate PKC.[121] At both higher and lower doses of PMA, integrin αIIbβ3 activation and P-selectin exposure were comparable between *Wt* and *Trpc6*$^{-/-}$ platelets (Figure 12).

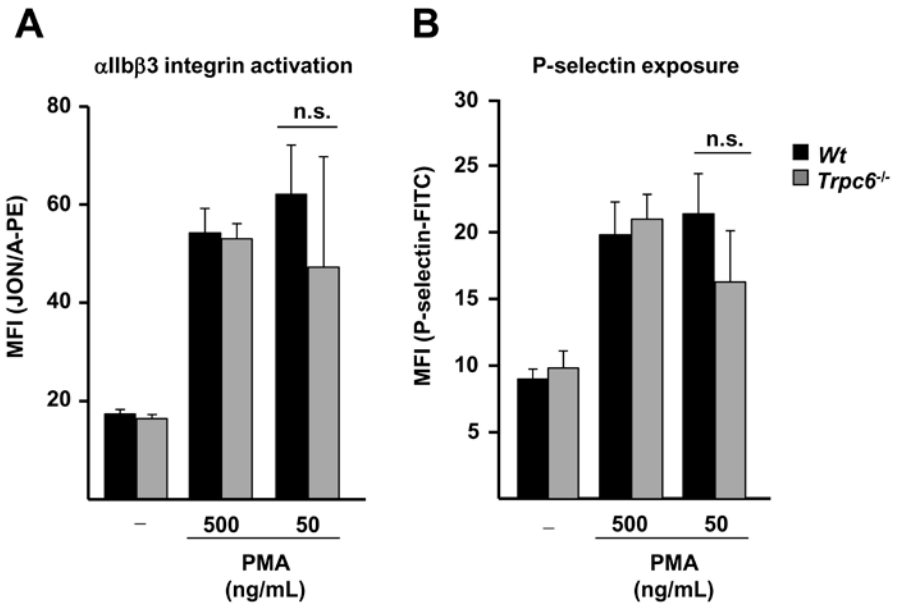

Figure 12: Normal PKC mediated platelet activation in *Trpc6*$^{-/-}$ mice. Washed platelets were activated by different concentrations of PMA to induce PKC mediated platelet activation. (A) Integrin activation and (B) degranulation was measured using flow cytometry. Results are shown as mean fluorescence intensity (MFI) ± SD of *Wt* and *Trpc6*$^{-/-}$mice of 4 mice per group.

Platelet aggregation requires both inside-out and outside-in signaling of integrins which is strengthened by secondary mediators and strongly dependent on increased intracellular Ca^{2+} concentrations. To study the role of TRPC6 in this process, standard aggregometry was performed. The loss of DAG dependent Ca^{2+} entry mediated by TRPC6 did not interfere with platelet aggregation responses to different agonists at all tested concentrations (Figure 13).

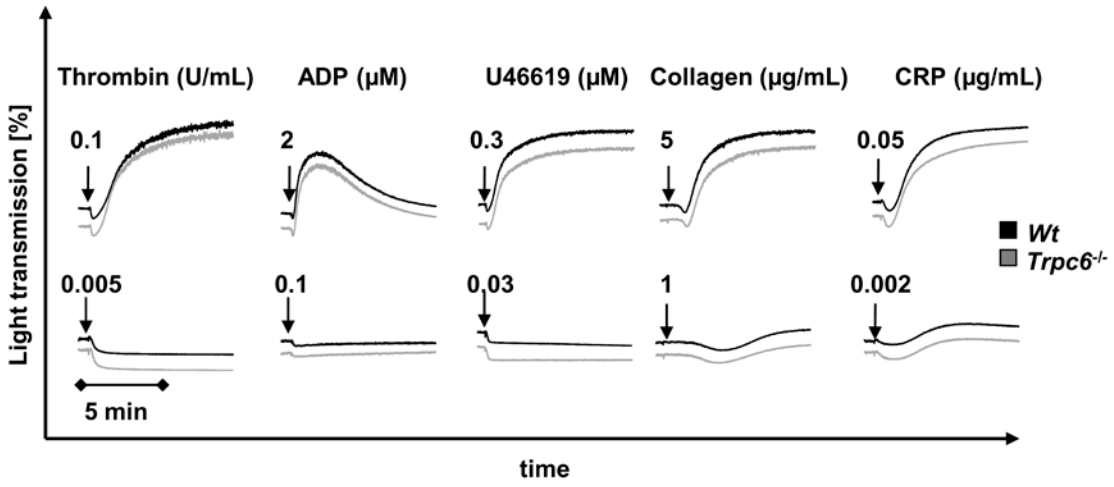

Figure 13: Unaltered aggregation of *Trpc6*$^{-/-}$ platelets. Aggregation curves of *Wt* and *Trpc6*$^{-/-}$platelets in response to the indicated agonist concentrations over a time span of 10 min. (Representative curves of 4 independent measurements).

4.1.6 *Trpc6*$^{-/-}$ platelets display normal spreading on fibrinogen

Another process requiring Ca^{2+} dependent outside-in signaling of integrins is spreading of platelets on extracellular matrix proteins. To investigate the role of TRPC6 in this process, *Wt* and *Trpc6*$^{-/-}$ platelets were allowed to spread on a fibrinogen coated surface in presence of thrombin (0.01 U/mL). Interestingly, *Trpc6*$^{-/-}$ platelets were able to form filopodia and lamellipodia to the same extent and with similar kinetics as *Wt* platelets (Figure 14). Both groups of platelets could spread fully within 20 min and overall morphological structure of spread *Trpc6*$^{-/-}$ platelets appeared similar to *Wt* platelets. These results showed that Ca^{2+} influx through TRPC6 does not play a crucial role for outside-in integrin signaling and for the reorganization of the actin cytoskeleton.

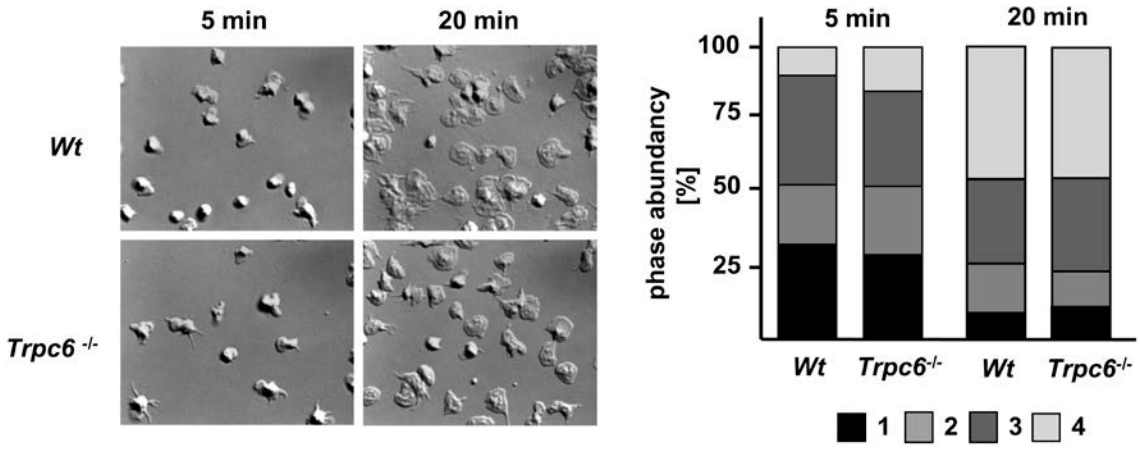

Figure 14: *Trpc6*$^{-/-}$ platelets display normal spreading on fibrinogen. Washed platelets of *Wt* and *Trpc6*$^{-/-}$ mice were stimulated with 0.01 U/mL thrombin and allowed to spread on fibrinogen (200 µg/mL). Representative differential interference contrast (DIC) images of 3 individual experiments from the indicated time points (left) and statistical evaluation of the percentage of platelets at different stages of spreading (right). 1: roundish, 2: only filopodia, 3: filopodia and lamellipodia, 4: fully spread.

4.1.7 Unaltered thrombus formation under flow and procoagulant activity of *Trpc6*$^{-/-}$ platelets

The experiments described above showed normal platelet activation responses and aggregation *in vitro* despite the loss of DAG mediated ROCE. Under high shear flow conditions in blood vessels, modest differences in Ca^{2+} homeostasis could, however, become a limiting factor, as agonist concentrations can drop rapidly by dilution and weak platelet interactions can result in reduced thrombus stability. Therefore, the ability of *Trpc6*$^{-/-}$ platelets to form platelet aggregates on a collagen-coated surface was analyzed in a whole blood perfusion system. At a shear rate of 1000 s^{-1}, mimicking flow conditions in large arteries, *Wt* and *Trpc6*$^{-/-}$ platelets formed large and stable three-dimensional aggregates that covered similar surface areas at the end of perfusion

time (53.2 ± 5.6% for *Wt* platelets and 48.3 ± 6.0% *Trpc6*$^{-/-}$ platelets; *P*=0.77). The relative thrombus volume was also similar between the two groups. These finding indicated that TRPC6 does not play an essential role in thrombus formation under flow conditions (Figure 15A).

Impaired agonist-induced Ca^{2+} responses may influence *phosphatidylserine* (PS) exposure and interfere with platelet-dependent coagulation. To address the role of TRPC6 in maintaining procoagulant activity in murine platelets, PS exposure was analyzed in *Trpc6*$^{-/-}$ platelets by Annexin V-Dylight488 binding to PS exposed surfaces on platelets upon agonist stimulation. Percentages of annexin V positive platelets were found to be similar in *Wt* and *Trpc6*$^{-/-}$ platelets, indicating that the Ca^{2+} influx through TRPC6 is not essential for procoagulant responses (Figure 15B).

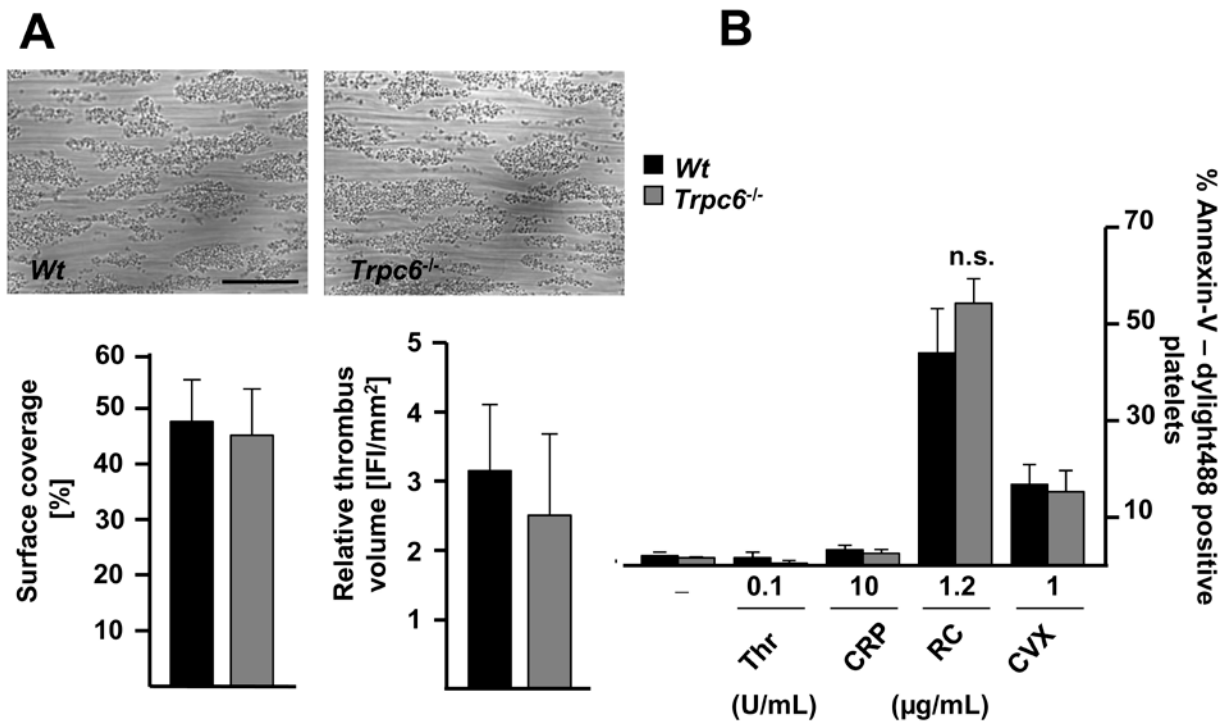

Figure 15: Flow adhesion assay and procoagulant activity of *Trpc6*$^{-/-}$ mice. (A) *Trpc6*$^{-/-}$ platelets form stable thrombi on a collagen-coated surface (0.2 mg/ml) in whole blood perfusion assay at a shear rate of 1000 s^{-1} over a run time of 4 min. Representative phase contrast images and statistical mean surface coverage and relative thrombus volume (A, lower panel) are shown (*n*=8) for *Wt* and *Trpc6*$^{-/-}$ mice. (B) procoagulant activity was analyzed using Annexin V-Dylight 488 binding to negatively charged PS. Platelets were activated with 0.1 U/mL thrombin, 10 µg/mL CRP, 1 µg/mL CVX or 1.2 µg/mL of RC and percentage of Annexin V-Dylight 488 positive platelets were analyzed by FACS.

4.1.8 Normal arterial thrombus formation and primary hemostasis in *Trpc6*$^{-/-}$ mice

To study *in vivo* thrombus formation, arterial thrombosis was induced using three different models. These experiments were done together with Ina Thielmann from our laboratories. In the first experiment, mechanical injury was induced on the abdominal aorta by a firm compression

followed by monitoring the blood flow with an ultrasonic flow probe for up to 30 min. Under these conditions, *Wt* as well as *Trpc6*$^{-/-}$ mice formed irreversible occlusive thrombi within the observation period (mean occlusion time of 217 ± 73 s (*Wt*) and 153 ± 4 s (*Trpc6*$^{-/-}$), *P*=0.95; Figure 16A).

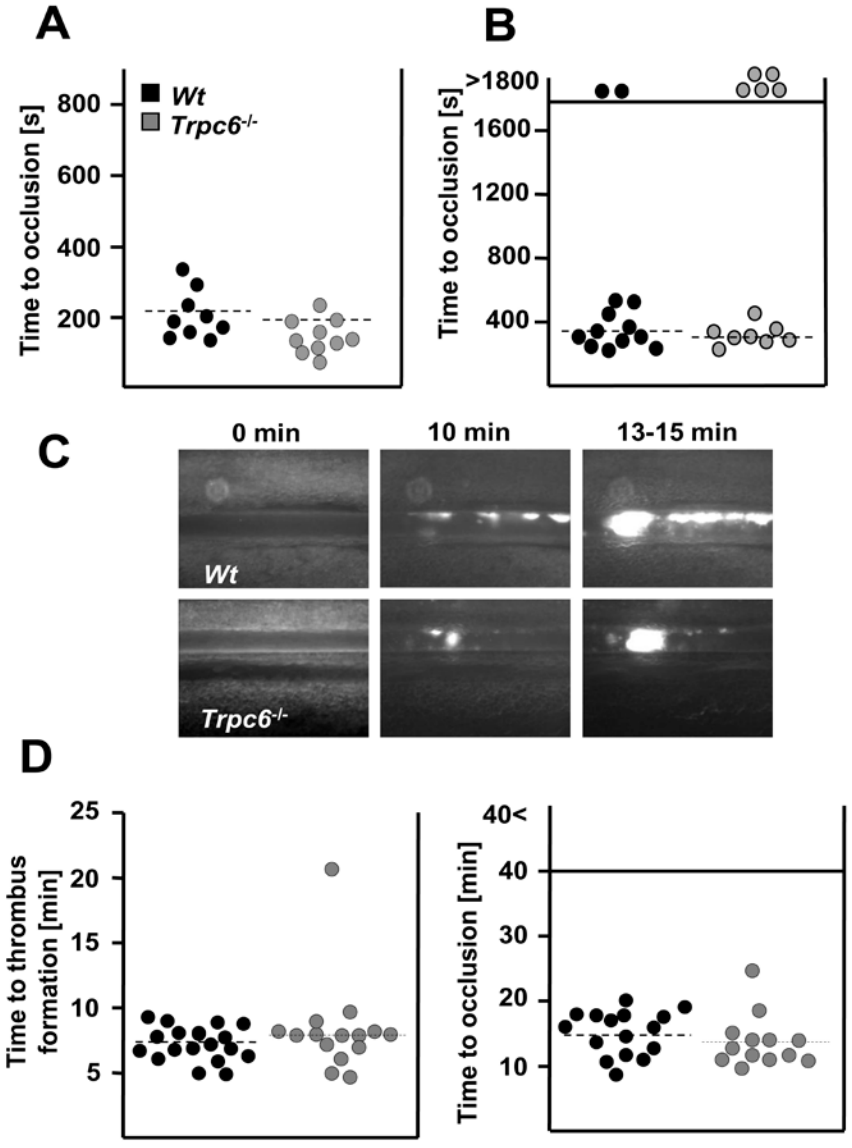

Figure 16: *Trpc6*$^{-/-}$ mice display normal thrombosis. (A) Vessel occlusion times for *Wt* and *Trpc6*$^{-/-}$ mice after mechanical injury of the abdominal aorta. (B) Thrombus formation in $FeCl_3$-injured carotid artery as monitored by ultrasonic flow probe. (C and D) Thrombus formation in $FeCl_3$-injured mesenteric arterioles was monitored for adhesion and thrombus formation of fluorescently labeled platelets by intravital microscopy. Representative images and time to complete vessel occlusion are shown. Each symbol represents one individual.

In a second set of experiments, the carotid artery injury model was used. Chemical injury was induced by application of 10 % *ferric-chloride* ($FeCl_3$) and the time to occlusion was monitored using an ultrasonic flow probe. In this injury model, 11 out of 13 *Wt* mice could form occlusive

thrombi in comparison to 8 out of 13 *Trpc6*$^{-/-}$ mice within the observation period of 30 min (mean occlusion time of 370.62 ± 111.7 s for *Wt* and 342.72 ± 67.55 s for *Trpc6*$^{-/-}$ mice; *P*=0.87; Figure 16B). Furthermore, *in vivo* thrombus formation was also analyzed in $FeCl_3$ injured mesenteric arterioles using intravital fluorescence microscopy. The kinetics of initial adhesion and accumulation of fluorescently labeled platelets over time was found to be comparable in *Wt* and *Trpc6*$^{-/-}$ animals and also the mean time to complete vessel occlusion was also similar between the two groups (15.7 ± 3.5 vs 14.2 ± 4.0 min, respectively; Figure 16C and D).

To determine the hemostatic function of *Trpc6*$^{-/-}$ platelets, tail bleeding assay was performed. 1 mm of the mouse tail tip was amputated and the tails were immediately immersed into saline at 37°C and the bleeding time was defined as time until cessation of blood flow (Figure 17). No significant hemostatic defect was observed in *Trpc6*$^{-/-}$ mice (mean tail bleeding time of *Trpc6*$^{-/-}$ was 218 ± 315 s (n=14), *Wt* was 114 ± 168 s (n=14); *P=0.16*).

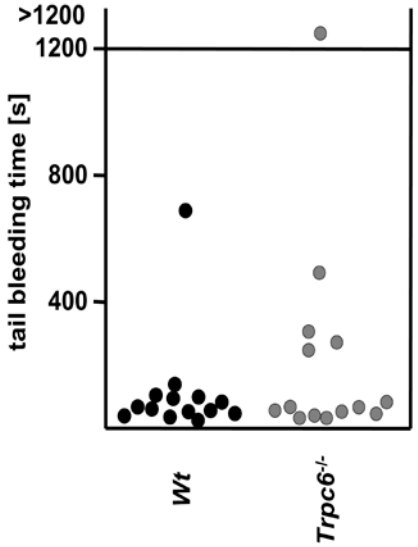

Figure 17: *Trpc6*$^{-/-}$ mice display normal hemostasis. Tail bleeding times of *Wt* and *Trpc6*$^{-/-}$ mice were analyzed by cutting a 1 mm of tail tip and immersion in saline at 37°C. Each symbol represents one individual.

Together, these results demonstrated that the absence of TRPC6-mediated Ca^{2+} signaling in platelets has no major effect on primary hemostasis and arterial thrombus formation in mice.

4.2 The PDLIM domain family member CLP36 is a crucial mediator of platelet activation in hemostasis and thrombosis

To study the role of CLP36 and its different domains in platelets, a genetrap approach was used.

- Mice carrying the intronic genetrap insertion in the *Clp36* gene after exon 5 were referred to as *Clp36*$^{\Delta LIM}$. These mice expressed truncated CLP36 protein where the C-terminal LIM domain was replaced by the β-Geomycin cassette. *Clp36*$^{\Delta LIM}$ mice expressed the chimeric CLP36 protein termed as CLP36$^{\Delta LIM}$-β-GEO protein.
- Mice carrying the intronic gentrap insertion in the Clp36 gene after exon 1 were denoted as *Clp36*$^{-/-}$. In these mice the CLP36 protein was absent.

For both mouse lines, respective wildtype littermates (referred as *Wt*) served as control animals. This part of the study was done together with Dr. Attila Braun from our group.

4.2.1 CLP36 is expressed in mouse platelets

The partially overlapping expression profile of PDLIMs in different mouse tissues and the similar domain structure of ALP, RIL and CLP36[101] indicated that the biological function of these proteins may be redundant *in vivo*. To assess the expression of various members of the PDLIM family in platelets, RT-PCR was performed. Interestingly, only *clp36* mRNA but no other PDLIM mRNAs, was found to be expressed in platelets (Figure 18). The unique expression of CLP36 in murine platelets suggested that disruption of CLP36 function cannot be compensated by other members of PDLIMs and thus CLP36 might play an important role in platelet physiology.

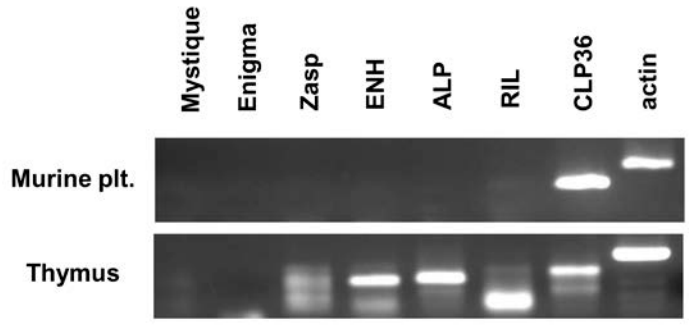

Figure 18: mRNA expression profile of PDLIM family members in platelets. mRNA was isolated from *Wt* platelets (plt.) and RT-PCR was performed. mRNA isolated from *Wt* thymus cells served as a positive control. Actin was used as loading control.

4.2.2 CLP36 colocalizes with the actin cytoskeleton in spread mouse platelets

To study protein expression and subcellular localization of CLP36, immunofluorescence confocal microscopy was performed on *Wt* platelets that were allowed to spread on fibrinogen after stimulation with thrombin (0.01 U/mL). CLP36 was found to be abundantly expressed with

dotted appearance throughout the platelet cytoskeleton (Figure 19). Interestingly, CLP36 was absent in the central granule body of platelets where actin fibers are absent.

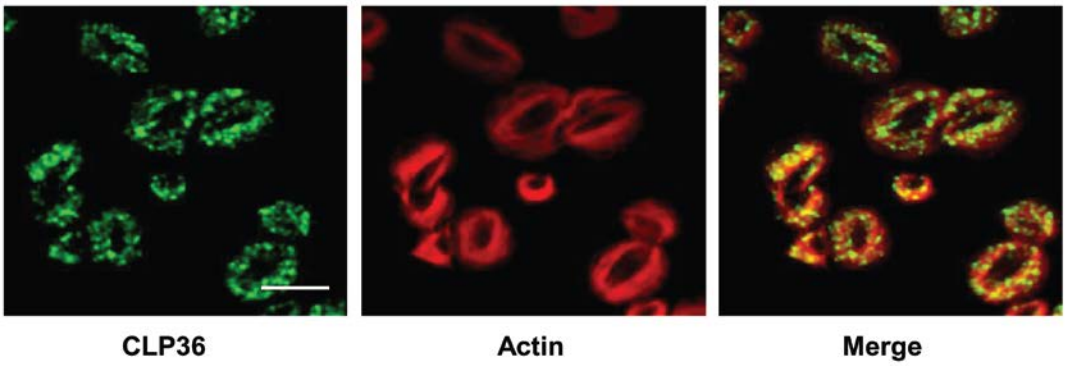

Figure 19: Subcellular localization of CLP36 in platelets. Washed platelets of *Wt* mice were spread on 200 µg/mL of immobilized fibrinogen after stimulation with 0.01 U/mL thrombin. Platelets were allowed to spread for 20 min and were then stained with phalloidin Atto647N and CLP36-PDZ antibody to detect CLP36 protein. Representative confocal microscopy images are shown. Scale bar: 3 µm.

4.2.3 Generation of the *Clp36$^{\Delta LIM}$* knockin mice

To study the function CLP36 in platelets, ES cells (XC 262, *BayGenomics*) were injected into the C57Bl/6 blastocysts to generate chimeric mice. In these ES cells the *Clp36* gene was disrupted by insertion of an intronic β-Geomycin gene-trap cassette into intron 5 located upstream of exons encoding the LIM domain (Figure 20). Insertion of the cassette in the intronic region between exon 5 and 6 resulted in expression of a chimeric CLP36$^{\Delta LIM}$-β-GEO fusion protein. Chimeric mice were backcrossed with C57Bl/6 and subsequent progenies were intercrossed to obtain homozygous mutant animals. The mice, homozygously expressing this truncated CLP36 variant, are further referred to as *Clp36$^{\Delta LIM}$* mice. *Clp36$^{\Delta LIM}$* mice were born following the Mendelian distribution and developed normally. Histological analysis of different hematopoietic organs of *Clp36$^{\Delta LIM}$* mice revealed no obvious hematological diseases or other developmental alterations until the age of 12 months (data not shown).

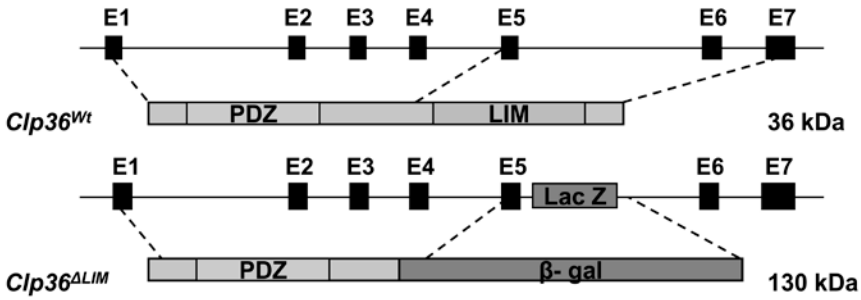

Figure 20: Targeting strategy of *Clp36$^{\Delta LIM}$* mice. Genetrap cassette β-Geomycin (GEO) is indicated. Exon-intron structure of *Clp36* gene is denoted as black box and line, respectively. Translated Wt and putative chimeric CLP36$^{\Delta LIM}$-β-GEO fusion proteins are indicated. (XC 262, *BayGenomics*)

4.2.4 Genotyping of *Clp36$^{\Delta LIM}$* knockin mice

A two-step approach was followed to genotype the mice. In the first step, the genetrap PCR was performed which could detect the insertion of the *β-Geomycin* gene-trap cassette. The mice negative for the genetrap PCR were referred as *Wt* controls. Mice found to be positive for the genetrap PCR were termed as either heterozygote (*Clp36$^{+/\Delta LIM}$*) or knockin (*Clp36$^{\Delta LIM}$*) (Figure 21A). To further distinguish between the *Clp36$^{+/\Delta LIM}$* and *Clp36$^{\Delta LIM}$*, Western blot was performed on platelet lysates. The fusion of β-GEO cassette to the C terminus of CLP36 resulted in expression of the chimeric CLP36$^{\Delta LIM}$-β-GEO fusion protein of 130 kDa. Two commercial antibodies were available that recognized different domains of CLP36. One of the antibodies recognized the N-terminal PDZ domain and the other antibody detected the C-terminal LIM domain of CLP36. Western blotting with the CLP36 N-terminal PDZ specific antibody detected 2 bands for *Clp36$^{+/\Delta LIM}$* mice; one at 36 kDa, corresponding to the *Wt* protein and another at ~130 kDa, corresponding to the CLP36$^{\Delta LIM}$-β-GEO protein. Western blot of platelet lysate from *Clp36$^{\Delta LIM}$* mice detected a single band at ~130 KDa (Figure 21B). Western blot, using the second antibody recognizing the C-terminal LIM domain, detected *Wt* protein of 36 kDa in *Clp36$^{+/\Delta LIM}$* mice but could not detect any band of similar size for *Clp36$^{\Delta LIM}$* mice (Figure 21B).

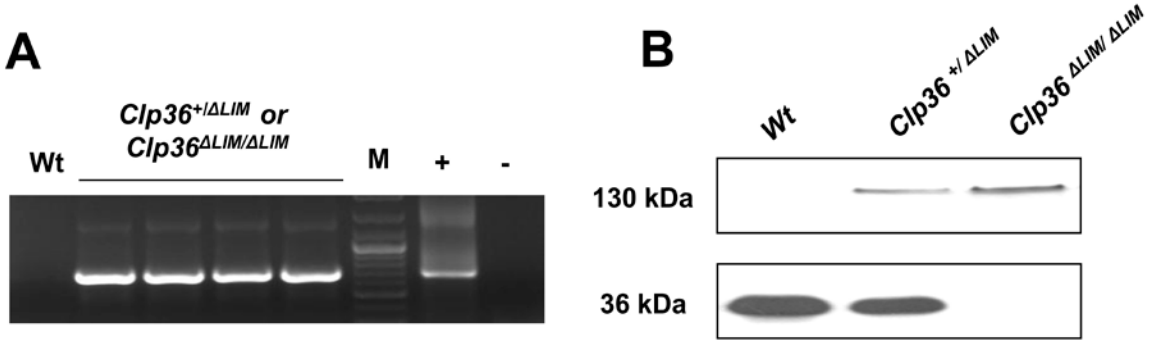

Figure 21: Detection of the insertion of the *β-Geomycin* genetrap cassette and Western blot detection of the CLP36$^{\Delta LIM}$-β-GEO chimeric protein. (A) The genetrap PCR was performed to distinguish between *Wt* and *Clp36$^{+/\Delta LIM}$* or *Clp36$^{\Delta LIM}$* mice. (B) In the next step, Western blot analysis with anti-PDZ domain of CLP36 and anti-LIM domain of CLP36 specific antibodies was performed to differentiate between *Clp36$^{+/\Delta LIM}$* and *Clp36$^{\Delta LIM}$* mice. In *Wt* platelets, the CLP36 protein migrated at 36 kDa; in the *Clp36$^{\Delta LIM}$* platelets a chimeric protein was detected at ~130 kDa.

4.2.5 *Clp36$^{\Delta LIM}$* platelets spread normally on fibrinogen and display an unaltered subcellular localization of the chimeric protein

CLP36 binds to α-actinin in resting platelets and translocates as the CLP36-α-actinin complex to the actin cytoskeleton upon platelet activation.[115] This interaction is mediated by the PDZ region of the CLP36 protein. To test whether the LIM domain of CLP36 was required for actin rearrangements in platelets, *Wt* and *Clp36$^{\Delta LIM}$* platelets were allowed to spread on

fibrinogen-coated coverslips in the presence of thrombin (0.01 U/mL). *Clp36*$^{\Delta LIM}$ platelets formed filopodia and lamellipodia with similar kinetics as *Wt* platelets. After 20 min, the number of fully spread platelets was also comparable between the two groups (Figure 22A). To determine whether *Clp36*$^{\Delta LIM}$ platelets have the capability to assemble actin filaments, flow cytometric analyses were performed to measure F-actin assembly after agonist stimulation. In these measurements, the amount of F-actin in resting and after stimulation with different agonists was found to be similar in *Wt* and *Clp36*$^{\Delta LIM}$ platelets (Figure 22B). These results suggested that the LIM domain of CLP36 is dispensable for actin rearrangements in murine platelets.

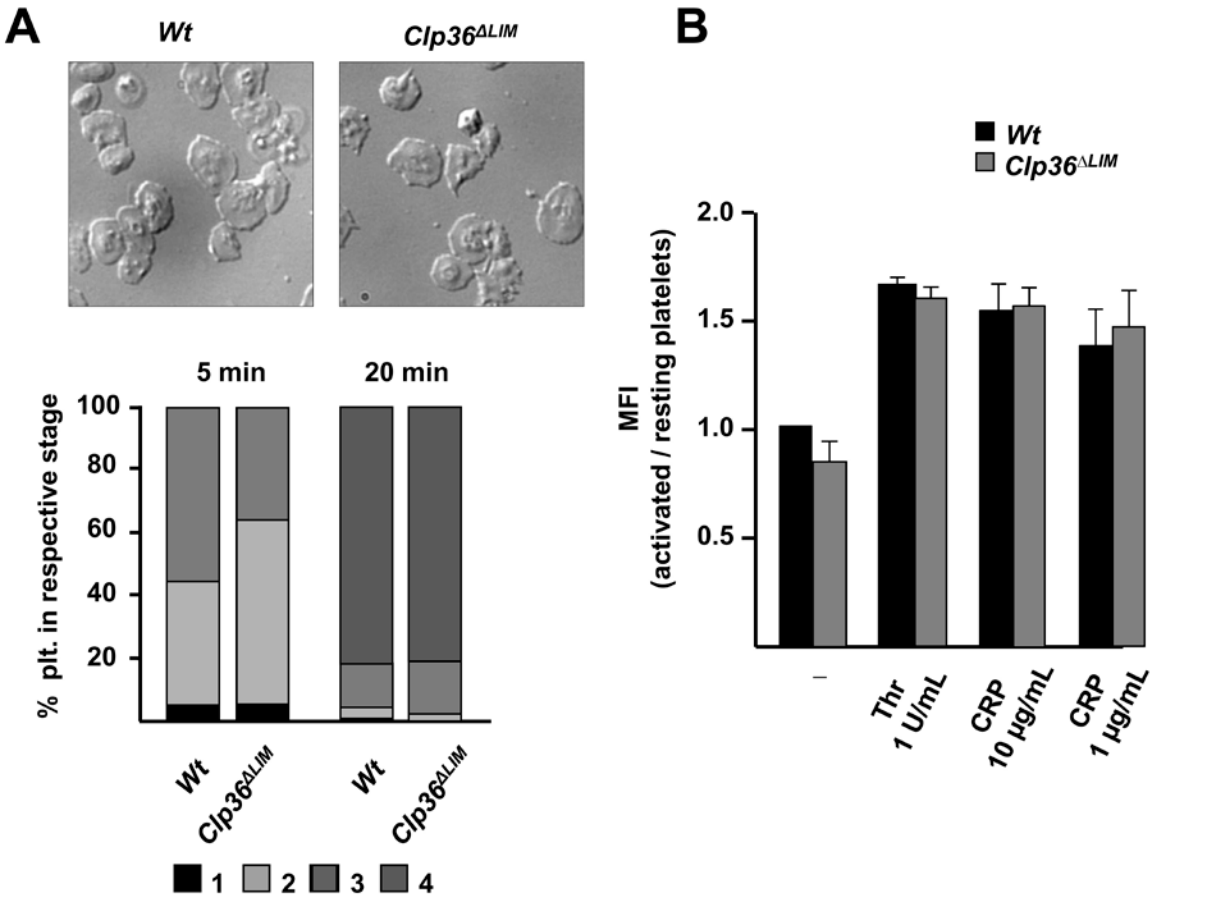

Figure 22: *Clp36*$^{\Delta LIM}$ platelets can spread on fibrinogen and display unaltered F-actin assembly. (A) Washed platelets of *Wt* and *Clp36*$^{\Delta LIM}$ mice were stimulated with 0.01 U/mL thrombin and were allowed to spread on fibrinogen (200 µg/mL). Representative differential interference contrast (DIC) images of 4 individual experiments from the indicated time points and statistical evaluation of the percentage of spread platelets at different spreading stages. 1: no filopodia, 2: only filopodia, 3: filopodia and lamellipodia, 4: full spreading. (B) Quantification of F-actin assembly in *Clp36*$^{\Delta LIM}$ platelets. After activation of washed platelets with thrombin (1 U/mL), CRP (10 µg/mL and 1 µg/mL) for 2 min at 37°C, platelets were fixed, permeabilized, stained with phalloidin-FITC and analyzed by flow cytometry. The mean fluorescence intensity (MFI) of resting control platelets was set to 1. MFI of resting and activated platelets was measured. The ratio of polymerized actin in activated *versus* resting platelets was determined.

Furthermore, confocal immunofluorescence microscopy of *Wt* and *Clp36*$^{\Delta LIM}$ platelets at different spreading stages was performed to visualize the actin cytoskeleton and the localization of the chimeric CLP36. Interestingly, localization of chimeric CLP36 in *Clp36*$^{\Delta LIM}$ platelets was similar to that of *Wt* platelets (Figure 23). The localization of α-actinin-1 was also found to be unaltered (data not shown).

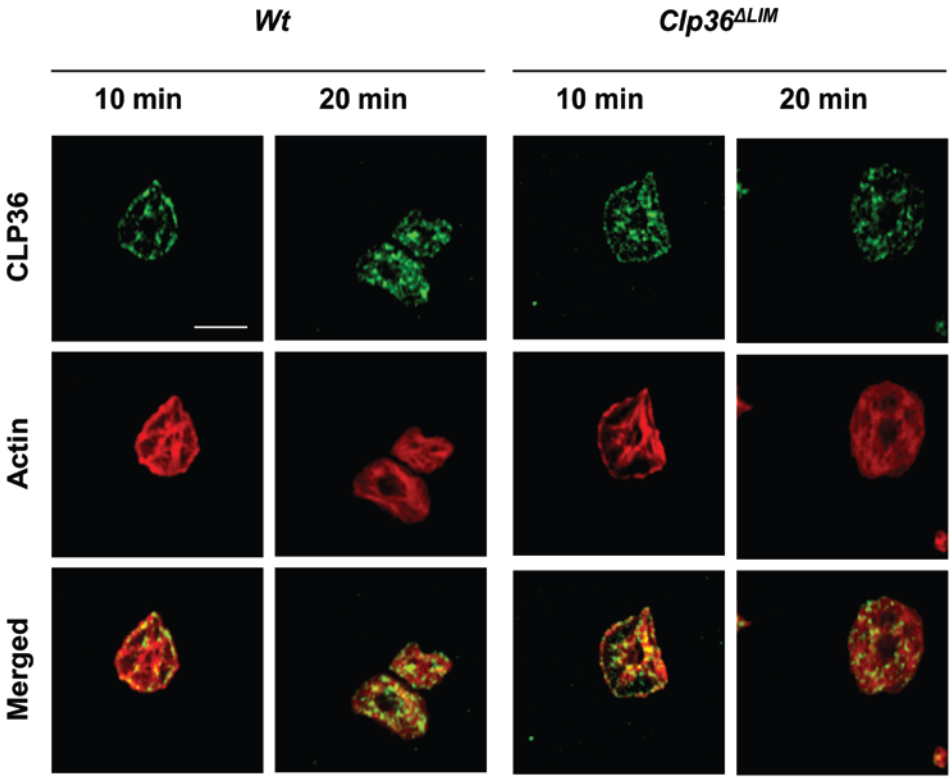

Figure 23: **Localization of the chimeric CLP36 in *Clp36*$^{\Delta LIM}$ platelets.** Washed platelets of *Wt* and *Clp36*$^{\Delta LIM}$ mice were allowed to spread on 200 µg/mL of immobilized fibrinogen after stimulation with 0.01 U/mL thrombin. Platelets were allowed to spread for 10 or 20 min and were stained with phalloidin Atto647N and CLP36-PDZ antibody to detect *Wt* (left panel) and *Clp36*$^{\Delta LIM}$ (right panel) protein. Representative confocal microscopy images are shown. Scale bar: 3 µm.

4.2.6 CLP36$^{\Delta LIM}$ protein co-immunoprecipates with α–actinin-1 in *Clp36*$^{\Delta LIM}$ platelets

To study if the chimeric CLP36 protein could still interact with α-actinin-1, immunoprecipitation studies were performed. The chimeric CLP36 protein was immunoprecipitated from platelet lysates using an antibody specific for the N-terminal PDZ domain. Western blot analysis showed that α-actinin-1 specifically co-immunoprecipitated with CLP36 in both *Wt* and *Clp36*$^{\Delta LIM}$ platelet lysates (Figure 24).

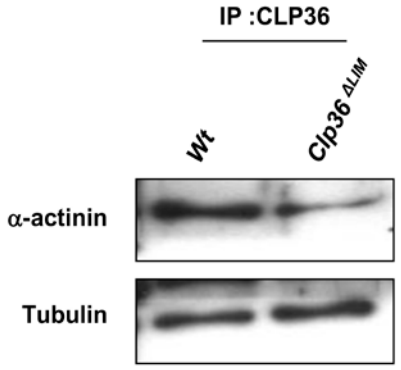

Figure 24: Chimeric CLP36$^{\Delta LIM}$ protein associates with α-actinin-1 in mouse platelets. Co-immunoprecipitation of α-actinin-1 in anti-CLP36 immunoprecipitates from *Wt* and *Clp36$^{\Delta LIM}$* platelet lysates. The fractions were resolved by SDS-PAGE, blotted and probed with anti-α-actinin-1 antibody. Tubulin was used as loading control.

4.2.7 *Clp36$^{\Delta LIM}$* platelets display normal clot retraction

Upon ligand binding, integrin αIIbβ3 can also mediate clot retraction which is governed by outside-in signaling by the integrin along with cytoskeletal contractibility of platelets.[128] CLP36 has been proposed to be important for actin stress fiber formation; therefore to study if CLP36 has a role in clot formation, coagulation of *platelet rich plasma* (prp) of *Wt* and *Clp36$^{\Delta LIM}$* mice was induced by high doses of thrombin (3 U/mL) in the presence of high Ca^{2+}-concentrations (20 mM) and clot retraction was monitored under non-stirring conditions for 4 h (Figure 25). Clot formation and retraction was comparable in both of *Wt* and *Clp36$^{\Delta LIM}$* prp, with partial and complete retraction after 1h and 4h, respectively. This result indicated that CLP36 does not play an essential role in integrin mediated clot retraction.

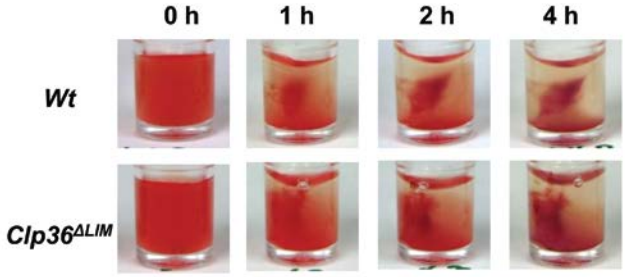

Figure 25: *Clp36$^{\Delta LIM}$* platelets show normal integrin-dependent clot retraction. Clot retraction of Wt and *Clp36$^{\Delta LIM}$* prp upon activation with 3 U/mL thrombin in presence of 20 mM $CaCl_2$ at the indicated time points. Representative images of 3 different experiments are depicted.

4.2.8 Blood cell analysis in *Clp36$^{\Delta LIM}$* mice

To study whether the absence of the LIM domain of CLP36 affected the biogenesis of other blood cells including granulocytes and lymphocytes, different cell populations were analyzed. Light scatter characteristics in combination with specific staining of surface markers were used to identify different blood cell populations by flow cytometry. These experiments were performed together with Timo Vögtle in our laboratories. Granulocytes were prepared from mouse blood

and stained with the neutrophil-specific marker combination CD11b and Gr1. $CD11b^+/Gr1^+$ double-positive neutrophils represented a clearly defined population in the FSC/SSC dot plots, and therefore could be identified by FSC/SSC characteristics and CD11b expression in the following experiments. Under these experimental settings, no differences were observed for different granulocyte populations which were termed as $Gr1^+/CD11^+$ and $Gr^{low}/CD11^+$. In the next experimental setting, cells were stained for different lymphocyte populations which included antibodies against CD4, CD8 and B220. No differences were observed in population of T cells ($CD4^+$ and $CD8^+$) and B cells ($B220^+$) from *Clp36*$^{\Delta LIM}$ mice in comparison to *Wt* controls thus indicating normal blood cellularity in these mice (Figure 26).

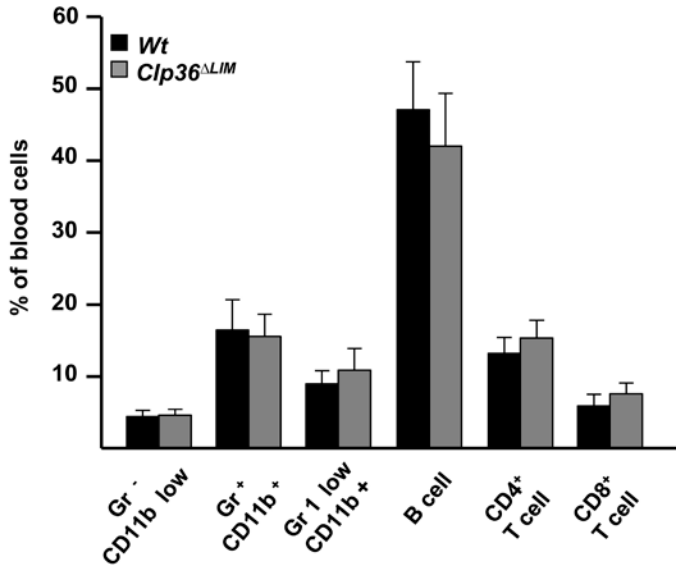

Figure 26: Normal granulocyte and lymphocyte populations in *Clp36*$^{\Delta LIM}$ mice. Blood cells were isolated and different cell populations were stained with antibodies against different lineage specific markers. The populations were analyzed by flow cytometry.

4.2.9 *Clp36*$^{\Delta LIM}$ platelets display normal surface glycoprotein expression and an unaltered life span *in vivo*

The *mean platelet volume* (MPV) and surface expression of major surface receptors including GPIb-V-IX, GPVI, and β1 and β3 integrins were analyzed using flow cytometry in *Wt* and *Clp36*$^{\Delta LIM}$ platelets. The abundance of major platelet surface receptors was normal except for a slight but significant elevation of CD9 surface expression. Apart from that, platelet count and platelet size were measured using Sysmex KX-21N automated hematology analyzer (Sysmex Corp., Kobe, Japan). *Clp36*$^{\Delta LIM}$ mice displayed decreased platelet counts and mildly increased mean platelet volumes (Figure 27A).

To study whether CLP36 plays a role in megakaryopoiesis, platelet life span in *Clp36*$^{\Delta LIM}$ and *Wt* mice was determined. A fluorescent non-cytotoxic anti-GPIX platelet labeling antibody was injected into mice and the labeled platelet population was monitored by flow cytometry over time. One hour after antibody treatment, >90% of circulating platelets were fluorescently labeled

in both *Clp36*$^{\Delta LIM}$ and *Wt* mice and this platelet population constantly declined over 5 days in both groups (Figure 27B). These findings demonstrated that the LIM domain of CLP36 is dispensable for platelet production.

A

	Wt	*Clp36*$^{\Delta LIM}$
GPIb	291 ± 5.6	285 ± 10.0
GPV	271 ± 2.6	280 ± 14.3
GPIX	440 ± 5.3	460 ± 25.0
GPVI	21 ± 1.25	21 ± 2.6
CD9	1585 ± 31.0	1657 ± 35.0 *
GPIIbIIIa	509 ± 38.0	506 ± 29.0
Integrin α	59 ± 3.8	57 ± 3.3
Integrin β1	167 ± 3.8	163 ± 18.0
Clec2	136 ± 13.0	138 ± 7.0
Platelets (nL^{-1})	128 ± 29.0	112 ± 11.21
MPV(fl)	5.2 ± 0.1542	5.4 ± 0.1857 *

B

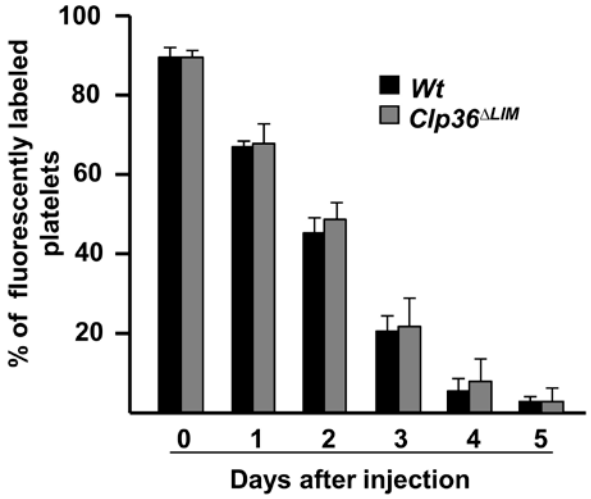

Figure 27: Normal surface glycoprotein expression and platelet life span in *Clp36*$^{\Delta LIM}$ mice.
(A) Expression levels of prominent glycoproteins were determined by flow cytometry. Diluted whole blood from the indicated mice was incubated with FITC-labeled antibodies at saturating concentrations for 15 min at RT and analyzed directly. Results are expressed as mean fluorescence intensity ± SD (n=5) and are representative of 4 individual experiments. Platelet count and platelet size were determined using a Sysmex automated cell analyzer. **P*<0.05. (B) The platelet life span was determined by percentage of fluorescently labeled platelets in *Wt* and *Clp36*$^{\Delta LIM}$ mice over a 5 day period after i.v. injection of a Dylight-488 anti-GPIX Ig derivative (0.5 mg/kg), (n=5).

4.2.10 Enhanced GPVI signaling in *Clp36*$^{\Delta LIM}$ platelets

Platelet activation involves a shift of integrin αIIbβ3 from low affinity "off" state to the active conformation, which results in fibrinogen/vWF-binding and platelet aggregation followed by release of granule contents that in turn further potentiate platelet activation. To test the functional consequences of the absence of the LIM domain for platelet activation, flow cytometric analysis of integrin αIIbβ3 activation using the JON/A-PE antibody[118] and of P-selectin surface exposure as a marker of α-granule release were analyzed upon agonist stimulation. This experimental setting involves use of highly diluted platelet suspension and thus, largely excludes the accumulation of released secondary mediators and thereby allows conclusions about the primary platelet signaling responses. *Clp36*$^{\Delta LIM}$ platelet activation was found to be normal in response to the *G protein-coupled receptor* (GPCR) agonists ADP, thrombin and stable TxA_2 analogue U46619 (Figure 28A, B). In contrast, upon stimulation of

Clp36$^{\Delta LIM}$ platelets with GPVI agonists (CRP, convulxin) markedly increased integrin αIIbβ3 activation and α-granule release were observed. This effect was most evident at low agonist concentrations (Figure 28C, D).

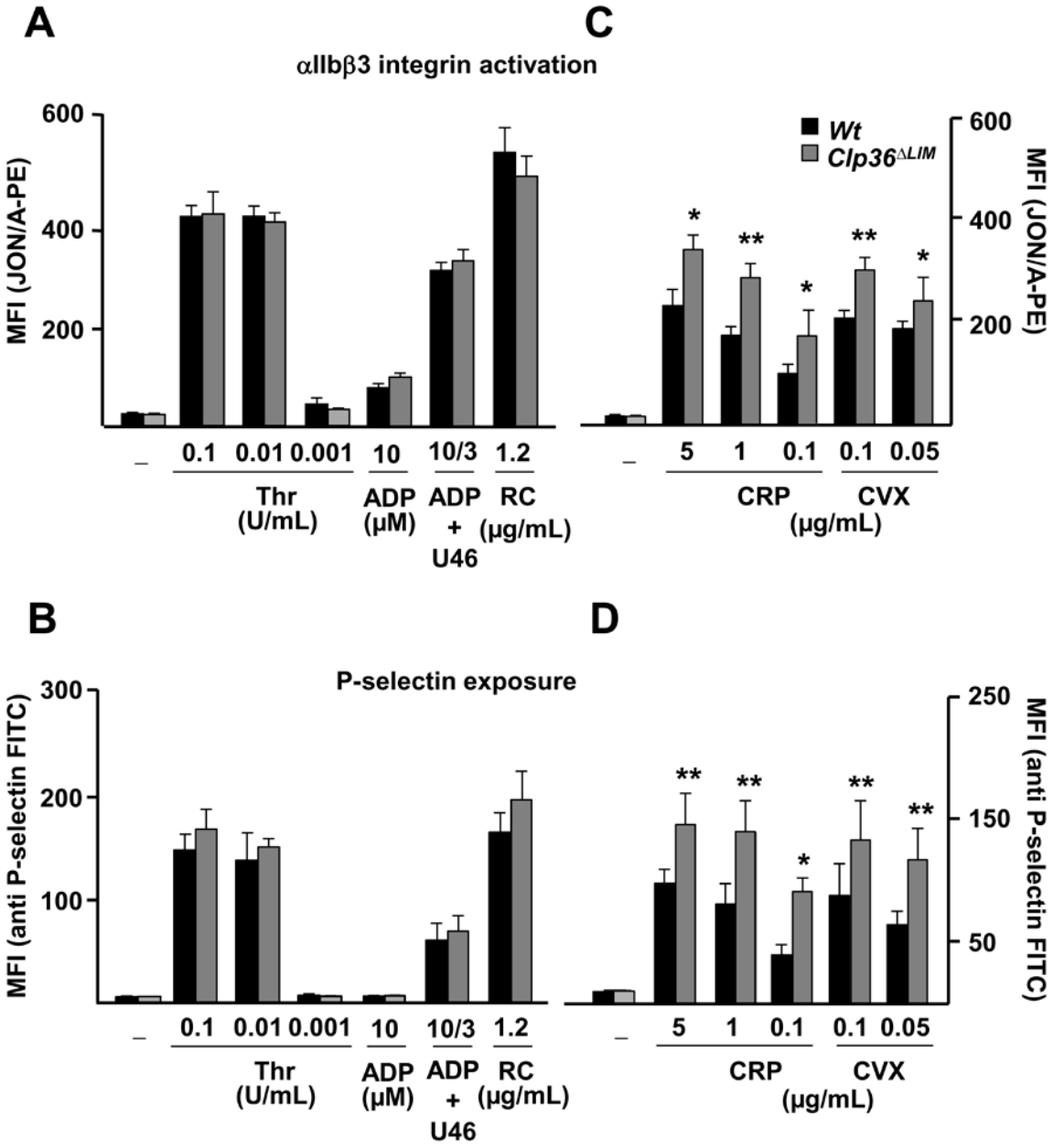

Figure 28: Increased integrin activation and α-granule release in *Clp36*$^{\Delta LIM}$ platelets upon GPVI stimulation. (A and B) Flow cytometric analysis of integrin αIIbβ3 activation (binding of JON/A-PE) and degranulation-dependent P-selectin exposure in *Wt* and *Clp36*$^{\Delta LIM}$ platelets in response to the indicated G-protein coupled receptor agonists and (C and D) in response to GPVI agonists. Results are given as mean fluorescence intensities (MFI) ± SD of 5 mice per group and are representative of 4 individual experiments. **P*<0.05, ***P*<0.01.

To assess whether the enhanced granule secretion was restricted only to α-granules, release of ATP from dense granules was measured upon agonist stimulation. The enhanced GPVI signaling was also associated with an increased dense-granule secretion as shown by faster and increased ATP release in response to low concentrations of CRP or collagen. In contrast, no differences in ATP release between *Wt* and *Clp36*$^{\Delta LIM}$ platelets were detectable in response to thrombin or at high concentrations of GPVI agonists (Figure 29). These observations confirmed that *Clp36*$^{\Delta LIM}$ platelets have unaltered granule content, but display a selectively increased granule release in response to GPVI stimulation.

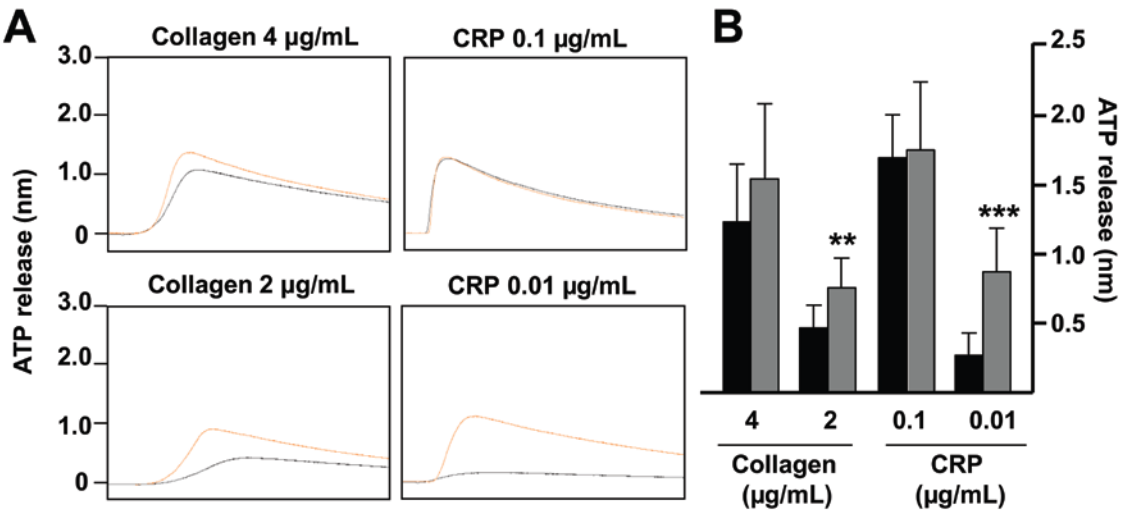

Figure 29: Enhanced dense granule release in *Clp36*$^{\Delta LIM}$ mice. Washed platelets from *Wt* (black line) or *Clp36*$^{\Delta LIM}$ (red line) (240 µl with 0.3x10^6 platelets/µL) were incubated with Luciferase-Luciferin reagent, followed by agonist addition. (A) ATP release and aggregation were measured simultaneously on a Lumi-Aggregometer. (B) The concentration (nM) of released ATP is given. Mean % of maximal aggregation ± SD of each group ***P*<0.01, ****P*<0.001.

4.2.11 Enhanced GPVI-induced aggregation of *Clp36*$^{\Delta LIM}$ platelets

CLP36 has been implicated in actin stress fiber formation and knockdown of CLP36 resulted in altered morphology of BeWo cells.[113] To investigate the role of CLP36 in platelet shape change and to define the functional consequences of increased αIIbβ3 integrin activation and degranulation in *Clp36*$^{\Delta LIM}$ platelets, aggregation studies were performed. *Clp36*$^{\Delta LIM}$ platelets aggregated normally in response to GPCR agonists (thrombin, ADP, U46619) at all tested concentrations (Figure 30A). In contrast, upon stimulation with GPVI agonists (collagen, CRP, CVX), an enhanced aggregation response were observed in *Clp36*$^{\Delta LIM}$ platelets. This effect was best detectable at threshold concentrations of these agonists that did not induce aggregation of *Wt* platelets (Figure 30B).

In contrast, at higher concentrations of GPVI agonists, no significant difference in aggregation was detected between *Wt* and mutant platelets. Notably, *Clp36*$^{\Delta LIM}$ platelets did not aggregate spontaneously or upon stimulation with epinephrine (data not shown), indicating that the platelets were not *per se* in a pre-activated state. Taken together, these findings demonstrated that CLP36 plays a critical role in GPVI mediated platelet activation, especially at lower concentrations of GPVI agonists which mimics physiological conditions.

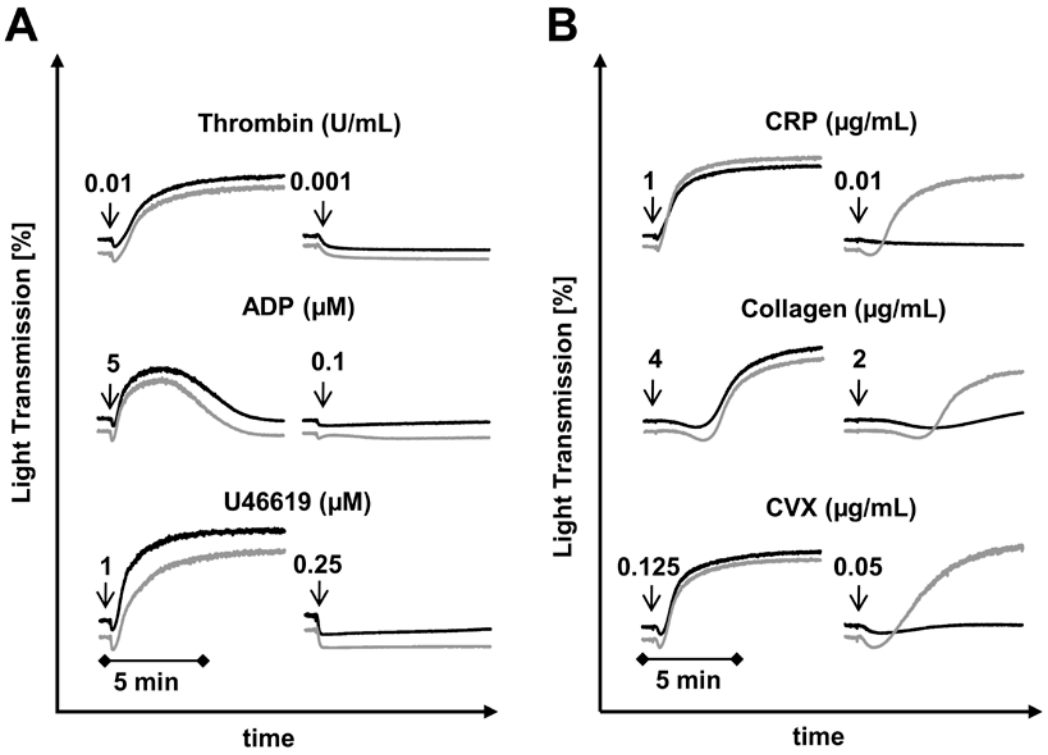

Figure 30: Enhanced GPVI-induced aggregation and ATP release in *Clp36*$^{\Delta LIM}$ platelets. (A,B) Washed platelets from *Wt* (black line) or *Clp36*$^{\Delta LIM}$ (grey line) were stimulated with the indicated agonists and light transmission was recorded on a Fibrintimer 4-channel aggregometer. ADP measurements were performed in prp. Representative aggregation curves traces of 4 individual experiments are shown.

4.2.12 Increased Ca^{2+} mobilization in *Clp36*$^{\Delta LIM}$ platelets

Agonist induced platelet activation and aggregation requires an increase in the intracellular Ca^{2+} concentration $[Ca^{2+}]_i$ that occurs through release of Ca^{2+} from intracellular stores followed by the Ca^{2+} entry through the plasma membrane. To test whether the observed GPVI-ITAM-induced activation response of *Clp36*$^{\Delta LIM}$ platelets was based on altered Ca^{2+} signaling, agonist-induced changes in $[Ca^{2+}]_i$ were studied fluorimetrically. Store release in the absence of extracellular Ca^{2+} in response to CRP (1 mg/mL) was significantly elevated in *Clp36*$^{\Delta LIM}$ platelets compared to *Wt* controls (*Wt:* 30 ± 12 nM; *Clp36*$^{\Delta LIM}$: 60 ± 10 nM; $P<0.05$, Figure 31A). As a result, the subsequent Ca^{2+} influx was also markedly increased in the presence of extracellular Ca^{2+} in

Clp36$^{\Delta LIM}$ platelets (*Wt*: 180 ± 20 nM; *Clp36*$^{\Delta LIM}$: 380 ± 35 nM, *P*<0.01, Figure 31B). In addition, Ca^{2+} mobilization was measured upon stimulation with thrombin and ADP. No differences were observed in Ca^{2+} store release or Ca^{2+} influx in response to the GPCR signaling agonists. (Figure 31A, B). These data pointed towards a selective defect in GPVI signaling pathway in *Clp36*$^{\Delta LIM}$ platelets.

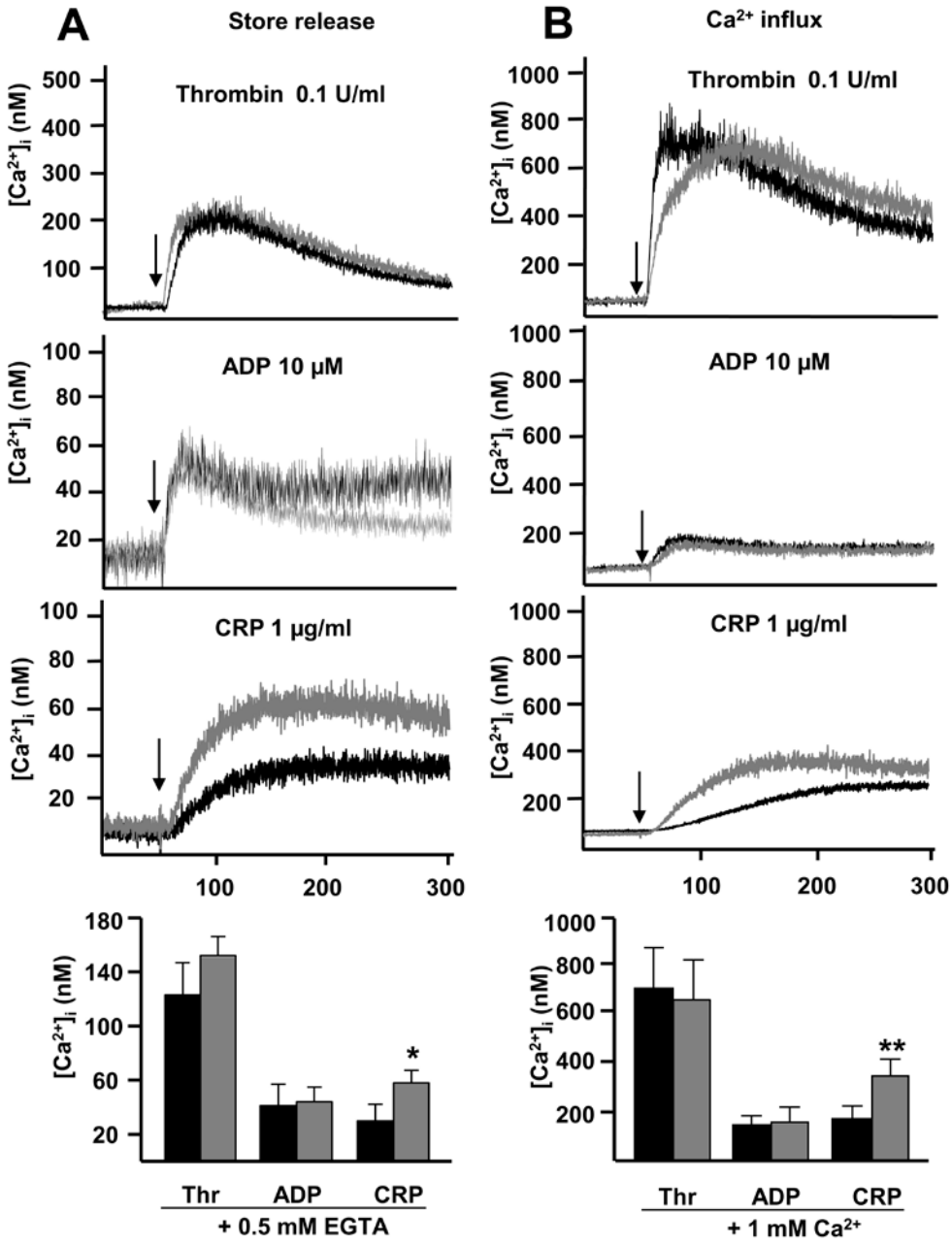

Figure 31: Enhanced GPVI-induced Ca^{2+} mobilization in *Clp36*$^{\Delta LIM}$ platelets. (A) Fura-2–loaded *Wt* (black line) or *Clp36*$^{\Delta LIM}$ (grey line) platelets were stimulated with 0.1 U/mL thrombin, 10 µM ADP or 1 µg/mL CRP in the presence of 0.5 mM EGTA or (B) in the presence of 1 mM Ca^{2+} and changes in $[Ca^{2+}]_i$ were monitored fluorimetrically. Representative measurements and maximal increase in $[Ca^{2+}]_i$ compared with baseline levels before stimulus ($\Delta[Ca^{2+}]_i$) ± SD (*n* = 5 mice per group) are shown. **P*<0.05, ***P*<0.01.

4.2.13 Increased GPVI-induced tyrosine phosphorylation and IP_3 production in *Clp36$^{\Delta LIM}$* platelets

GPVI signaling involves a series of tyrosine phosphorylation events that finally culminate in PLCγ2 activation and subsequent hydrolysis of PIP_2 into IP_3 and DAG. IP_3 in turn is responsible for emptying of intracellular Ca^{2+} stores. Increased Ca^{2+} store depletion in response to GPVI agonists suggested a modulating function of CLP36 in GPVI signaling upstream of IP_3 receptors. Hence, changes in tyrosine phosphorylation patterns upon GPVI stimulation were analyzed in *Wt* and *Clp36$^{\Delta LIM}$* platelets. At low concentrations of CRP (0.1 µg/mL), *Wt* platelets displayed only a small increase in tyrosine phosphorylation whereas a marked increase of tyrosine phosphorylation of numerous platelet proteins, including those co-migrating with PLCγ2, Fyn, Lyn and the FcRγ-chain was observed in *Clp36$^{\Delta LIM}$* platelets (Figure 32A). At high concentrations of CRP (5 µg/mL) the increases in tyrosine phosphorylation was similar in *Wt* and mutant platelets (data not shown). To confirm that the enhanced phosphorylation of signaling molecules in *Clp36$^{\Delta LIM}$* platelets resulted in an increased PLCγ2 activity, we measured the amount of IP_3 indirectly using an IP_1 ELISA.[129] The half-life of IP_3 in cells is very short before it is degraded to IP_2 and IP_1. The IP_1 can accumulate in the cell after addition of Li^+ which inhibits its further degradation to myo-inositol. We quantified IP_1 concentration upon platelet activation with thrombin (1 U/mL), CRP (1 µg/mL and 0.1 µg/mL) in presence of indomethacin (10 µM) and apyrase (2 U/mL). While IP_1 production in response to thrombin was similar in *Wt* and *Clp36$^{\Delta LIM}$* platelets (*Wt*: 1551 ± 307 vs *Clp36$^{\Delta LIM}$* : 1742 ± 186, P=0.42), the response to CRP at both tested concentrations was markedly elevated in *Clp36$^{\Delta LIM}$* platelets compared to *Wt* controls (Wt: 427 ± 45 vs *Clp36$^{\Delta LIM}$* : 842 ± 197, P<0.001 for CRP 1 µg/mL and Wt: 311 ± 99 vs *Clp36$^{\Delta LIM}$*: 1049 ± 493, P<0.01 for CRP 1 µg/mL , Figure 32B), suggesting an enhanced activity of PLCγ2 in mutant platelets. Taken together, these results suggested that the LIM domain of CLP36 acts as a negative regulator of GPVI signaling that controls PLCγ2 activity.

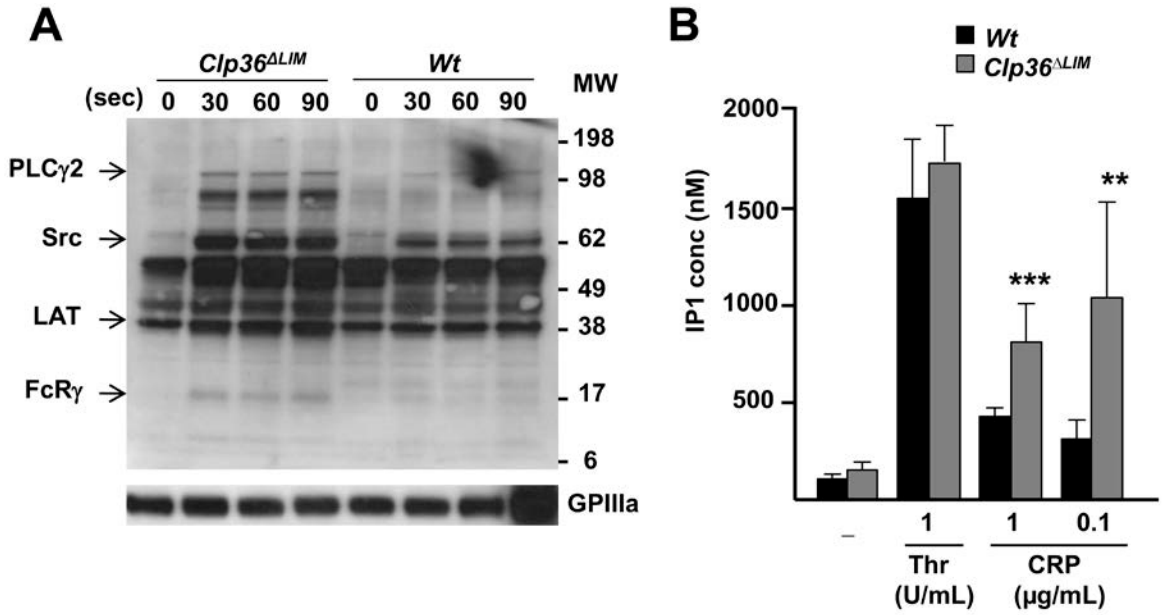

Figure 32: Enhanced GPVI-induced tyrosine phosphorylation in *Clp36$^{\Delta LIM}$* platelets. (A) Determination of whole cell tyrosine phosphorylation. Washed platelets from *Wt* and *Clp36$^{\Delta LIM}$* mice were stimulated with 0.1 µg/mL CRP under stirring conditions at 37°C. 50 µL aliquotes were taken at the indicated time points. Samples were blotted onto a PVDF membrane and immunoblotted with the anti-phosphotyrosine antibody 4G10. GPIIIa protein levels served as loading controls. (B) Quantification of produced IP_1 upon platelet activation. Washed platelets from *Wt* and *Clp36$^{\Delta LIM}$* mice were stimulated with the indicated agonists (thrombin (Thr.): 1 U/mL; CRP: 1 µg/mL and 0.1 µg/mL) for 5 min at 37°C (450 rpm). Platelets were lysed and IP_1, a specific metabolite of IP_3, was quantified using an ELISA assay. Results are given as the mean IP_1 concentration (nM) ± SD (n=4 per group). ***P*<0.01, ****P*<0.001.

4.2.14 *Clp36$^{\Delta LIM}$* platelets display increased thrombus formation on collagen under flow

At sites of vessel wall injury, secondary mediators released from activated platelets play an essential role in the recruitment of other platelets to promote thrombus growth. GPVI-collagen interaction plays a major role in the process of thrombus formation under flow conditions. To study the effect of enhanced GPVI induced αIIbβ3 integrin activation and degranulation of *Clp36$^{\Delta LIM}$* platelets on thrombus formation under flow, whole anti-coagulated blood was perfused over collagen at physiological shear rates. At the high shear rates of 1700 s^{-1}, that modeled flow conditions in arterioles, no significant difference in surface coverage was observed between the two groups but increased thrombus volumes were observed for *Clp36$^{\Delta LIM}$* platelets compared to *Wt* platelets (data not shown). In contrast, at intermediate shear rates of 1000 s^{-1}, which models flow conditions in large arteries, *Clp36$^{\Delta LIM}$* platelets displayed an increased platelet surface coverage and thrombus volumes when compared to the *Wt* controls. (*Wt*: 31.4 ± 4 % vs *Clp36$^{\Delta LIM}$*: 46.5 ± 5 %, *P*<0.001, Figure 33).

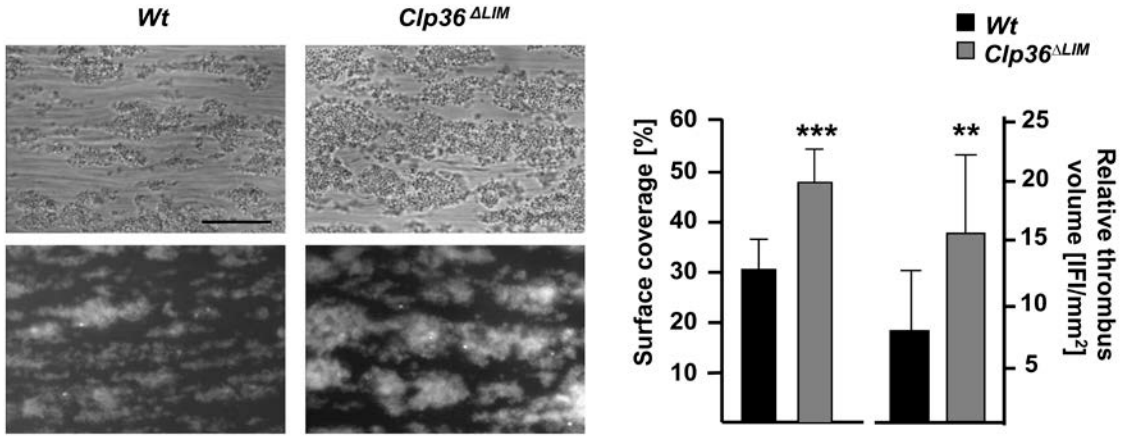

Figure 33: Increased thrombus formation of *Clp36$^{\Delta LIM}$* platelets on collagen under flow. Heparinized whole blood from *Wt* and *Clp36$^{\Delta LIM}$* was perfused over 0.2 mg/mL of immobilized collagen at a shear rate of 1000 s^{-1} (4 min) followed by 1 min perfusion with Tyrode HEPES buffer at the same shear rate. Representative phase contrast images (upper panel) and fluorescent images (platelets stained with anti-GPIX-DyLight488; lower panel) are shown (bar: 50 µm). Right panel: mean surface coverage and relative thrombus volume ± SD (n=10 per group). ***P*<0.01, ****P*<0.001.

4.2.15 *Clp36$^{\Delta LIM}$* platelets display increased procoagulant activity on collagen

Activated αIIbβ3 integrin and increased Ca^{2+} mobilization have been implicated in the coagulant activity of platelets[130,131] achieved by a Ca^{2+}-activated scramblase mechanism. The activation of scramblase in turns leads to disturbed phospholipid asymmetry in the plasma membrane, which results in the exposure of *phosphatidylserine* (PS) at the outer membrane surface.[132,133] Exposed PS provides high affinity binding sites for key coagulation factors and thus facilitates the assembly of tenase and prothrombinase complexes, which are then responsible for the formation of factor Xa and thrombin, respectively.[132] To determine the role of CLP36 in this process, anti-coagulated whole blood from *Wt* or *Clp36$^{\Delta LIM}$* mice was perfused over a collagen coated surface at the shear rate of 1700 s^{-1} in presence of high dose of heparin (5 U/ml) to inhibit thrombin. The shear rate of 1700 s^{-1} was used to perform these experiments as in these conditions no differences in surface coverage were observed in *Wt* or *Clp36$^{\Delta LIM}$* blood. PS exposure was determined using Annexin V-Dylight488 staining which specifically binds to platelets exposing PS at their outer surface. The numbers of PS positive platelets were significantly increased in *Clp36$^{\Delta LIM}$* blood samples compared to *Wt* controls (Figure 34). These results indicated that the enhanced GPVI-mediated Ca^{2+} store release and subsequent Ca^{2+} influx were responsible for the elevated procoagulant activity of *Clp36$^{\Delta LIM}$* platelets.

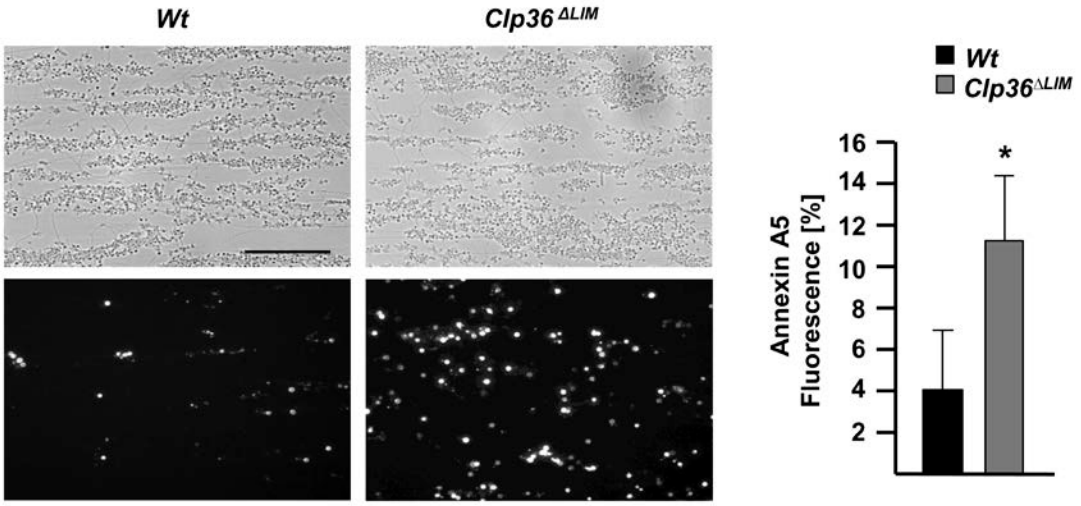

Figure 34: Increased procoagulant activity of *Clp36$^{\Delta LIM}$* platelets on collagen under flow. *Clp36$^{\Delta LIM}$* platelets display enhanced procoagulant activity. Whole blood was perfused over a collagen-coated (0.2 mg/mL) surface at a shear rate of 1700 s^{-1} for 4 min. Adherent platelets were stained with Annexin V-Dylight488 (0.25 µg/mL). Representative phase contrast (upper panel) and fluorescence images (lower panel) are shown (Bar: 50 µm). Mean percentage of Annexin V positive platelets ± SD ($n \geq 3$) for the indicated shear rates. *P<0.05.

4.2.16 Accelerated arterial thrombus formation, but normal bleeding times in *Clp36$^{\Delta LIM}$* bone marrow chimeric mice

To rule out the possibility that deficiency of the LIM domain in cells of the vessel wall might influence thrombus formation and hemostatic function, the mutation of the LIM domain was restricted to the hematopoietic system by transferring bone marrow cells from *Clp36 $^{\Delta LIM}$* donor mice into lethally irradiated *Wt* recipient mice and *vice versa*. Thrombus growth was studied in an arterial thrombosis model, where the abdominal aorta is mechanically injured and blood flow is monitored by an ultrasonic perivascular Doppler flowmeter. While irreversible occlusion of the aorta occurred with similar kinetics to wild-type controls and *Clp36^{Wt}* bone marrow chimeras (mean time to occlusion for wild type control: 260 ± 59 s vs *Clp36^{Wt}*: 350 ± 131 s, P=0.07). Whereas, occlusion times were markedly reduced in *Clp36$^{\Delta LIM}$* bone marrow chimeras (mean time to occlusion for wild type control: 260 ± 59 s vs *Clp36$^{\Delta LIM}$*: 132 ± 56 s, P<0.001; Figure 35A).

Finally, tail bleeding times were measured to determine hemostatic function of *Clp36$^{\Delta LIM}$* platelets in the bone marrow chimeric mice. No significant hemostatic defect was observed in bone marrow chimeric mice transplanted with *Clp36^{wt}* or *Clp36$^{\Delta LIM}$* cells (mean bleeding time: 47 ± 22 s (*Clp36^{wt}*) vs 57 ± 54 s (*Clp36$^{\Delta LIM}$*) *P=0.48*; (Figure 35B))

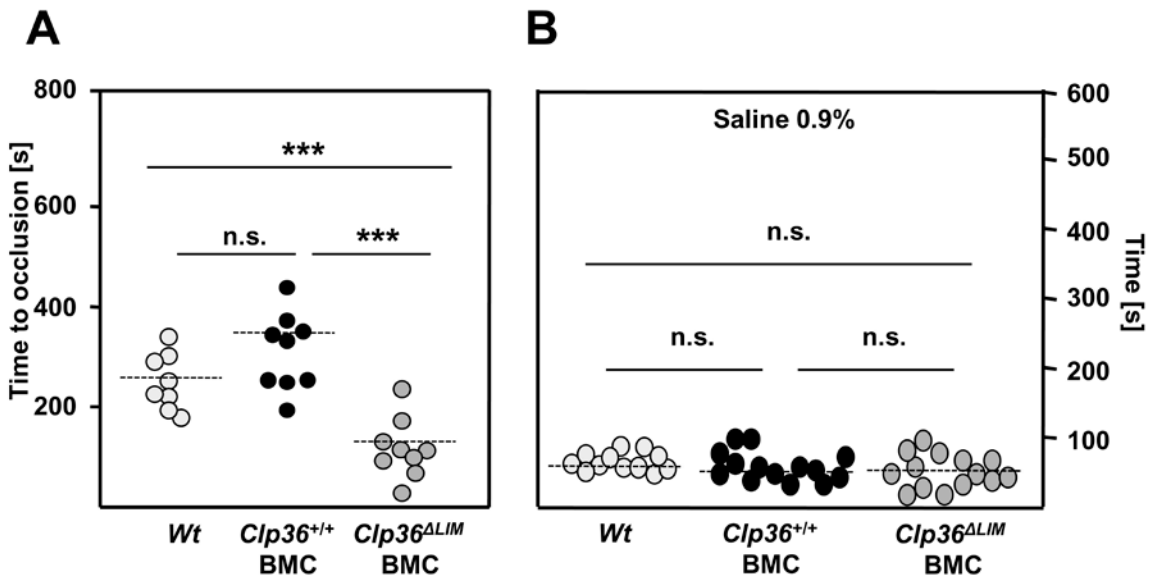

Figure 35: Accelerated thrombotic occlusion of the aorta but normal bleeding times in *Clp36$^{\Delta LIM}$* chimeric mice (A) The abdominal aorta of *Wt* and *Clp36$^{\Delta LIM}$* bone marrow chimeric mice was injured by tight compression with a forceps and blood flow was monitored for 30 min with an ultrasonic flow probe. The time to stable vessel occlusion is shown. Each symbol represents one individual. (B) Normal hemostasis in *Clp36$^{\Delta LIM}$* bone marrow chimeric mice. Tail bleeding times of *Wt* and *Clp36$^{\Delta LIM}$* bone marrow chimeric mice were measured in saline at 37°C. Each symbol represents one individual. The white dots represent *Wt* mice, the black dots and grey dots represent *Wt* and *Clp36$^{\Delta LIM}$* bone marrow chimeric mice respectively. ****P*<0.001.

4.2.17 *Clp36$^{\Delta LIM}$* mice, but not BMCs, are protected from ischemic brain infarction

Cerebral ischemia is the second leading cause of death and disability in developed nations[4] and has been proposed to be a complex thrombo-inflammatory disease.[134] Cerebral ischemia involves the disturbance in microvascular integrity but the signaling events involved in formation of intravascular thrombus formation in the brain are still not understood. To determine whether the observed thrombus instability and prolonged occlusion times observed in *Clp36$^{\Delta LIM}$* mice also affect the outcome in this experimental setting, mice were challenged in a tMCAO model, performed in collaboration with Dr. Peter Kraft, Department of Neurology, University Clinic, Würzburg, Germany. To initiate transient cerebral ischemia, a thread was advanced through the carotid artery into the middle cerebral artery to reduce cerebral blood flow by >90% [36] and allowed to remain for one hour after which reperfusion was allowed. The extent of infraction was quantified 24h after reperfusion on 2, 3, 5-triphenyltetrazolium chloride (TTC)-stained brain slices. In *Clp36$^{\Delta LIM}$* mice, brain infract volumes were reduced by about 50 % of the infract volumes in Wt mice (infarct volume for Wt: 107 ± 36 mm^3 vs *Clp36$^{\Delta LIM}$*: 50 ± 25 mm^3 ; *P*<0,001; Figure 36A, C). This reduction in *Clp36$^{\Delta LIM}$* mice in ischemic lesions of *Clp36$^{\Delta LIM}$* mice also resulted in significantly less neurological deficits compared to *Wt*, determined as Bederson score assessing the global neurological function (3.0 ± 0.2 vs 1.5 ± 0.5; *P*<0.001; Figure 36B)

and grip test which indicates motor function and coordination of the mice (2.3 ± 0.83 vs 3.6 ±0.8; *P*<0.05; Figure 36D). Again, to study the role of *Clp36*$^{\Delta LIM}$ platelets in development of stroke, lethally irradiated *Wt* mice were reconstituted with *Clp36*$^{\Delta LIM}$ bone marrow cells and *vice versa* for *Clp36*$^{\Delta LIM}$ mice. Interestingly, Wt mice transfused with *Clp36*$^{\Delta LIM}$ bone marrow showed infarct volumes, Bederson score and grip test similar to that of *Wt* control mice (Figure 36E, F, G). The stroke results indicated towards the role of CLP36 in other cell types including the cells lining the vessel walls.

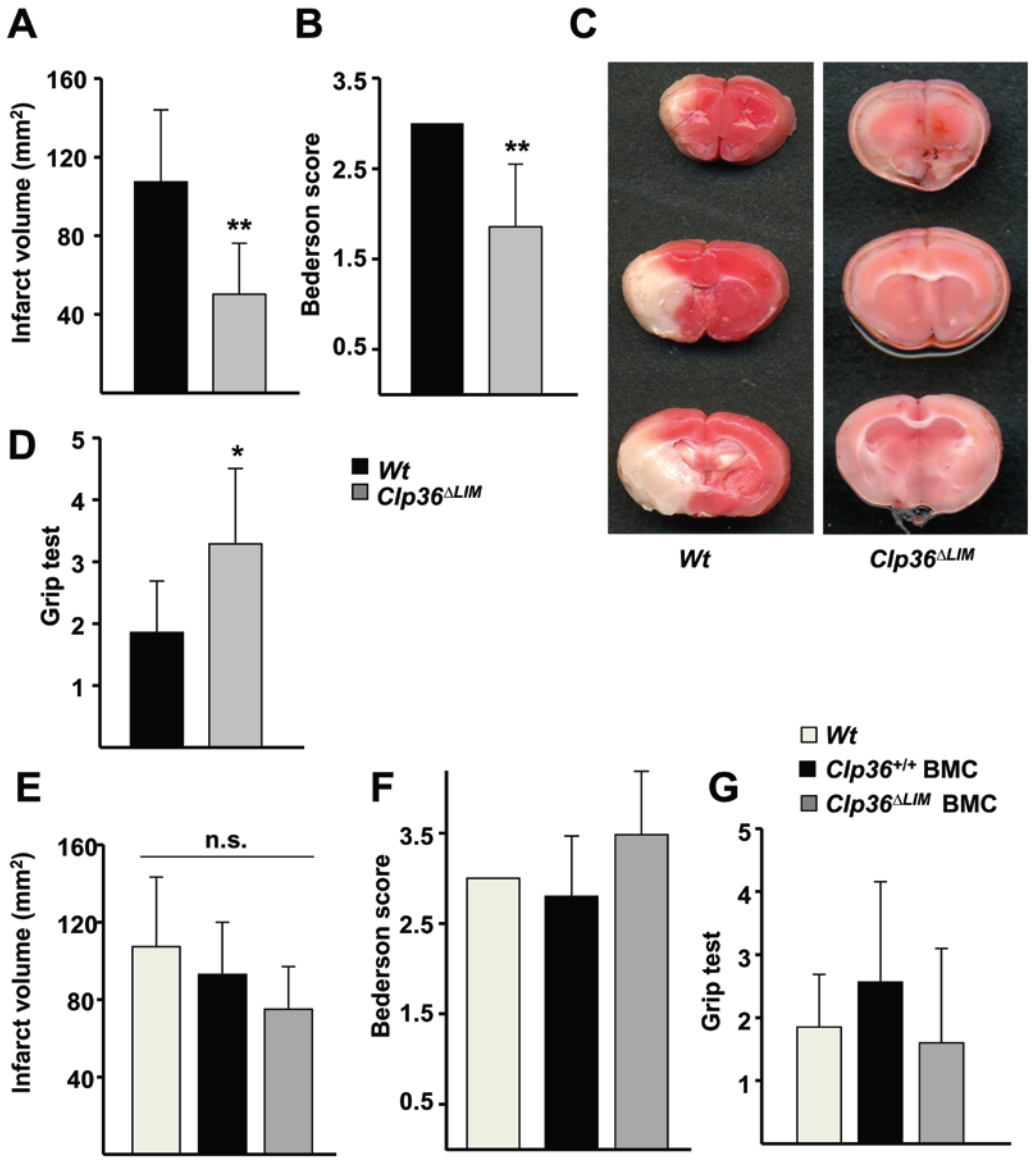

Figure 36: *Clp36*$^{\Delta LIM}$ mice but *Clp36*$^{\Delta LIM}$ bone marrow chimeric mice are protected in a model of tMACO. Formation of cerebral brain infarction and consequential neurological defects were investigated in a murine stroke model. (A) Brain infract volumes (B) Bederson score and (D) grip test in *Wt* and *Clp36*$^{\Delta LIM}$ mice presented as mean ± SD. (C) Representative images of the three corresponding coronal sections from Wt and Clp36$^{\Delta LIM}$ mice stained with TTC 24 h after tMCAO. (E) Brain infracts volumes in *Wt, Clp36*^{Wt} bone marrow and *Clp36*$^{\Delta LIM}$ bone marrow chimeric mice presented as mean SD, (F) Bederson score and (G) grip test, determined 24 h after tMCAO **P*<0.05, ***P*<0.01.

4.3 Analysis of *Clp36* knockout mice

4.3.1 Generation of *Clp36*$^{-/-}$ mice

The function of the N-terminal PDZ domain of CLP36 has been studied by different groups as discussed in detail in the introduction. All studies performed pointed towards an essential role of the N-terminal PDZ domain and its intermediate region in actin rearrangements and stress fiber formation by mediating interaction with actin reorganizing proteins like α-actinin[111] and palladin.[114,115] To study the physiological function of the CLP36 protein in platelet signaling, especially in platelet actin dynamics, we generated mice in which the *Clp36* gene was disrupted by insertion of an intronic β-Geomycin gene-trap cassette into intron one located upstream of exon 2 (ES cells source: IST12013D3, *TIGM*) (Figure 37). This insertion resulted in a frame shift mutation and premature termination of the transcription of the CLP36 protein.

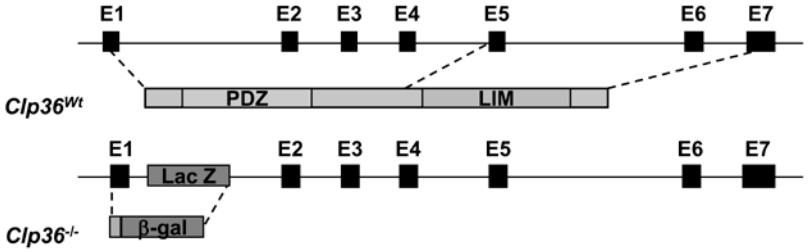

Figure 37: Targeting strategy of Cl*p36*$^{-/-}$ mice. The β-Geomycin genetrap cassette (GEO) is indicated. The exon-intron structure of the *Clp36* gene is depicted with black boxes and lines. (IST12013D3, *TIGM*)

4.3.2 Genotyping of *Clp36*$^{-/-}$ mice

A genetrap PCR was performed to detect the insertion of β-Geomycin gene-trap cassette into intron one. Mice negative for the genetrap PCR served as *Wt* (*Clp36*$^{+/+}$) controls. To further distinguish between the heterozygous (*Clp36*$^{+/-}$) and homozygous (*Clp36*$^{-/-}$) knockout mice, western blot was performed with platelet lysates using the antibody recognizing the LIM domain of CLP36. The antibody detected a *Wt* protein of 36 kDa in *Clp36*$^{+/-}$ but could not detect any band of similar size in *Clp36*$^{-/-}$ platelet samples (Figure 38).

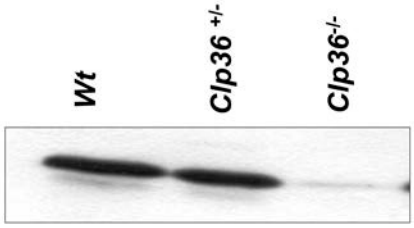

Figure 38: Genotyping of *Clp36*$^{-/-}$ mice by Western blotting: Western blot analysis with an anti-LIM domain of CLP36 specific antibody was performed to differentiate between *Clp36*$^{+/-}$ and *Clp36*$^{-/-}$ mice. In *Wt* and *Clp36*$^{+/-}$ platelets, CLP36 protein migrated at 36 kDa whereas; in *Clp36*$^{-/-}$ platelets the protein was absent.

4.3.3 *Clp36*$^{-/-}$ platelets spread normally on fibrinogen and exhibit normal clot retraction

The N terminal PDZ domain of the CLP36 binds to α-actinin in resting platelets and translocates as the CLP36-α-actinin complex to the actin cytoskeleton upon platelet activation.[115] To directly test the role of CLP36 especially its PDZ domain in platelet actin rearrangements upon agonist stimulation, *Wt* and *Clp36*$^{-/-}$ platelets were allowed to spread on fibrinogen-coated coverslips in the presence of thrombin (0.01 U/mL). Surprisingly, *Clp36*$^{-/-}$ platelets could form filopodia and lamellipodia and could spread after 20 min. The kinetics of spreading was similar in *Clp36*$^{-/-}$ platelets in comparison to *Wt* control platelets. The numbers of fully spread platelets after the observation period of 20 min were similar between the two groups (Figure 39).

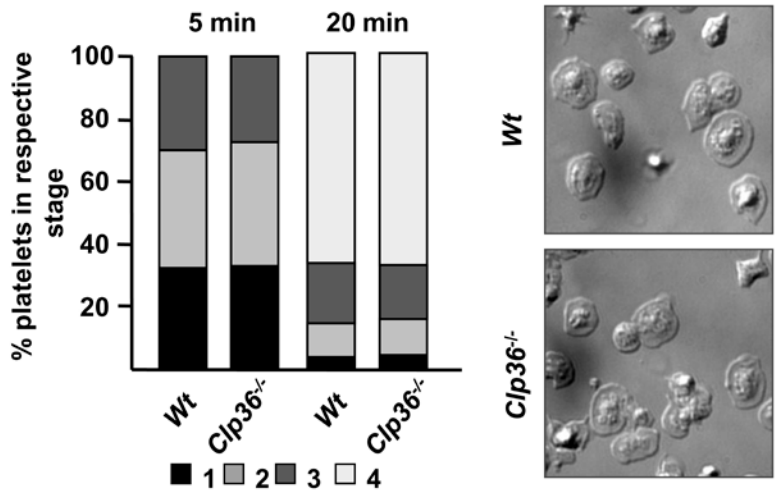

Figure 39: *Clp36*$^{-/-}$ platelets can spread on fibrinogen upon thrombin stimulation. Washed platelets of *Wt* and *Clp36*$^{-/-}$ mice were stimulated with 0.01 U/mL thrombin and were allowed to spread on 200 µg/mL of immoblized fibrinogen coated coverslips. Representative differential interference contrast (DIC) images of 4 individual experiments from the indicated time points (right) and statistical evaluation of the percentage of spread platelets at different spreading stages (left). 1: no filopodia, 2: only filopodia, 3: filopodia and lamellipodia, 4: full spreading.

Clot formation and retraction requires outside-in signaling of integrins along with cytoskeletal contractibility of platelets.[128] Therefore clot formation in prp of *Wt* and *Clp36*$^{-/-}$ mice was induced by high doses of thrombin (3 U/mL) in the presence of high Ca^{2+} concentrations (20 mM) and clot retraction was monitored under non-stirring conditions over time (Figure 40). Consistent with the results of the spreading assay, no differences were observed in the beginning of clot formation and also at the later time points clot retraction was found to be similar between *Wt* and *Clp36*$^{-/-}$. The above results indicated that CLP36 is dispensable for actin rearrangements and stress fiber formation upon platelet activation.

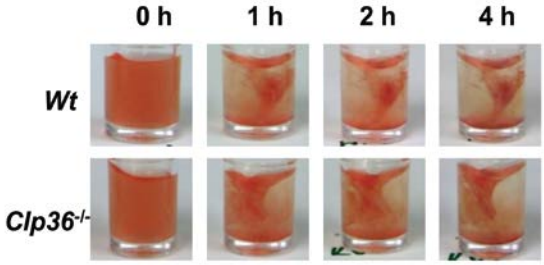

Figure 40: *Clp36*$^{-/-}$ platelets show normal clot retraction. Clot retraction of Wt and *Clp36*$^{-/-}$ prp upon activation with 3 U/mL thrombin in the presence of 20 mM $CaCl_2$ at the indicated time points. Representative images of 3 different experiments are depicted

4.3.4 *Clp36*$^{-/-}$ mice display unaltered platelet life span and normal platelet surface glycoprotein expression

Platelet biogenesis and proplatelet formation are mediated by a microtubule extension but also requires reorganization of the actin-spectrin cytoskeleton.[135] To study whether CLP36 plays a role in actin rearrangements during megakaryopoesis, platelet life span in *Clp36*$^{-/-}$ and *Wt* was determined *in vivo*. Circulating platelets were labeled with a fluorescent non-cytotoxic anti GPIX antibody derivative injected into mice and the labeled platelet population was monitored by flow-cytometry over time. One hour after antibody treatment, >90% of circulating platelets were labeled in both *Clp36*$^{-/-}$ and *Wt* mice and this platelet population constantly declined over 5 days in both groups (Figure 41A). To further investigate *Clp36*$^{-/-}$ platelets in more detail, the mean platelet volume, and surface expression of major surface receptors like GPIb-V-IX, GPVI, Clec-2 and β1 and β3 integrins were analyzed. The abundance of these platelet surface receptors was found to be normal (Figure 41B). Thus, these findings demonstrated that CLP36 is dispensable for platelet production and the absence of CLP36 does not interfere with platelet production and expression of major platelet receptors.

A

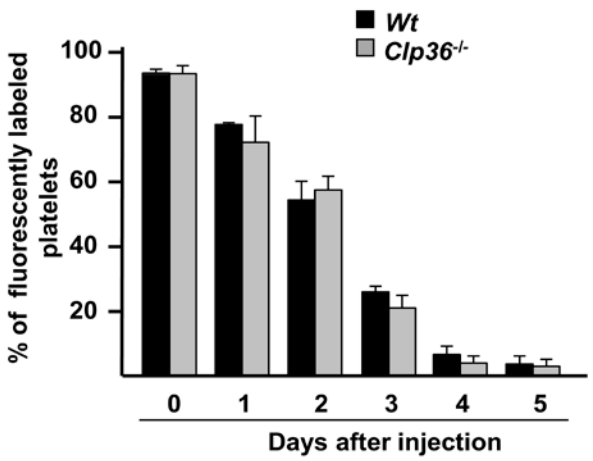

B

	Wt	Clp36$^{-/-}$
GPIb	420 ± 36.0	406 ± 30.0
GPV	316 ± 45.6	333 ± 27.3
GPIX	525 ± 28.0	510 ± 21.0
GPVI	27 ± 3.6	28 ± 5.6
CD9	1700 ± 220.0	1679 ± 142
GPIIbIIIa	589 ± 62.0	626 ± 46.0
Integrin α	70 ± 6.0	83 ± 4.3
Integrin β1	146 ± 4.2	175 ± 1.5
Clec2	124 ± 13.0	135 ± 7.0
Platelets (nL^{-1})	120 ± 39.0	108 ± 10.0
MPV(fl)	5.1 ± 0.16	5.3 ± 0.2

Figure 41: Normal surface glycoprotein expression and platelet life span in *Clp36*$^{-/-}$ mice.
(A) Platelet life span was determined by percentage of fluorescently labeled platelets in *Wt* and *Clp36*$^{-/-}$ mice over a 5 day period after i.v. injection of a Dylight488 anti-GPIX Ig derivative (0.5 mg/kg), (n=5). (B) Expression levels of prominent glycoproteins were determined by flow cytometry. Diluted whole blood from the indicated mice was incubated with FITC-labeled antibodies at saturating concentrations for 15 min at RT and platelets were analyzed directly. Results are expressed as mean fluorescence intensity ± SD (n=5) and are representative of 3 individual experiments. Platelet count and platelet size were determined using a Sysmex automated cell analyzer.

4.3.5 Enhanced GPVI signaling in *Clp36*$^{-/-}$ platelets

Platelet activation involves inside out activation of αIIbβ3 integrin and release of granule content with both the processes requiring actin rearrangements. To test the functional consequences of the absence of CLP36 on platelet activation, flow cytometric analysis of integrin αIIbβ3 activation using the JON/A-PE antibody[118] and P-selectin surface exposure as a marker of α-granule release were analyzed for *Wt* and *Clp36*$^{-/-}$ platelets upon agonist stimulation. This experimental setting involved the use of highly diluted platelet suspension and thus the accumulation of released secondary mediators is largely excluded. Activation of *Clp36*$^{-/-}$ platelets was normal in response to the GPCR agonists ADP, thrombin and U46619. In contrast, in response to GPVI agonist CRP, *Clp36*$^{-/-}$ platelets displayed a markedly increased integrin activation and degranulation. This effect was most evident at lower agonist concentrations and was similar to the aggregation responses observed in *Clp36*$^{\Delta LIM}$ platelets (Figure 42).

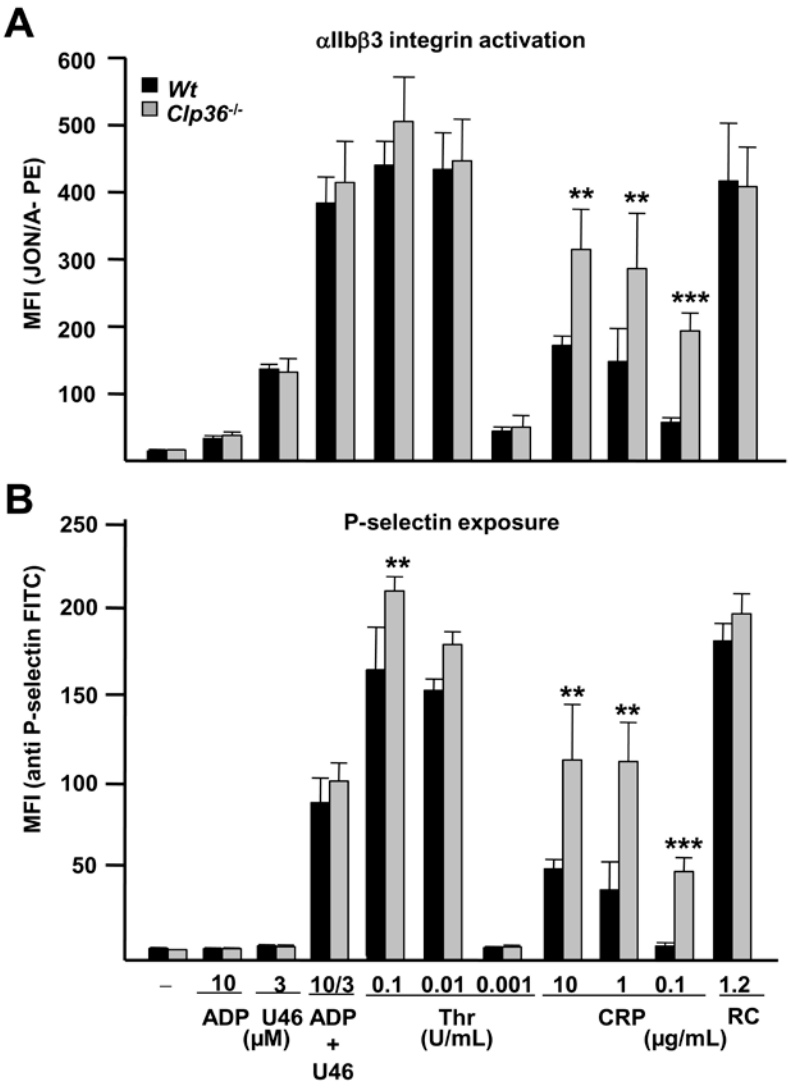

Figure 42: Increased integrin activation and α-granule release in *Clp36*$^{-/-}$ platelets upon GPVI stimulation. (A) Flow cytometric analysis of integrin αIIbβ3 activation (binding of JON/A-PE) and (B) degranulation-dependent P-selectin exposure in *Wt* and *Clp36*$^{-/-}$ platelets in response to the indicated agonists. Results are given as mean fluorescence intensities (MFI) ± SD of 4 mice per group and are representative of 3 individual experiments. ***P*<0.01, ****P*<0.001.

4.3.6 *Clp36*$^{-/-}$ platelets display enhanced aggregation in response to GPVI activation and display an increased thrombus formation on collagen under flow

Platelet shape change and aggregation upon agonist stimulation requires actin reorganization which is mediated by complex signaling machinery. CLP36 has been implicated in actin stress fiber formation and loss of the PDZ domain of CLP36 has been shown to result in altered cell morphology. To further investigate the role of the PDZ domain of CLP36 in actin rearrangements leading to platelet shape change and aggregation, platelet aggregation was performed using different agonists. *Clp36*$^{-/-}$ platelets aggregated normally in response to GPCR

agonists (thrombin, ADP) at all tested concentrations. In contrast, upon stimulation with the GPVI agonist, CRP, a markedly enhanced aggregation response at low doses of the agonist was observed in *Clp36*$^{-/-}$ platelets which were comparable to that observed for *Clp36*$^{\Delta LIM}$ platelets. At higher concentrations of GPVI agonists, no significant difference in aggregation was detected between *Wt* and *Clp36*$^{-/-}$ platelets (Figure 43). Notably, *Clp36*$^{-/-}$ platelets did not aggregate spontaneously or upon stimulation with epinephrine (data not shown), indicating that the platelets were not *per se* in a pre-activated state.

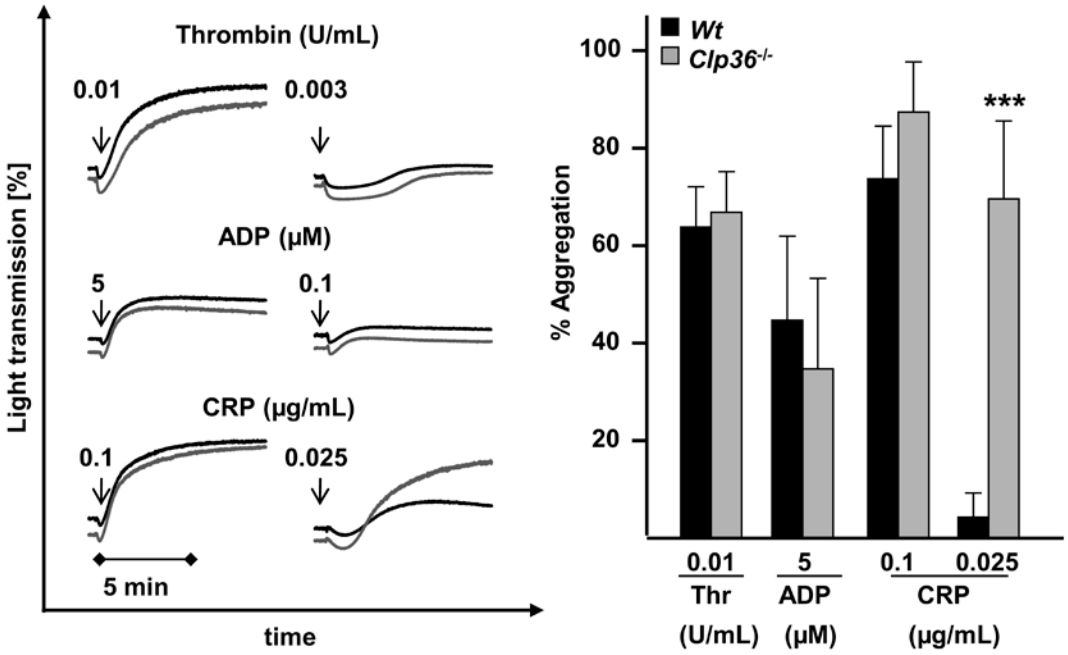

Figure 43: Enhanced GPVI-induced aggregation in *Clp36*$^{-/-}$ platelets. Washed platelets from *Wt* (black line) or *Clp36*$^{-/-}$ (grey line) mice were stimulated with the indicated agonists and light transmission was recorded on a Fibrintimer 4-channel aggregometer. Bar graphs representations of results obtained by aggregometry. Results are given as the mean percent of aggregation ± SD.

GPVI-collagen interaction plays a major role in the process of thrombus formation under flow conditions. To study the effect of enhanced αIIbβ3 integrin activation and degranulation of *Clp36*$^{-/-}$ platelets in response to GPVI signaling on thrombus formation under flow, whole anti-coagulated blood was perfused over collagen at physiological shear rates. At intermediate shear rate of 1000 s^{-1} which modeled flow conditions in large arteries, *Clp36*$^{-/-}$ platelets displayed an increased platelet surface coverage when compared to the *Wt* controls. The increased ability to form aggregates correlated with enhanced three dimensional thrombus volumes observed under flow conditions. These results reveal a significant influence of CLP36 on the negative regulation of the GPVI signaling in platelets under flow. (*Wt*: 38.4± 4.1 % , *Clp36*$^{-/-}$: 60.5± 9.8 %, *P*<0.001: Figure 44). Interestingly, the result obtained for *Clp36*$^{-/-}$ platelets was similar to that of *Clp36*$^{\Delta LIM}$ platelets, thus indicating on the one hand that CLP36 might act as a negative

regulator of GPVI signaling and on the other hand that this regulation is achieved by its C-terminal LIM domain.

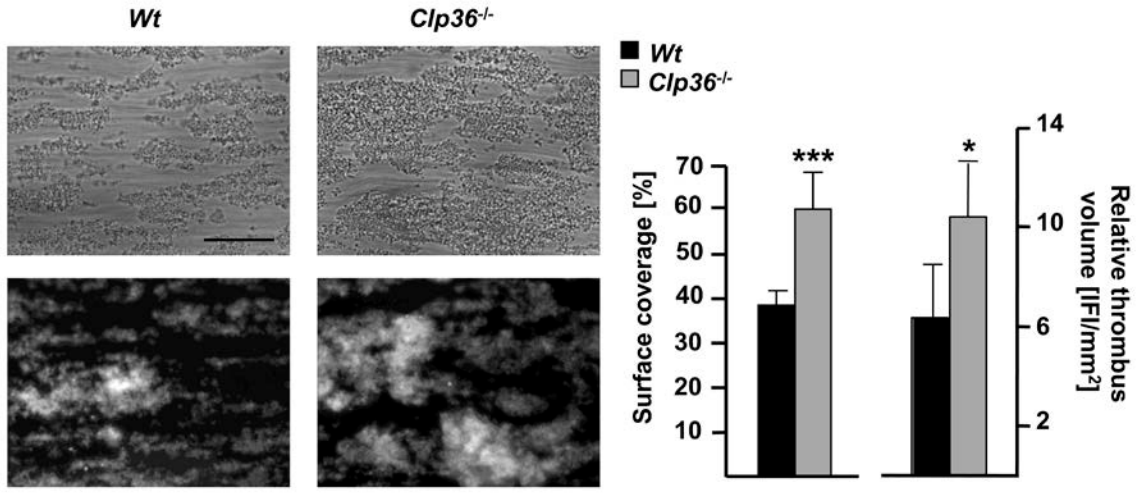

Figure 44: Increased thrombus formation of *Clp36*$^{-/-}$ platelets on collagen under flow. Heparinized whole blood from *Wt* and *Clp36*$^{-/-}$ was perfused over immobilized collagen (0.2 mg/mL) at a shear rate of 1000 s^{-1} (4 min) followed by 1 min perfusion with Tyrode HEPES buffer at the same shear rate. Representative phase contrast images (upper panel) and fluorescent images (platelets stained with anti-GPIX-DyLight488; lower panel) are shown (bar: 50 µm). Right panel: mean surface coverage and relative thrombus volume ± SD (n=10 per group).

4.3.7 *Clp36*$^{-/-}$ mice are protected from ischemic brain infarction

To determine whether the increased thrombus formation *in vitro* observed in *CLP36*$^{-/-}$ mice also affects the outcome in *in vivo* experimental settings; mice were challenged in a tMCAO model as described in result section for *Clp36*$^{\Delta LIM}$ mice. The experiments were performed in collaboration with Dr. Peter Kraft from the Department of Neurology, Würzburg.

To initiate transient cerebral ischemia, a thread was advanced through the carotid artery into the middle cerebral artery to reduce cerebral blood flow by >90%[36] and allowed to remain for one hour (tMCAO) after which reperfusion was allowed. The extent of infarction was quantified 24h after reperfusion on 2, 3, 5-triphenyltetrazolium chloride (TTC)-stained brain slices. In *Clp36*$^{-/-}$ mice, brain infract volumes were reduced by 50% of the infract volumes in *Wt* mice (*Clp36*$^{-/-}$: 62 ± 42 mm^3 vs *Wt*: 113 ± 20 mm^3; *P*<0.001; Figure 45A). This reduction in *Clp36*$^{-/-}$ mice in ischemic lesions also resulted in significantly fewer neurological deficits compared to *Wt*, determined by the Bederson score assessing the global neurological function (*Clp36*$^{-/-}$: 1.5 ± 0.5 vs *Wt:* 3.1 ± 0.2; *P*<0.001; Figure 45B) and grip test which measures motor function and coordination of these mice (*Clp36*$^{-/-}$: 3.6 ± 0.8 vs *Wt:* 2.3 ± 0.8; *P*<0.05; Figure 45C). These data were in contrast to the observed *in vitro* data where the *Clp36*$^{-/-}$ mice displayed an increased

thrombus formation under static and flowing conditions. As CLP36 is widely expressed including its expression in endothelium vascular wall lining. The observed protection in tMCAO could be due to the fact that CLP36 might be required for the proper morphology of the endothelial lining and this might affect thrombus formation in brain vessels.

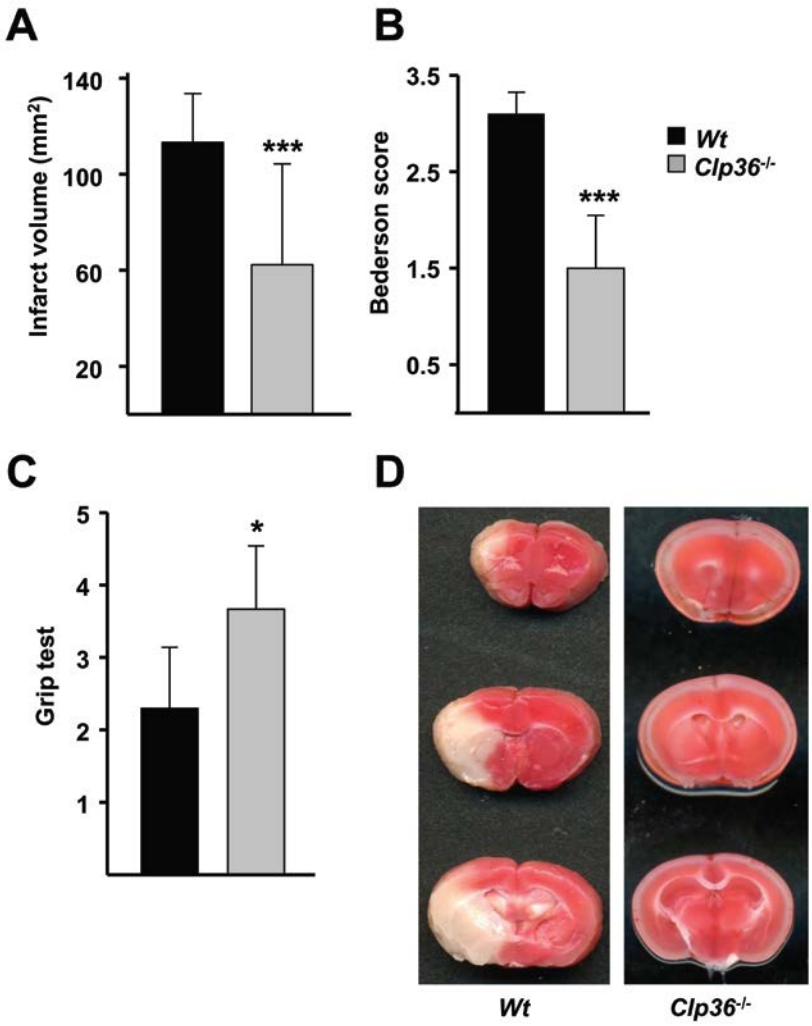

Figure 45: ***Clp36*$^{-/-}$ mice are protected in the tMACO model**. Formation of cerebral brain infarction and consequential neurological defects were investigated in a murine stroke model. (A) Brain infarct volumes in *Wt* and *Clp36*$^{-/-}$ mice presented as mean ± SD. (B) Bederson score, and (C) Grip test determined 24 h after tMCAO. (D) Representative images of the three corresponding coronal sections from *Wt* and *Clp36*$^{-/-}$ mice stained with TTC 24 h after tMACO. The infarct areas are white in color. *, P<0.05, ***, P<0.001.

5 DISCUSSION

Platelets represent an essential component of the blood system as they safeguard the vasculature at the sites of injury. However, under pathological conditions, uncontrolled platelet activation and aggregation may also lead to full vessel occlusion or embolism resulting in life threatening diseases like myocardial infarction or stroke. These cardiovascular diseases are a leading cause of mortality worldwide.[136] Therefore, anti-platelet therapy using agents such as aspirin, clopidogrel and integrin αIIbβ3 antagonists have been beneficial in the prophylaxis and treatment of cardiovascular diseases[137] but their use is limited because they often induce increased bleeding complications. Thus, a comprehensive analysis of platelet activation and their respective signaling pathways has emerged as an essential and developing field in cardiovascular research.

In recent years, the mouse model has become an essential tool for platelet research. The manipulation of the mouse genome by gene targeting approaches has proven as a milestone in thrombosis research. The analysis of genetically modified mice in different *in vivo* models of thrombosis and ischemic stroke has been instrumental for the identification of potential antithrombotic therapeutical targets. It is important to note that some differences in the expression or function of platelet proteins between humans and mice exist. Therefore, the results obtained in mice cannot be directly transferred to the human situation.[138] Nevertheless, the knowledge obtained from the mouse system may serve as the basis for the development of new antithrombotic strategies.

In this study, the role of DAG activated ROCE channel TRPC6 in platelet function and thrombus formation was investigated by using knockout mice. The results presented here establish TRPC6 as the only relevant DAG activated Ca^{2+} channel to be expressed in murine platelets. Loss of TRPC6 did not affect major platelet functions. Further, the role of PDLIM family member CLP36 was analyzed using a knockin and a knockout approach. Our results reveal a critical role of CLP36 in the regulation of GPVI signaling that is mediated by the C-terminal LIM domain of the protein.

5.1 Defective diacylglycerol-induced Ca^{2+} entry but normal agonist-induced activation responses in TRPC6-deficient mouse platelets

Agonist induced platelet activation results in the release of Ca^{2+} from intracellular stores followed by Ca^{2+} influx mediated by various channels present on the platelet plasma membrane. These channels include SOC channel- *calcium-release activated calcium modulator 1* (CRACM1) or Orai1, channels of the TRP family (TRPC1 and TRPC6) and the purinergic receptor, P2X1.

Studies on *Stim1*$^{-/-}$ and *Orai1*$^{-/-}$ platelets established these two proteins as key players of store operated calcium entry (SOCE) in platelets, with STIM1 being responsible for the detection of Ca^{2+} depletion of the intracellular stores and for the regulation of Orai1, the major SOC channel on the platelet surface.[58,59] The reduced Ca^{2+} responses in platelets from knockout mice resulted in a significant protection in different *in vivo* models of thrombotic diseases due to reduced thrombus stability and profound protection against ischemia/reperfusion induced brain injury. Interestingly, despite the reduced Ca^{2+} responses to both PLCβ and PLCγ activating platelet agonists, both *Stim1*$^{-/-}$ and *Orai1*$^{-/-}$ platelets showed unaltered αIIbβ3 activation, aggregation and degranulation through the GPCR/PLCβ pathway and only a mild defect in response to GPVI/ PLCγ2 agonists in the absence of flow *in vitro*,[58,59] indicating the role of alternative Ca^{2+} entry mechanisms mediated by so far unknown Ca^{2+} channels in platelets. *Trpc1* knockout mice showed no significant defects in platelet Ca^{2+} homeostasis or function.[62] Studies performed on *P2X1*$^{-/-}$ platelets showed decreased aggregation and granule release in response to low doses of the GPVI agonist collagen whereas these platelets responded normally to GPCR agonists. Platelets from *P2X1*$^{-/-}$ mice showed reduced thrombus formation at higher shear rates both *in vitro* and *in vivo*.[139] Conversely, over-expression of the receptor in mice resulted in a pro-thrombotic phenotype.[140]

TRPC6 was found to be expressed in megakaryocytes and platelets of both humans and murine mice.[141-143] Upon receptor stimulation, DAG produced by different PLC isoforms was shown to activate TRPC6 directly in the plasma membrane[121] and TRPC6 was proposed to be the major DAG activated ROC channel in human platelets.[141] The exact role of the DAG-operated ROC channel TRPC6 in platelet activation and thrombus formation remained elusive. The present study used TRPC6-deficient mice to investigate the contribution of TRPC6-mediated Ca^{2+} entry in PLC-DAG mediated signaling and the impact of TRPC6 deficiency on platelet function *in vitro* and *in vivo*. *Trpc6*$^{-/-}$ platelets displayed unaltered integrin αIIbβ3 activation, degranulation, aggregation, adhesion and occlusive thrombus formation *in vivo* in comparison to *Wt* controls. Cytoskeletal reorganization and kinetics of spreading were also similar between *Wt* and *Trpc6*$^{-/-}$ platelets.

Using the membrane permeable DAG analogue OAG, the present study established TRPC6 as the major DAG activated ROCE channel to be expressed on murine platelets. In accordance with earlier reports, OAG induced a change in $[Ca^{2+}]_i$ of approximately 50-80 nM in *Wt* platelets.[144] Interestingly, this transient elevation of $[Ca^{2+}]_i$ was abolished in *Trpc6*$^{-/-}$ platelets (Figure 7A). Furthermore, Jardin *et al.* suggested a role for TRPC6 in the regulation of SOCE.[145] They reported that human platelets upon incubation with an anti-human TRPC6 antibody resulted in a reduced TG or 2,5-di-(tert-butyl)-1,4-hydroquinone (TBHQ) induced Ca^{2+} influx.[122] The study showed that in human platelets, upon Ca^{2+} store depletion, TRPC6 rapidly interacted

with the STIM1-Orai1 complex and this association was displaced by human TRPC3 following stimulation with the DAG analogue, OAG.[145] The proposed model of dynamic coupling of TRPC6 with components of the SOCE and non-SOCE pathways suggested an essential role of TRPC6 in Ca^{2+} signaling and regulation of SOCE. However, this coupling mechanism cannot be extrapolated to murine platelets due to the lack of TRPC3 expression. Studies by DeHaven *et al.* suggested that activation of TRPC6 channel occurs by mechanisms dependent on PLC and does not involve its interactions with STIM1. They further demonstrated that TRPC6 and STIM1/Orai signaling occurred in different PM domains.[146] Interestingly, in the present study TG-induced SOCE was found to be unaltered in *Trpc6*$^{-/-}$ platelet and TRPC6 dependent Ca^{2+} influx in *Stim1*$^{-/-}$ and *Orai1*$^{-/-}$ platelets was found to be unaltered (data not shown). Therefore, the physiological significance of TRPC6 coupling to the SOC complex, if there is any, remains elusive. PKC isoforms have been shown to play an important role in platelet function by regulating many diverse signaling events.[144,147,148] Platelets deficient in PKCα or PKCβ displayed reduced Ca^{2+} signaling, but in the absence of PKCθ isoform these responses were found to be enhanced.[144,148] Studies performed by Bousquet *et al.* and Kawasaki *et al.* proposed PKC-mediated phosphorylation of TRPC6 and Orai1 in mammalian cells which resulted in the inhibition of these channels.[63,149] To study whether PKC mediated phosphorylation regulates TRPC6 channel activity, OAG-induced Ca^{2+} entry was measured in presence of the broad spectrum PKC inhibitor, Gö6983. Interestingly, the Ca^{2+} entry was further potentiated in *Wt* platelets, but this effect was found to be absent in *Trpc6*$^{-/-}$ platelets, indicating that PKC negatively regulates TRPC6 function (Figure 7B). The functional consequences of the TRPC6 phosphorylation mediated by PKC isoforms (PKCα, PKCβ and PKCθ) needs to be addressed. PMA activates PKC and has been shown to enhance purinoreceptor-activated ROCE[150] and non-capacitive Ca^{2+} entry[151] thereby stimulating platelet activation. The molecular identity of the Ca^{2+} channels involved in this process is still unclear. Interestingly, PMA induced integrin αIIbβ3 activation and P-selectin exposure was found to be unaltered in *Trpc6*$^{-/-}$ platelets compared to *Wt* controls.

To study the role of TRPC6 in intravascular thrombus formation, *Trpc6*$^{-/-}$ mice were subjected to different *in vivo* thrombosis models. The kinetics of thrombus formation were studied in different vascular beds, and types of injury including mechanical injury of the abdominal aorta as well as $FeCl_3$ induced injury on mesenteric arterioles and carotid artery. No differences in initiation of thrombus formation and complete vessel occlusion were observed between *Wt* and *Trpc6*$^{-/-}$ mice (Figure 16). Moreover, the hemostatic function in these mice was also comparable to Wt controls. Interestingly, Paez Espinosa *et al*.[152] recently demonstrated a significant hemostatic defect and protection from arterial thrombus formation in the *in vivo* model of $FeCl_3$ induced chemical injury on the carotid artery in *Trpc6*$^{-/-}$ mice. Their results stand in contrast to the

observation reported in the presented thesis. These discrepancies are difficult to explain, but they are most likely due to differences in the experimental conditions. The severity of the injury induced may vary depending on the used $FeCl_3$ concentration, application method via liquid drop or filter paper and the exposure time of the vessel to the applied chemical. Similarly, tail bleeding times, a measure of hemostatic function, can vary depending on the size of the injury as well as external conditions used while determining the bleeding times. Further studies will be required to address these questions directly. TRPC6 is highly expressed in vascular smooth muscle cells and *Trpc6*$^{-/-}$ mice displayed enhanced agonist-induced smooth muscle contractility.[71] This was later found to be due to upregulated expression of the TRPC3 channel in TRPC6 deficient vascular smooth muscle cells.[71] However, since murine platelets do not express TRPC3[142] (Figure 6B) loss of TRPC6 function cannot be compensated by this channel. Recently, Weissmann *et al*. proposed an important role played by TRPC6 in development of lung ischemia after *lung ischemia reperfusion induced oedema* (LIRE). Lung endothelial cells of *Trpc6*$^{-/-}$ mice showed attenuated ischemia and were protected in the LIRE model.[153] Based on expression profiling,[154] and the analysis of STIM1 and Orai1 function in platelets[59,130,155] it is concluded that STIM1-Orai1 mediated SOCE is the dominant Ca^{2+} entry pathway which may dominate the role of TRPC6 mediated Ca^{2+} influx. Alternatively, other so far unknown Ca^{2+} channels could also compensate for the lack of TRPC6. However, these channels – if existent - are not members of the TRPC family and cannot be activated by DAG.

Ca^{2+} is a central and common second messenger downstream of most signaling pathways in virtually all cells. Thus, regulators of Ca^{2+} signaling might be interesting targets for platelet inhibition.[156] Indeed, studies performed on mice lacking molecules like STIM1, Orai1 and P2X1 displayed a strong antithrombotic protection *in vivo* with only a mild hemostatic defect. Both *Stim1*$^{-/-}$ and *Orai1*$^{-/-}$ bone marrow chimeras were found to be largely protected against ischemia/reperfusion induced brain injury without any detectable tendency towards intracranial hemorrhage.[58,59] This protection was clinically relevant, because the global motor and neurological function of these animals were significantly better after ischemia than those of control mice. The ROC channel, P2X1 is another attractive antithrombotic candidate molecule. Mice deficient in the protein were found to be protected in models of laser-induced arterial thrombosis, and collagen/epinephrine-induced pulmonary thromboembolism, whereas their hemostatic capacity was normal.[139] Since many of the Ca^{2+} signaling molecules are widely expressed, a cell–specific targeting of platelets would be required to achieve selective antithrombotic therapy. The presented study revealed clear evidence for the central role of TRPC6 in DAG-activated ROCE in murine platelets. Furthermore, it was shown that platelet SOCE occurs independently of TRPC6 channel function. But, the lack of TRPC6 had no effect on arterial thrombus formation and hemostasis. It will be of interest to study TRPC6 function under pathological conditions or in case of gain of function mutations.

5.2 CLP36 as a negative regulator of GPVI signaling in mouse platelets

Platelet activation by multiple signaling pathways leads to shape change, release of intracellularly stored granules, and spreading on immobilized ligands. The molecular basis and the key regulators of actin dynamics essential for stress fiber formation and platelet shape change are an area of active research. Studies performed in our lab on Rho family GTPases like Rac1, Cdc42 and RhoA using conditional knockout approaches has allowed novel insights into their role in platelet function and contribution to thrombus formation under *in vivo* conditions. We demonstrated that Rac1 is essential for platelet lamellipodia formation, but also for PLCγ2 activation downstream of the collagen receptor GPVI.[129] The signaling defect resulted in a profound protection of Rac1-deficient mice from arterial thrombosis. On the other hand, platelets from Cdc42-deficient mice showed that the protein is not per se required for filopodia formation upon platelet activation. Interestingly, these platelets displayed an increased granule release after activation that translated into accelerated thrombus formation *in vivo*.[157] RhoA has been implicated as a critical mediator of stress fiber formation in numerous cell types.[158-160] A recent study from our group by Pleines *et al.* indicated that RhoA deficient platelets could spread upon thrombin stimulation and RhoA was only partially involved in stress formation and proper granule centralization. However, the study revealed a role of RhoA in the organization of microtubule structures in spread platelets. These results suggested that microtubule assembly may be regulated by the Rho/ROCK pathway upon platelet activation (Figure 46A, B). Interestingly, RhoA deficiency resulted in protection from irreversible thrombus formation *in vivo* caused mainly by impaired degranulation-dependent release of soluble mediators.[161]

The actin-depolymerizing factor (ADF)/cofilin family consists of F-actin severing proteins like ADF and non-muscle cofilin. The studies done by Bender *et al.* demonstrated that *Adf*$^{-/-}$ platelets spread with the same kinetics as control platelets. In contrast, n-cofilin platelets displayed a profoundly delayed filopodia and subsequent lamellipodia formation. Stimulated emission depletion (STED) microscopy revealed normal actin cytoskeleton reorganization (Figure 46C). Deletion of both the proteins in platelets led to severely impaired actin rearrangements.[162]

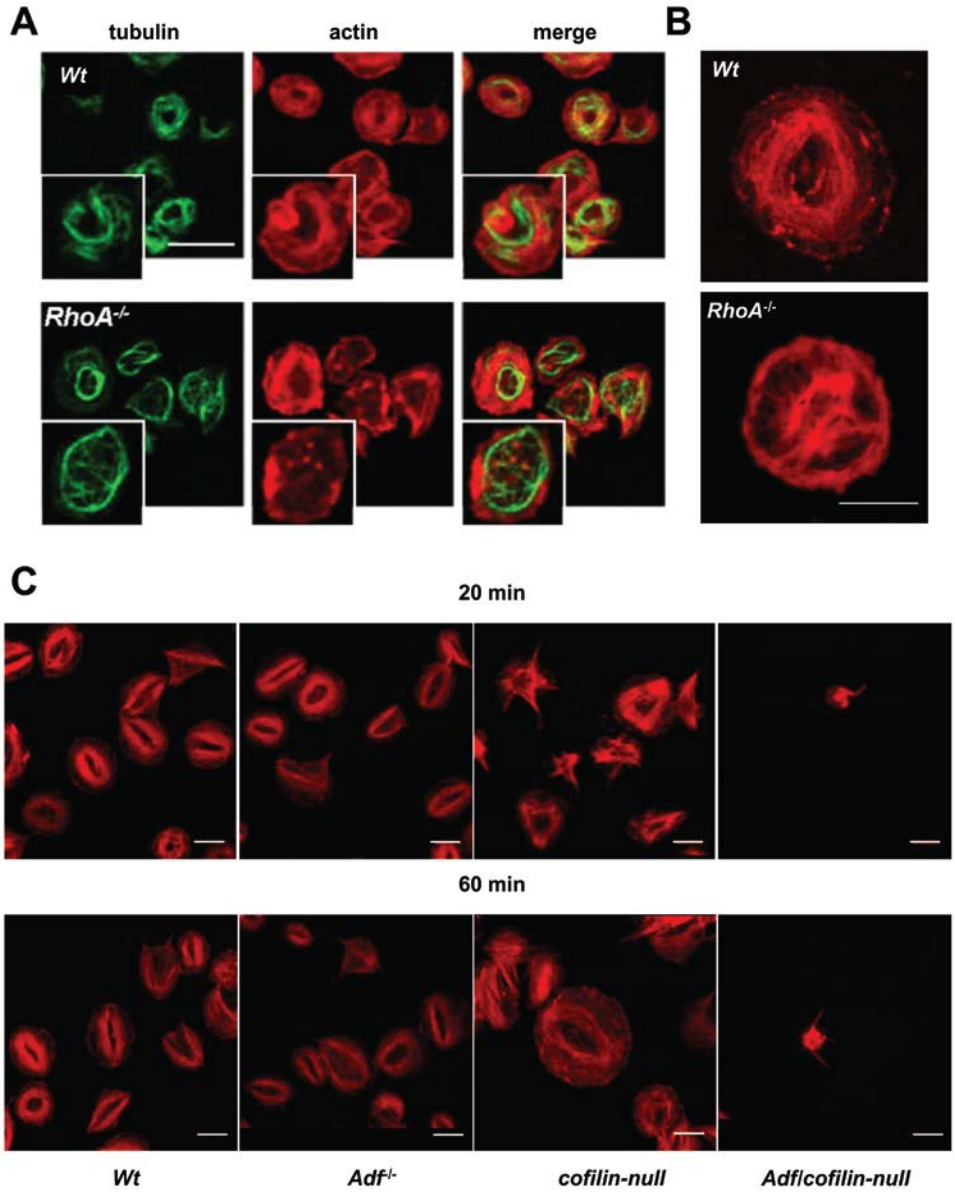

Figure 46: (A) Analysis of filamentous actin (red) and tubulin (green) structure in spread (30 min) *RhoA*$^{-/-}$ and *Wt* platelets by confocal microscopy. Scale bar represents 5 µm. (B) Visualisation of actin cytoskeleton of *RhoA*$^{-/-}$ and *Wt* platelets by STED microscopy 30 min after spreading. Scale bar represents 5 µm (C) STED microscopy of *Wt*, *Adf*$^{-/-}$, *cofilin-null* and *Adf*$^{-/-}$*/cofilin-null* platelets spread for 20 and 60 min on fibrinogen and stained with phalloidin. Scale bar represents 3 µm.

Members of the PDLIM family have been well characterized for their association with actin stress fibers and to the focal adhesion complex via α-actinin.[89,101,115,163] PDLIMs were proposed to play critical roles in stress fiber formation[164] and integrin mediated focal adhesion.[113] The PDLIM protein family contains muscle specific and ubiquitously expressed proteins that associate with actin cytoskeletal proteins (β-tropomyosin, α-actinin) and different kinases (Src, Clik, PKC) to stress fibers and focal adhesion complexes. Muscle specific PDLIM proteins are associated with Z-disc structures via α-actinin and their loss leads to cardio- and skeletal myopathies in mice.[96,165] In the presented thesis, the expression pattern of different PDLIM family members in

platelets was analyzed. Interestingly, only CLP36 was found to be expressed in platelets, indicating a unique role played by this protein in integrin mediated adhesion and stress fiber formation. Moreover, immunofluorescence confocal microscopy on spread mouse platelets showed CLP36 to be localized throughout the body of the platelet along the actin stress fibers with dotted appearance as previously described in human platelets by Bauer *et al*..[115] CLP36 was found to be absent from the central core of the platelet where the granules are localized (Figure 19). In order to study the function of CLP36 and its C-terminal LIM domain in platelets, *Clp36*$^{-/-}$ and *Clp36*$^{\Delta LIM}$ mice, respectively, were generated and analyzed. The targeting strategy used to generate *Clp36*$^{\Delta LIM}$ mice did not ablate CLP36 expression but resulted in the expression of a truncated CLP36 protein fused with β-GEO protein (termed as CLP36$^{\Delta LIM}$). *Clp36*$^{\Delta LIM}$ platelets expressing the chimeric protein displayed normal spreading, unaltered F-actin polymerization and stress fiber formation. Interestingly, the subcellular localization of the CLP36$^{\Delta LIM}$ protein in spread platelets was similar to *Wt* platelets (Figure 23). This could be attributed to the intact N-terminal PDZ domain of the chimeric CLP36 protein, which could still associate to the actin cytoskeleton. These data indicated that at least the LIM domain of CLP36 is not required for this association and CLP36 may regulate actin dynamics independently of its LIM domain. Surprisingly, *Clp36*$^{-/-}$ platelets could also form filopodia, lamellipodia and finally spread with similar kinetics as *Wt* platelets (Figure 39). Altogether, these findings indicated that CLP36 is dispensable for actin rearrangements in platelets. Bozulic *et al.* proposed CLP36 to be involved in the regulation of Ca^{2+} homeostasis in human platelets.[103] It was shown that the PDZ domain of CLP36 interacts with plasma membrane Ca^{2+}-ATPase (PMCA4b) and the authors speculated that this association might regulate late events during platelet activation, such as clot retraction and stability. Interestingly, no impairment of clot formation and retraction was observed in *Clp36*$^{\Delta LIM}$ and *Clp36*$^{-/-}$ platelets (Figure 25, Figure 40), indicating that CLP36 and its interaction with PMCA4b does not play an essential role in regulation of actin rearrangements, clot retraction and stability.

This is the first study describing the role of CLP36 and its LIM domain in platelet physiology using genetically modified mice. *Clp36*$^{\Delta LIM}$ and *Clp36*$^{-/-}$ mice developed normally without any obvious defects. Moreover, both mouse lines showed an unaltered platelet life span, platelet counts and glycoprotein expression profiles with a slightly but significantly increased platelet size thus indicating that CLP36 is dispensable for platelet production. These results stand in contrast to other actin organizing protein family members like RhoA, Cdc42 and Cofilin whose absence resulted in thrombocytopenia and altered platelet production.[157,161,162]

Further characterization of *Clp36*$^{\Delta LIM}$ and *Clp36*$^{-/-}$ platelets displayed enhanced integrin αIIbβ3 activation and α– and dense–granule secretion in response to GPVI agonists. This selective hyperresponsiveness of the GPVI-ITAM- PLCγ2 cascade in *Clp36*$^{\Delta LIM}$ and *Clp36*$^{-/-}$ platelets was

mapped to abnormal function of downstream signaling molecules of GPVI that are not required for GPCR signaling. It is known that the activating signal of PLCγ2 is different from that of PLCβ based on structural differences. Amino acid sequences of PLCγ2 and PLCβ diverged during evolution. PLCγ2 contains two SH2 domains, a single SH3 domain and PH domain which are absent in PLCβ.[166] SFKs bind and phosphorylate these domains and thereby regulate subcellular localization and enzymatic activity of PLCγ2, but not of PLCβ. The increased activation also resulted in enhanced aggregation under stirring conditions in response to various GPVI agonists, and the formation of larger aggregates on collagen under flow conditions. Of note, the surface expression of GPVI on both *Clp36*$^{-/-}$ and *Clp36*$^{\Delta LIM}$ platelets was not altered when compared to *Wt* controls excluding the possibility of enhanced signaling due to higher receptor number on platelet surface.

Clp36$^{\Delta LIM}$ platelets displayed an enhanced IP_3 production upon GPVI activation that further on led to a faster and enhanced Ca^{2+} release from the intracellular stores which subsequently increased store-operated Ca^{2+} entry (SOCE). This altered Ca^{2+} signaling was more pronounced at lower agonist concentrations where the *Wt* platelets failed to respond. Notably, passive store depletion with thapsigargin (TG) did not lead to any differences in the kinetics of store release or SOCE between *Wt* and *Clp36*$^{\Delta LIM}$ platelets (data not shown). These results demonstrated that the LIM domain of CLP36 has no direct effect on the regulation of Ca^{2+} store depletion or on the assembly and activation of SOC complex. Based on the integrin activation and degranulation results, obtained for *Clp36*$^{-/-}$ platelets, similar IP_3 production and Ca^{2+} mobilization are expected but further experiments are required to clarify the role of CLP36 protein in these processes.

GPVI signaling upon activation involves a series of tyrosine phosphorylation cascades that finally culminate in PLCγ2 activation and subsequent hydrolysis of PIP2 into IP_3 and DAG. IP_3 in turn is responsible for emptying of intracellular Ca^{2+} stores. Increased integrin activation, degranulation, aggregation and enhanced Ca^{2+} mobilization in response to the GPVI agonists collagen and CRP observed in *Clp36*$^{\Delta LIM}$ platelets suggested a modulating role of the LIM domain of CLP36 in platelet signaling downstream of GPVI receptor. Interestingly, an increased degree of phosphorylation was observed for *Clp36*$^{\Delta LIM}$ platelets at very low concentrations of CRP, while *Wt* platelets displayed only a weak or no tyrosine phosphorylation profile at such low doses. The tyrosine phosphorylation blot of *Clp36*$^{\Delta LIM}$ platelets displayed phosphorylation of numerous platelet proteins, including proteins that co-migrated with PLCγ2, Fyn, Lyn and the FcRγ-chain (Figure 32). Since the whole GPVI signaling was found to be phosphorylated in the tyrosine phosphorylation blots, CLP36 may be a regulator of the GPVI signalosome at the top of the signaling cascade. Several proteins have been identified by knockout approaches to negatively regulate GPVI-ITAM-PLCγ2 signaling, such as PECAM,[167] TULA-2[168] and CEACAM1.[169] Mice lacking these proteins, like *Clp36*$^{\Delta LIM}$ mice, display platelet hyperreactivity

towards GPVI agonists and a prothombotic phenotype *in vivo*, demonstrating the (patho-) physiological importance of the negative feedback loop that controls GPVI signaling in platelets. The identification of the phosphorylated proteins upon GPVI stimulation in *Clp36*$^{\Delta LIM}$ platelets remains to be determined.

The presented study proposed the LIM domain of CLP36 may regulate the localization and/or activity of tyrosine kinases in the GPVI signalosome, but the identity of these kinases remains yet to be determined. Using Expasy (Swiss Institute of Bioinformatics) a putative active binding site on the LIM domain of CLP36 was identified which could be phosphorylated by SFKs (Figure 47). The bioinformatic analysis indicated a possible interaction of CLP36 with SFKs that may influence signaling downstream of GPVI. This hypothesis was further strengthened by the previous observation that PDLIMs act as adapters between kinases and the actin cytoskeleton by associating on one hand to actin cytoskeleton via α-actinin or β-tropomyosin with their PDZ domain and on the other hand, to different kinases via their LIM domains.

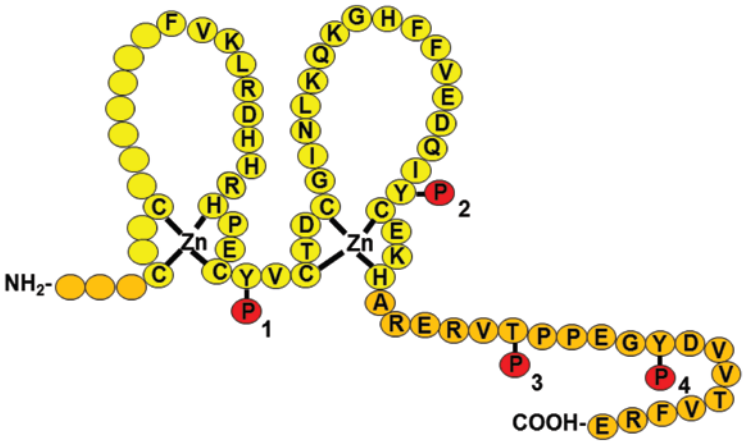

Figure 47: Putative active phosphorylation sites of the LIM domain of CLP36. P1: Src/SH2 binding site, P2: *Anaplastic lymphoma kinase* (ALK) phosphorylation site P3: CLIK1 kinase phosphorylation site, P4: Src kinase phosphorylation site identified by mass spectrometry; Expasy, Proteome database.

The analysis of *Clp36*$^{\Delta LIM}$ platelets showed their hyperactivation specific to GPVI signaling. But surprisingly, *Clp36*$^{\Delta LIM}$ and *Clp36*$^{-/-}$ mice displayed a significant protection from ischemic stroke. Previous studies performed by other groups show a wide expression of CLP36 in different cell types and tissue. In order to study the cause of contradictory *in vitro* and *in vivo* results and a possible role of CLP36 in maintaining vascular endothelial wall integrity, criss-cross bone marrow chimeras were generated. Interestingly, the *in vivo* analysis of the *Wt* mice transplanted with *Clp36*$^{\Delta LIM}$ bone marrow displayed significantly faster occlusive thrombus formation when compared to the *Wt* and *Clp36*$^{\Delta LIM}$ mice transplanted with *Wt* bone marrow. In contrast, tail bleeding times were not altered in these mice suggesting that the negative regulation of GPVI signaling may be particularly important to prevent intravascular occlusive thrombus formation.

The contrasting in *vivo* tMCAO results obtained for the *Clp36*$^{\Delta LIM}$ mice indicates the importance of CLP36 in other cell types including the cells lining the vascular endothelium. These results indicated the important role played by CLP36 in maintaining the vessel wall integrity which is essential for a stable thrombus formation. This mouse model thus may serve as an important tool to improve the understanding of the mechanisms that regulate thrombus formation *in vivo*.

Taken together, this study for the first time demonstrated a role of CLP36 in thrombosis and hemostasis. The results presented in the thesis showed that absence of CLP36 in platelets does not interfere with actin rearrangements. But, the loss of the LIM domain of CLP36 in platelets leads to increased PLCγ2 activity downstream of GPVI and thereby accelerates Ca^{2+} store release and Ca^{2+} influx, which in turn induces faster α– and dense granule secretion and integrin activation. During the last years, GPVI has been established as an attractive antithrombotic target.[34,37] This is particularly due to the observation that injection of anti-GPVI antibodies (JAQ1-3) into mice induces specific downregulation of the receptor from the surface of circulating platelets, resulting in a long-term antithrombotic protection but only a minimal hemostatic defect.[34,37,38,170,171] All these observation have made the downstream signaling cascade of GPVI an interesting target for inhibition. Therefore, the pathway involving CLP36 downstream of GPVI might be an attractive target for new anti-platelet agents to prevent thrombotic events. These findings establish CLP36 as an important regulator of platelet activation and might be effective in the prophylaxis or treatment of ischemic cerebro- or cardiovascular diseases.

5.3 Concluding remarks and future plans

Historically, most of the understanding about platelet function was derived from the diagnosis of patients suffering from bleeding or thrombotic disorders and the subsequent identification and characterization of the involved proteins. In recent years, the advent of gene targeting and transgenic techniques in mice has proved to be a powerful *in vitro* and *in vivo* approach to manipulate and study platelets. Nearly all known adhesion molecules, receptors and many signaling molecules involved in platelet function have been knocked out, mutated, or overexpressed in mice. As a consequence, mice are frequently used as a model to explore the molecular mechanisms underlying hemorrhagic and thrombotic disorders. Although the relevance of mouse studies to human pathology may not always be straightforward, mice have already been proven to provide an excellent model to study thrombosis. However, great care should be taken in selecting a particular thrombosis model, conclusions drawn, and the limitations of each model need to be taken into account. Interestingly, gene deletions to study platelet function are sometimes associated with compensatory changes or additional new

findings. For example, in the current study with *Clp36$^{\Delta LIM}$ and Clp36$^{-/-}$* mice, the protection observed in tMCAO model gave new insights into the role of CLP36 in maintaining endothelium vessel wall integrity. Similarly, recent studies performed by Weissmann *et al*. extended our knowledge about TRPC6 function in endothelium. *Trpc6$^{-/-}$* mice were protected in lung ischemia–reperfusion-induced oedema (LIRE), a condition that causes pulmonary oedema induced by endothelial dysfunction.[172] Thus, manipulation of mouse genetics in combination with upcoming *in vivo* models can serve as a useful practical tool for identifying and validating novel targets for therapeutic intervention.

The presented thesis established TRPC6 as the only DAG activated Ca^{2+} channel in murine platelets. Loss of TRPC6 function in murine platelets cannot be compensated by other DAG-operated channels. Since Orai1 is already established as the major Ca^{2+} channel in platelets but its absence does not affect GPCR signaling, it will be interesting to study the consequences of lack of function of both the Ca^{2+} channels on platelet signaling and also on the process of megakaryopoiesis and platelet production. For this part of the study double mutant mice lacking Orai1 and TRPC6 will be generated and analyzed for *in vitro* and *in vivo* platelet function. Additionally, to study the functional relevance of *Trpc6$^{-/-}$* platelets in cerebral ischemia, *Trpc6$^{-/-}$* mice will be analyzed in the tMCAO model of ischemic stroke in collaboration with the Department of Neurology, University Hospital, Würzburg. It will be interesting to study the role played by TRPC6 in vascular endothelium in the development of ischemic stroke and in the model of collagen/epinephrine-induced pulmonary thromboembolism.

In the second part of the thesis, further studies are planned in our group to investigate the role of CLP36 in different *in vivo* models of thrombosis. The contrasting tMCAO results obtained for both *Clp36$^{\Delta LIM}$ and Clp36$^{-/-}$* mice makes them a useful model to study the mechanism of thrombus formation and various factors apart from platelets, decide thrombus formation at the sites of injury. This mouse model can provide useful insights in the study of thrombus formation and stroke development. In another set of experiments, the proteins involved in the regulation of the GPVI signalosome with special emphasis on CLP36 will be analyzed. The studies are planned to decipher the binding partners of CLP36 and how CLP36 regulates the GPVI signaling. The preliminary analysis has shown an association of CLP36 with the GPVI signalosome. Further experiments are planned in our group to study if the calpain-mediated cleavage of CLP36 regulates GPVI signaling upon platelet activation. In addition, it will be interesting to study if absence of CLP36 also has an impact on another ITAM signaling pathways, especially the Clec-2 signaling pathway in mouse platelets.

6 REFERENCES

1. Italiano JE, Jr., Patel-Hett S, Hartwig JH. Mechanics of proplatelet elaboration. *J Thromb Haemost*. 2007;5 Suppl 1:18-23.
2. Junt T, Schulze H, Chen Z, Massberg S, Goerge T, Krueger A, Wagner DD, Graf T, Italiano JE, Jr., Shivdasani RA, von Andrian UH. Dynamic visualization of thrombopoiesis within bone marrow. *Science*. 2007;317:1767-1770.
3. Ruggeri ZM. Platelets in atherothrombosis. *Nat Med*. 2002;8:1227-1234.
4. Murray CJ, Lopez AD. Mortality by cause for eight regions of the world: Global Burden of Disease Study. *Lancet*. 1997;349:1269-1276.
5. Bertozzi CC, Hess PR, Kahn ML. Platelets: covert regulators of lymphatic development. *Arterioscler Thromb Vasc Biol*. 2010;30:2368-2371.
6. Bertozzi CC, Schmaier AA, Mericko P, Hess PR, Zou Z, Chen M, Chen CY, Xu B, Lu MM, Zhou D, Sebzda E, Santore MT, Merianos DJ, Stadtfeld M, Flake AW, Graf T, Skoda R, Maltzman JS, Koretzky GA, Kahn ML. Platelets regulate lymphatic vascular development through CLEC-2-SLP-76 signaling. *Blood*. 2010;116:661-670.
7. Turitto VT, Baumgartner HR. Platelet interaction with subendothelium in flowing rabbit blood: effect of blood shear rate. *Microvasc Res*. 1979;17:38-54.
8. Savage B, Almus-Jacobs F, Ruggeri ZM. Specific synergy of multiple substrate-receptor interactions in platelet thrombus formation under flow. *Cell*. 1998;94:657-666.
9. Varga-Szabo D, Pleines I, Nieswandt B. Cell adhesion mechanisms in platelets. *Arterioscler Thromb Vasc Biol*. 2008;28:403-412.
10. Offermanns S. Activation of platelet function through G protein-coupled receptors. *Circ Res*. 2006;99:1293-1304.
11. Jackson SP, Nesbitt WS, Kulkarni S. Signaling events underlying thrombus formation. *J Thromb Haemost*. 2003;1:1602-1612.
12. Wettschureck N, Offermanns S. Rho/Rho-kinase mediated signaling in physiology and pathophysiology. *J Mol Med (Berl)*. 2002;80:629-638.
13. Clapham DE, Neer EJ. G protein beta gamma subunits. *Annu Rev Pharmacol Toxicol*. 1997;37:167-203.
14. Berridge MJ, Bootman MD, Roderick HL. Calcium signalling: dynamics, homeostasis and remodelling. *Nat Rev Mol Cell Biol*. 2003;4:517-529.
15. Bird GS, Aziz O, Lievremont JP, Wedel BJ, Trebak M, Vazquez G, Putney JW, Jr. Mechanisms of phospholipase C-regulated calcium entry. *Curr Mol Med*. 2004;4:291-301.
16. Varga-Szabo D, Braun A, Nieswandt B. STIM and Orai in platelet function. *Cell Calcium*. 2011;50:270-278.

17. Braun A, Vogtle T, Varga-Szabo D, Nieswandt B. STIM and Orai in hemostasis and thrombosis. *Front Biosci*. 2012;17:2144-2160.
18. Stegner D, Nieswandt B. Platelet receptor signaling in thrombus formation. *J Mol Med (Berl)*. 2011;89:109-121.
19. Clemetson JM, Polgar J, Magnenat E, Wells TN, Clemetson KJ. The platelet collagen receptor glycoprotein VI is a member of the immunoglobulin superfamily closely related to FcalphaR and the natural killer receptors. *J Biol Chem*. 1999;274:29019-29024.
20. Watson SP, Auger JM, McCarty OJ, Pearce AC. GPVI and integrin alphaIIb beta3 signaling in platelets. *J Thromb Haemost*. 2005;3:1752-1762.
21. Poole A, Gibbins JM, Turner M, van Vugt MJ, van de Winkel JG, Saito T, Tybulewicz VL, Watson SP. The Fc receptor gamma-chain and the tyrosine kinase Syk are essential for activation of mouse platelets by collagen. *Embo J*. 1997;16:2333-2341.
22. Nieswandt B, Bergmeier W, Schulte V, Rackebrandt K, Gessner JE, Zirngibl H. Expression and function of the mouse collagen receptor glycoprotein VI is strictly dependent on its association with the FcRgamma chain. *J Biol Chem*. 2000;275:23998-24002.
23. Berlanga O, Tulasne D, Bori T, Snell DC, Miura Y, Jung S, Moroi M, Frampton J, Watson SP. The Fc receptor gamma-chain is necessary and sufficient to initiate signalling through glycoprotein VI in transfected cells by the snake C-type lectin, convulxin. *Eur J Biochem*. 2002;269:2951-2960.
24. Nieswandt B, Watson SP. Platelet-collagen interaction: is GPVI the central receptor? *Blood*. 2003;102:449-461.
25. Jung SM, Tsuji K, Moroi M. Glycoprotein (GP) VI dimer as a major collagen-binding site of native platelets: direct evidence obtained with dimeric GPVI-specific Fabs. *J Thromb Haemost*. 2009;7:1347-1355.
26. Bender M, Hofmann S, Stegner D, Chalaris A, Bosl M, Braun A, Scheller J, Rose-John S, Nieswandt B. Differentially regulated GPVI ectodomain shedding by multiple platelet-expressed proteinases. *Blood*. 2010;116:3347-3355.
27. Bergmeier W, Rabie T, Strehl A, Piffath CL, Prostredna M, Wagner DD, Nieswandt B. GPVI down-regulation in murine platelets through metalloproteinase-dependent shedding. *Thromb Haemost*. 2004;91:951-958.
28. Gardiner EE, Karunakaran D, Shen Y, Arthur JF, Andrews RK, Berndt MC. Controlled shedding of platelet glycoprotein (GP)VI and GPIb-IX-V by ADAM family metalloproteinases. *J Thromb Haemost*. 2007;5:1530-1537.
29. Herr AB. Direct evidence of a native GPVI dimer at the platelet surface. *J Thromb Haemost*. 2009;7:1344-1346.

30. Horii K, Brooks MT, Herr AB. Convulxin forms a dimer in solution and can bind eight copies of glycoprotein VI: implications for platelet activation. *Biochemistry*. 2009;48:2907-2914.
31. Inoue O, Suzuki-Inoue K, McCarty OJ, Moroi M, Ruggeri ZM, Kunicki TJ, Ozaki Y, Watson SP. Laminin stimulates spreading of platelets through integrin alpha6beta1-dependent activation of GPVI. *Blood*. 2006;107:1405-1412.
32. Asselin J, Knight CG, Farndale RW, Barnes MJ, Watson SP. Monomeric (glycine-proline-hydroxyproline)10 repeat sequence is a partial agonist of the platelet collagen receptor glycoprotein VI. *Biochem J*. 1999;339 (Pt 2):413-418.
33. Kanaji S, Kanaji T, Furihata K, Kato K, Ware JL, Kunicki TJ. Convulxin binds to native, human glycoprotein Ib alpha. *J Biol Chem*. 2003;278:39452-39460.
34. Nieswandt B, Schulte V, Bergmeier W, Mokhtari-Nejad R, Rackebrandt K, Cazenave JP, Ohlmann P, Gachet C, Zirngibl H. Long-term antithrombotic protection by in vivo depletion of platelet glycoprotein VI in mice. *J Exp Med*. 2001;193:459-469.
35. Gruner S, Prostredna M, Koch M, Miura Y, Schulte V, Jung SM, Moroi M, Nieswandt B. Relative antithrombotic effect of soluble GPVI dimer compared with anti-GPVI antibodies in mice. *Blood*. 2005;105:1492-1499.
36. Kleinschnitz C, Pozgajova M, Pham M, Bendszus M, Nieswandt B, Stoll G. Targeting platelets in acute experimental stroke: impact of glycoprotein Ib, VI, and IIb/IIIa blockade on infarct size, functional outcome, and intracranial bleeding. *Circulation*. 2007;115:2323-2330.
37. Massberg S, Gawaz M, Gruner S, Schulte V, Konrad I, Zohlnhofer D, Heinzmann U, Nieswandt B. A crucial role of glycoprotein VI for platelet recruitment to the injured arterial wall in vivo. *J Exp Med*. 2003;197:41-49.
38. Schulte V, Rabie T, Prostredna M, Aktas B, Gruner S, Nieswandt B. Targeting of the collagen-binding site on glycoprotein VI is not essential for in vivo depletion of the receptor. *Blood*. 2003;101:3948-3952.
39. Gardiner EE, Arthur JF, Kahn ML, Berndt MC, Andrews RK. Regulation of platelet membrane levels of glycoprotein VI by a platelet-derived metalloproteinase. *Blood*. 2004;104:3611-3617.
40. Rabie T, Varga-Szabo D, Bender M, Pozgaj R, Lanza F, Saito T, Watson SP, Nieswandt B. Diverging signaling events control the pathway of GPVI down-regulation in vivo. *Blood*. 2007;110:529-535.
41. Ezumi Y, Shindoh K, Tsuji M, Takayama H. Physical and functional association of the Src family kinases Fyn and Lyn with the collagen receptor glycoprotein VI-Fc receptor gamma chain complex on human platelets. *J Exp Med*. 1998;188:267-276.

42. Quek LS, Pasquet JM, Hers I, Cornall R, Knight G, Barnes M, Hibbs ML, Dunn AR, Lowell CA, Watson SP. Fyn and Lyn phosphorylate the Fc receptor gamma chain downstream of glycoprotein VI in murine platelets, and Lyn regulates a novel feedback pathway. *Blood*. 2000;96:4246-4253.
43. Suzuki-Inoue K, Tulasne D, Shen Y, Bori-Sanz T, Inoue O, Jung SM, Moroi M, Andrews RK, Berndt MC, Watson SP. Association of Fyn and Lyn with the proline-rich domain of glycoprotein VI regulates intracellular signaling. *J Biol Chem*. 2002;277:21561-21566.
44. Bori-Sanz T, Inoue KS, Berndt MC, Watson SP, Tulasne D. Delineation of the region in the glycoprotein VI tail required for association with the Fc receptor gamma-chain. *J Biol Chem*. 2003;278:35914-35922.
45. Schmaier AA, Zou Z, Kazlauskas A, Emert-Sedlak L, Fong KP, Neeves KB, Maloney SF, Diamond SL, Kunapuli SP, Ware J, Brass LF, Smithgall TE, Saksela K, Kahn ML. Molecular priming of Lyn by GPVI enables an immune receptor to adopt a hemostatic role. *Proc Natl Acad Sci U S A*. 2009;106:21167-21172.
46. Kurosaki T, Johnson SA, Pao L, Sada K, Yamamura H, Cambier JC. Role of the Syk autophosphorylation site and SH2 domains in B cell antigen receptor signaling. *J Exp Med*. 1995;182:1815-1823.
47. Abtahian F, Bezman N, Clemens R, Sebzda E, Cheng L, Shattil SJ, Kahn ML, Koretzky GA. Evidence for the requirement of ITAM domains but not SLP-76/Gads interaction for integrin signaling in hematopoietic cells. *Mol Cell Biol*. 2006;26:6936-6949.
48. Asazuma N, Wilde JI, Berlanga O, Leduc M, Leo A, Schweighoffer E, Tybulewicz V, Bon C, Liu SK, McGlade CJ, Schraven B, Watson SP. Interaction of linker for activation of T cells with multiple adapter proteins in platelets activated by the glycoprotein VI-selective ligand, convulxin. *J Biol Chem*. 2000;275:33427-33434.
49. Yablonski D, Kadlecek T, Weiss A. Identification of a phospholipase C-gamma1 (PLC-gamma1) SH3 domain-binding site in SLP-76 required for T-cell receptor-mediated activation of PLC-gamma1 and NFAT. *Mol Cell Biol*. 2001;21:4208-4218.
50. Gross BS, Lee JR, Clements JL, Turner M, Tybulewicz VL, Findell PR, Koretzky GA, Watson SP. Tyrosine phosphorylation of SLP-76 is downstream of Syk following stimulation of the collagen receptor in platelets. *J Biol Chem*. 1999;274:5963-5971.
51. Clements JL, Lee JR, Gross B, Yang B, Olson JD, Sandra A, Watson SP, Lentz SR, Koretzky GA. Fetal hemorrhage and platelet dysfunction in SLP-76-deficient mice. *J Clin Invest*. 1999;103:19-25.
52. Judd BA, Myung PS, Obergfell A, Myers EE, Cheng AM, Watson SP, Pear WS, Allman D, Shattil SJ, Koretzky GA. Differential requirement for LAT and SLP-76 in GPVI versus T cell receptor signaling. *J Exp Med*. 2002;195:705-717.

53. Atkinson BT, Ellmeier W, Watson SP. Tec regulates platelet activation by GPVI in the absence of Btk. *Blood*. 2003;102:3592-3599.
54. Suzuki-Inoue K, Inoue O, Frampton J, Watson SP. Murine GPVI stimulates weak integrin activation in PLCgamma2-/- platelets: involvement of PLCgamma1 and PI3-kinase. *Blood*. 2003;102:1367-1373.
55. Elvers M, Pozgaj R, Pleines I, May F, Kuijpers MJ, Heemskerk JM, Yu P, Nieswandt B. Platelet hyperreactivity and a prothrombotic phenotype in mice with a gain-of-function mutation in phospholipase Cgamma2. *J Thromb Haemost*. 2010;8:1353-1363.
56. Hathaway DR, Adelstein RS. Human platelet myosin light chain kinase requires the calcium-binding protein calmodulin for activity. *Proc Natl Acad Sci U S A*. 1979;76:1653-1657.
57. Shattil SJ, Brass LF. Induction of the fibrinogen receptor on human platelets by intracellular mediators. *J Biol Chem*. 1987;262:992-1000.
58. Varga-Szabo D, Braun A, Kleinschnitz C, Bender M, Pleines I, Pham M, Renne T, Stoll G, Nieswandt B. The calcium sensor STIM1 is an essential mediator of arterial thrombosis and ischemic brain infarction. *J Exp Med*. 2008;205:1583-1591.
59. Braun A, Varga-Szabo D, Kleinschnitz C, Pleines I, Bender M, Austinat M, Bosl M, Stoll G, Nieswandt B. Orai1 (CRACM1) is the platelet SOC channel and essential for pathological thrombus formation. *Blood*. 2009;113:2056-2063.
60. Rosado JA, Sage SO. Coupling between inositol 1,4,5-trisphosphate receptors and human transient receptor potential channel 1 when intracellular Ca2+ stores are depleted. *Biochem J*. 2000;350 Pt 3:631-635.
61. Rosado JA, Sage SO. Activation of store-mediated calcium entry by secretion-like coupling between the inositol 1,4,5-trisphosphate receptor type II and human transient receptor potential (hTrp1) channels in human platelets. *Biochem J*. 2001;356:191-198.
62. Varga-Szabo D, Authi KS, Braun A, Bender M, Ambily A, Hassock SR, Gudermann T, Dietrich A, Nieswandt B. Store-operated Ca(2+) entry in platelets occurs independently of transient receptor potential (TRP) C1. *Pflugers Arch*. 2008;457:377-387.
63. Bousquet SM, Monet M, Boulay G. Protein kinase C-dependent phosphorylation of transient receptor potential canonical 6 (TRPC6) on serine 448 causes channel inhibition. *J Biol Chem*. 2010;285:40534-40543.
64. Aires V, Hichami A, Boulay G, Khan NA. Activation of TRPC6 calcium channels by diacylglycerol (DAG)-containing arachidonic acid: a comparative study with DAG-containing docosahexaenoic acid. *Biochimie*. 2007;89:926-937.
65. Shi J, Mori E, Mori Y, Mori M, Li J, Ito Y, Inoue R. Multiple regulation by calcium of murine homologues of transient receptor potential proteins TRPC6 and TRPC7 expressed in HEK293 cells. *J Physiol*. 2004;561:415-432.

66. Nishida M, Watanabe K, Sato Y, Nakaya M, Kitajima N, Ide T, Inoue R, Kurose H. Phosphorylation of TRPC6 channels at Thr69 is required for anti-hypertrophic effects of phosphodiesterase 5 inhibition. *J Biol Chem*. 2010;285:13244-13253.
67. Mwanjewe J, Grover AK. Role of transient receptor potential canonical 6 (TRPC6) in non-transferrin-bound iron uptake in neuronal phenotype PC12 cells. *Biochem J*. 2004;378:975-982.
68. Sossin WS, Barker PA. Something old, something new: BDNF-induced neuron survival requires TRPC channel function. *Nat Neurosci*. 2007;10:537-538.
69. Eder P, Molkentin JD. TRPC channels as effectors of cardiac hypertrophy. *Circ Res*. 2011;108:265-272.
70. Welsh DG, Morielli AD, Nelson MT, Brayden JE. Transient receptor potential channels regulate myogenic tone of resistance arteries. *Circ Res*. 2002;90:248-250.
71. Dietrich A, Mederos YSM, Gollasch M, Gross V, Storch U, Dubrovska G, Obst M, Yildirim E, Salanova B, Kalwa H, Essin K, Pinkenburg O, Luft FC, Gudermann T, Birnbaumer L. Increased vascular smooth muscle contractility in TRPC6-/- mice. *Mol Cell Biol*. 2005;25:6980-6989.
72. Kuwahara K, Wang Y, McAnally J, Richardson JA, Bassel-Duby R, Hill JA, Olson EN. TRPC6 fulfills a calcineurin signaling circuit during pathologic cardiac remodeling. *J Clin Invest*. 2006;116:3114-3126.
73. Cho KO, Hunt CA, Kennedy MB. The rat brain postsynaptic density fraction contains a homolog of the Drosophila discs-large tumor suppressor protein. *Neuron*. 1992;9:929-942.
74. Woods DF, Bryant PJ. The discs-large tumor suppressor gene of Drosophila encodes a guanylate kinase homolog localized at septate junctions. *Cell*. 1991;66:451-464.
75. Itoh M, Nagafuchi A, Yonemura S, Kitani-Yasuda T, Tsukita S. The 220-kD protein colocalizing with cadherins in non-epithelial cells is identical to ZO-1, a tight junction-associated protein in epithelial cells: cDNA cloning and immunoelectron microscopy. *J Cell Biol*. 1993;121:491-502.
76. Harris BZ, Lim WA. Mechanism and role of PDZ domains in signaling complex assembly. *J Cell Sci*. 2001;114:3219-3231.
77. Ponting CP, Phillips C, Davies KE, Blake DJ. PDZ domains: targeting signalling molecules to sub-membranous sites. *Bioessays*. 1997;19:469-479.
78. Ponting CP. Evidence for PDZ domains in bacteria, yeast, and plants. *Protein Sci*. 1997;6:464-468.
79. Jelen F, Oleksy A, Smietana K, Otlewski J. PDZ domains - common players in the cell signaling. *Acta Biochim Pol*. 2003;50:985-1017.

80. Karlsson O, Thor S, Norberg T, Ohlsson H, Edlund T. Insulin gene enhancer binding protein Isl-1 is a member of a novel class of proteins containing both a homeo- and a Cys-His domain. *Nature*. 1990;344:879-882.
81. Way JC, Chalfie M. mec-3, a homeobox-containing gene that specifies differentiation of the touch receptor neurons in C. elegans. *Cell*. 1988;54:5-16.
82. Guy PM, Kenny DA, Gill GN. The PDZ domain of the LIM protein enigma binds to beta-tropomyosin. *Mol Biol Cell*. 1999;10:1973-1984.
83. Zhou Q, Ruiz-Lozano P, Martone ME, Chen J. Cypher, a striated muscle-restricted PDZ and LIM domain-containing protein, binds to alpha-actinin-2 and protein kinase C. *J Biol Chem*. 1999;274:19807-19813.
84. Faulkner G, Pallavicini A, Formentin E, Comelli A, Ievolella C, Trevisan S, Bortoletto G, Scannapieco P, Salamon M, Mouly V, Valle G, Lanfranchi G. ZASP: a new Z-band alternatively spliced PDZ-motif protein. *J Cell Biol*. 1999;146:465-475.
85. Xia H, Winokur ST, Kuo WL, Altherr MR, Bredt DS. Actinin-associated LIM protein: identification of a domain interaction between PDZ and spectrin-like repeat motifs. *J Cell Biol*. 1997;139:507-515.
86. Wu RY, Gill GN. LIM domain recognition of a tyrosine-containing tight turn. *J Biol Chem*. 1994;269:25085-25090.
87. Kuroda S, Tokunaga C, Kiyohara Y, Higuchi O, Konishi H, Mizuno K, Gill GN, Kikkawa U. Protein-protein interaction of zinc finger LIM domains with protein kinase C. *J Biol Chem*. 1996;271:31029-31032.
88. Durick K, Wu RY, Gill GN, Taylor SS. Mitogenic signaling by Ret/ptc2 requires association with enigma via a LIM domain. *J Biol Chem*. 1996;271:12691-12694.
89. Vallenius T, Luukko K, Makela TP. CLP-36 PDZ-LIM protein associates with nonmuscle alpha-actinin-1 and alpha-actinin-4. *J Biol Chem*. 2000;275:11100-11105.
90. Bashirova AA, Markelov ML, Shlykova TV, Levshenkova EV, Alibaeva RA, Frolova EI. The human RIL gene: mapping to human chromosome 5q31.1, genomic organization and alternative transcripts. *Gene*. 1998;210:239-245.
91. Wang H, Harrison-Shostak DC, Lemasters JJ, Herman B. Cloning of a rat cDNA encoding a novel LIM domain protein with high homology to rat RIL. *Gene*. 1995;165:267-271.
92. Torrado M, Senatorov VV, Trivedi R, Fariss RN, Tomarev SI. Pdlim2, a novel PDZ-LIM domain protein, interacts with alpha-actinins and filamin A. *Invest Ophthalmol Vis Sci*. 2004;45:3955-3963.
93. Kotaka M, Kostin S, Ngai S, Chan K, Lau Y, Lee SM, Li H, Ng EK, Schaper J, Tsui SK, Fung K, Lee C, Waye MM. Interaction of hCLIM1, an enigma family protein, with alpha-actinin 2. *J Cell Biochem*. 2000;78:558-565.

94. Te Velthuis AJ, Isogai T, Gerrits L, Bagowski CP. Insights into the molecular evolution of the PDZ/LIM family and identification of a novel conserved protein motif. *PLoS One*. 2007;2:e189.
95. Jo K, Rutten B, Bunn RC, Bredt DS. Actinin-associated LIM protein-deficient mice maintain normal development and structure of skeletal muscle. *Mol Cell Biol*. 2001;21:1682-1687.
96. Pashmforoush M, Pomies P, Peterson KL, Kubalak S, Ross J, Jr., Hefti A, Aebi U, Beckerle MC, Chien KR. Adult mice deficient in actinin-associated LIM-domain protein reveal a developmental pathway for right ventricular cardiomyopathy. *Nat Med*. 2001;7:591-597.
97. Lorenzen-Schmidt I, McCulloch AD, Omens JH. Deficiency of actinin-associated LIM protein alters regional right ventricular function and hypertrophic remodeling. *Ann Biomed Eng*. 2005;33:888-896.
98. Klaavuniemi T, Kelloniemi A, Ylanne J. The ZASP-like motif in actinin-associated LIM protein is required for interaction with the alpha-actinin rod and for targeting to the muscle Z-line. *J Biol Chem*. 2004;279:26402-26410.
99. Andersen O, Ostbye TK, Gabestad I, Nielsen C, Bardal T, Galloway TF. Molecular characterization of a PDZ-LIM protein in Atlantic salmon (Salmo salar): a fish ortholog of the alpha-actinin-associated LIM-protein (ALP). *J Muscle Res Cell Motil*. 2004;25:61-68.
100. te Velthuis AJ, Ott EB, Marques IJ, Bagowski CP. Gene expression patterns of the ALP family during zebrafish development. *Gene Expr Patterns*. 2007;7:297-305.
101. Kotaka M, Ngai SM, Garcia-Barcelo M, Tsui SK, Fung KP, Lee CY, Waye MM. Characterization of the human 36-kDa carboxyl terminal LIM domain protein (hCLIM1). *J Cell Biochem*. 1999;72:279-285.
102. Vallenius T, Makela TP. Clik1: a novel kinase targeted to actin stress fibers by the CLP-36 PDZ-LIM protein. *J Cell Sci*. 2002;115:2067-2073.
103. Bozulic LD, Malik MT, Powell DW, Nanez A, Link AJ, Ramos KS, Dean WL. Plasma membrane Ca(2+) -ATPase associates with CLP36, alpha-actinin and actin in human platelets. *Thromb Haemost*. 2007;97:587-597.
104. Loughran G, Healy NC, Kiely PA, Huigsloot M, Kedersha NL, O'Connor R. Mystique is a new insulin-like growth factor-I-regulated PDZ-LIM domain protein that promotes cell attachment and migration and suppresses Anchorage-independent growth. *Mol Biol Cell*. 2005;16:1811-1822.
105. van den Berk LC, Landi E, Harmsen E, Dente L, Hendriks WJ. Redox-regulated affinity of the third PDZ domain in the phosphotyrosine phosphatase PTP-BL for cysteine-containing target peptides. *Febs J*. 2005;272:3306-3316.

106. Omasu F, Ezura Y, Kajita M, Ishida R, Kodaira M, Yoshida H, Suzuki T, Hosoi T, Inoue S, Shiraki M, Orimo H, Emi M. Association of genetic variation of the RIL gene, encoding a PDZ-LIM domain protein and localized in 5q31.1, with low bone mineral density in adult Japanese women. *J Hum Genet*. 2003;48:342-345.
107. Cuppen E, Gerrits H, Pepers B, Wieringa B, Hendriks W. PDZ motifs in PTP-BL and RIL bind to internal protein segments in the LIM domain protein RIL. *Mol Biol Cell*. 1998;9:671-683.
108. Tanaka T, Soriano MA, Grusby MJ. SLIM is a nuclear ubiquitin E3 ligase that negatively regulates STAT signaling. *Immunity*. 2005;22:729-736.
109. Tanaka T, Grusby MJ, Kaisho T. PDLIM2-mediated termination of transcription factor NF-kappaB activation by intranuclear sequestration and degradation of the p65 subunit. *Nat Immunol*. 2007;8:584-591.
110. Schulz TW, Nakagawa T, Licznerski P, Pawlak V, Kolleker A, Rozov A, Kim J, Dittgen T, Kohr G, Sheng M, Seeburg PH, Osten P. Actin/alpha-actinin-dependent transport of AMPA receptors in dendritic spines: role of the PDZ-LIM protein RIL. *J Neurosci*. 2004;24:8584-8594.
111. Iida Y, Matsuzaki T, Morishima T, Sasano H, Asai K, Sobue K, Takata K. Localization of reversion-induced LIM protein (RIL) in the rat central nervous system. *Acta Histochem Cytochem*. 2009;42:9-14.
112. Ohno K, Kato H, Funahashi S, Hasegawa T, Sato K. Characterization of CLP36/Elfin/PDLIM1 in the nervous system. *J Neurochem*. 2009;111:790-800.
113. Tamura N, Ohno K, Katayama T, Kanayama N, Sato K. The PDZ-LIM protein CLP36 is required for actin stress fiber formation and focal adhesion assembly in BeWo cells. *Biochem Biophys Res Commun*. 2007;364:589-594.
114. Maeda M, Asano E, Ito D, Ito S, Hasegawa Y, Hamaguchi M, Senga T. Characterization of interaction between CLP36 and palladin. *Febs J*. 2009;276:2775-2785.
115. Bauer K, Kratzer M, Otte M, de Quintana KL, Hagmann J, Arnold GJ, Eckerskorn C, Lottspeich F, Siess W. Human CLP36, a PDZ-domain and LIM-domain protein, binds to alpha-actinin-1 and associates with actin filaments and stress fibers in activated platelets and endothelial cells. *Blood*. 2000;96:4236-4245.
116. Nieswandt B, Bergmeier W, Rackebrandt K, Gessner JE, Zirngibl H. Identification of critical antigen-specific mechanisms in the development of immune thrombocytopenic purpura in mice. *Blood*. 2000;96:2520-2527.
117. May F, Hagedorn I, Pleines I, Bender M, Vogtle T, Eble J, Elvers M, Nieswandt B. CLEC-2 is an essential platelet-activating receptor in hemostasis and thrombosis. *Blood*. 2009;114:3464-3472.

118. Bergmeier W, Schulte V, Brockhoff G, Bier U, Zirngibl H, Nieswandt B. Flow cytometric detection of activated mouse integrin alphaIIbbeta3 with a novel monoclonal antibody. *Cytometry*. 2002;48:80-86.

119. Dirnagl U. Bench to bedside: the quest for quality in experimental stroke research. *J Cereb Blood Flow Metab*. 2006;26:1465-1478.

120. Carter RN, Tolhurst G, Walmsley G, Vizuete-Forster M, Miller N, Mahaut-Smith MP. Molecular and electrophysiological characterization of transient receptor potential ion channels in the primary murine megakaryocyte. *J Physiol*. 2006;576:151-162.

121. Hofmann T, Obukhov AG, Schaefer M, Harteneck C, Gudermann T, Schultz G. Direct activation of human TRPC6 and TRPC3 channels by diacylglycerol. *Nature*. 1999;397:259-263.

122. Jardin I, Redondo PC, Salido GM, Rosado JA. Phosphatidylinositol 4,5-bisphosphate enhances store-operated calcium entry through hTRPC6 channel in human platelets. *Biochim Biophys Acta*. 2008;1783:84-97.

123. Redondo PC, Jardin I, Lopez JJ, Salido GM, Rosado JA. Intracellular Ca2+ store depletion induces the formation of macromolecular complexes involving hTRPC1, hTRPC6, the type II IP3 receptor and SERCA3 in human platelets. *Biochim Biophys Acta*. 2008;1783:1163-1176.

124. Jardin I, Gomez LJ, Salido GM, Rosado JA. Dynamic interaction of hTRPC6 with the Orai1-STIM1 complex or hTRPC3 mediates its role in capacitative or non-capacitative Ca(2+) entry pathways. *Biochem J*. 2009;420:267-276.

125. Dowling MR, Josefsson EC, Henley KJ, Hodgkin PD, Kile BT. Platelet senescence is regulated by an internal timer, not damage inflicted by hits. *Blood*.116:1776-1778.

126. Mason KD, Carpinelli MR, Fletcher JI, Collinge JE, Hilton AA, Ellis S, Kelly PN, Ekert PG, Metcalf D, Roberts AW, Huang DC, Kile BT. Programmed anuclear cell death delimits platelet life span. *Cell*. 2007;128:1173-1186.

127. McCloskey C, Jones S, Amisten S, Snowden RT, Kaczmarek LK, Erlinge D, Goodall AH, Forsythe ID, Mahaut-Smith MP. Kv1.3 is the exclusive voltage-gated K+ channel of platelets and megakaryocytes: roles in membrane potential, Ca2+ signalling and platelet count. *J Physiol*.588:1399-1406.

128. Morgenstern E, Ruf A, Patscheke H. Ultrastructure of the interaction between human platelets and polymerizing fibrin within the first minutes of clot formation. *Blood Coagul Fibrinolysis*. 1990;1:543-546.

129. Pleines I, Elvers M, Strehl A, Pozgajova M, Varga-Szabo D, May F, Chrostek-Grashoff A, Brakebusch C, Nieswandt B. Rac1 is essential for phospholipase C-gamma2 activation in platelets. *Pflugers Arch*. 2009;457:1173-1185.

130. Gilio K, van Kruchten R, Braun A, Berna-Erro A, Feijge MA, Stegner D, van der Meijden PE, Kuijpers MJ, Varga-Szabo D, Heemskerk JW, Nieswandt B. Roles of platelet STIM1 and Orai1 in glycoprotein VI- and thrombin-dependent procoagulant activity and thrombus formation. *J Biol Chem*. 2010;285:23629-23638.
131. Elvers M, Stegner D, Hagedorn I, Kleinschnitz C, Braun A, Kuijpers ME, Boesl M, Chen Q, Heemskerk JW, Stoll G, Frohman MA, Nieswandt B. Impaired alpha(IIb)beta(3) integrin activation and shear-dependent thrombus formation in mice lacking phospholipase D1. *Sci Signal*. 2010;3:ra1.
132. Zwaal RF, Schroit AJ. Pathophysiologic implications of membrane phospholipid asymmetry in blood cells. *Blood*. 1997;89:1121-1132.
133. Heemskerk JW, Kuijpers MJ, Munnix IC, Siljander PR. Platelet collagen receptors and coagulation. A characteristic platelet response as possible target for antithrombotic treatment. *Trends Cardiovasc Med*. 2005;15:86-92.
134. Stoll G, Kleinschnitz C, Nieswandt B. Combating innate inflammation: a new paradigm for acute treatment of stroke? *Ann N Y Acad Sci*. 2010;1207:149-154.
135. Patel-Hett S, Wang H, Begonja AJ, Thon JN, Alden EC, Wandersee NJ, An X, Mohandas N, Hartwig JH, Italiano JE, Jr. The spectrin-based membrane skeleton stabilizes mouse megakaryocyte membrane systems and is essential for proplatelet and platelet formation. *Blood*. 2011;118:1641-1652.
136. WHO publishes definitive atlas on global heart disease and stroke epidemic. *Indian J Med Sci*. 2004;58:405-406.
137. Michelson AD. Antiplatelet therapies for the treatment of cardiovascular disease. *Nat Rev Drug Discov*. 2010;9:154-169.
138. Rowley JW, Oler AJ, Tolley ND, Hunter BN, Low EN, Nix DA, Yost CC, Zimmerman GA, Weyrich AS. Genome-wide RNA-seq analysis of human and mouse platelet transcriptomes. *Blood*. 2011;118:e101-111.
139. Hechler B, Lenain N, Marchese P, Vial C, Heim V, Freund M, Cazenave JP, Cattaneo M, Ruggeri ZM, Evans R, Gachet C. A role of the fast ATP-gated P2X1 cation channel in thrombosis of small arteries in vivo. *J Exp Med*. 2003;198:661-667.
140. Oury C, Kuijpers MJ, Toth-Zsamboki E, Bonnefoy A, Danloy S, Vreys I, Feijge MA, De Vos R, Vermylen J, Heemskerk JW, Hoylaerts MF. Overexpression of the platelet P2X1 ion channel in transgenic mice generates a novel prothrombotic phenotype. *Blood*. 2003;101:3969-3976.
141. Hassock SR, Zhu MX, Trost C, Flockerzi V, Authi KS. Expression and role of TRPC proteins in human platelets: evidence that TRPC6 forms the store-independent calcium entry channel. *Blood*. 2002;100:2801-2811.

142. Carter RN, Tolhurst G, Walmsley G, Vizuete-Forster M, Miller N, Mahaut-Smith MP. Molecular and electrophysiological characterization of transient receptor potential ion channels in the primary murine megakaryocyte. *J Physiol*. 2006;576:151-162.
143. Brownlow SL, Sage SO. Transient receptor potential protein subunit assembly and membrane distribution in human platelets. *Thromb Haemost*. 2005;94:839-845.
144. Harper MT, Poole AW. Protein kinase Ctheta negatively regulates store-independent Ca2+ entry and phosphatidylserine exposure downstream of glycoprotein VI in platelets. *J Biol Chem*. 2010;285:19865-19873.
145. Jardin I, Gomez LJ, Salido GM, Rosado JA. Dynamic interaction of hTRPC6 with the Orai1-STIM1 complex or hTRPC3 mediates its role in capacitative or non-capacitative Ca(2+) entry pathways. *Biochem J*. 2009;420:267-276.
146. DeHaven WI, Jones BF, Petranka JG, Smyth JT, Tomita T, Bird GS, Putney JW, Jr. TRPC channels function independently of STIM1 and Orai1. *J Physiol*. 2009;587:2275-2298.
147. Konopatskaya O, Gilio K, Harper MT, Zhao Y, Cosemans JM, Karim ZA, Whiteheart SW, Molkentin JD, Verkade P, Watson SP, Heemskerk JW, Poole AW. PKCalpha regulates platelet granule secretion and thrombus formation in mice. *J Clin Invest*. 2009;119:399-407.
148. Gilio K, Harper MT, Cosemans JM, Konopatskaya O, Munnix IC, Prinzen L, Leitges M, Liu Q, Molkentin JD, Heemskerk JW, Poole AW. Functional divergence of platelet protein kinase C (PKC) isoforms in thrombus formation on collagen. *J Biol Chem*. 2010;285:23410-23419.
149. Kawasaki T, Ueyama T, Lange I, Feske S, Saito N. Protein kinase C-induced phosphorylation of Orai1 regulates the intracellular Ca2+ level via the store-operated Ca2+ channel. *J Biol Chem*. 2010;285:25720-25730.
150. Harper MT, Mason MJ, Sage SO, Harper AG. Phorbol ester-evoked Ca2+ signaling in human platelets is via autocrine activation of P(2X1) receptors, not a novel non-capacitative Ca2+ entry. *J Thromb Haemost*. 2010;8:1604-1613.
151. Rosado JA, Sage SO. Protein kinase C activates non-capacitative calcium entry in human platelets. *J Physiol*. 2000;529 Pt 1:159-169.
152. Paez Espinosa EV, Murad JP, Ting HJ, Khasawneh FT. Mouse transient receptor potential channel 6: Role in hemostasis and thrombogenesis. *Biochem Biophys Res Commun*. 2012;417:853-856.
153. Weissmann N, Sydykov A, Kalwa H, Storch U, Fuchs B, Schnitzler MM, Brandes RP, Grimminger F, Meissner M, Freichel M, Offermanns S, Veit F, Pak O, Krause KH, Schermuly RT, Brewer AC, Schmidt HH, Seeger W, Shah AM, Gudermann T, Ghofrani

HA, Dietrich A. Activation of TRPC6 channels is essential for lung ischaemia-reperfusion induced oedema in mice. *Nat Commun*. 2012;3:649.

154. Tolhurst G, Carter RN, Amisten S, Holdich JP, Erlinge D, Mahaut-Smith MP. Expression profiling and electrophysiological studies suggest a major role for Orai1 in the store-operated Ca2+ influx pathway of platelets and megakaryocytes. *Platelets*. 2008;19:308-313.
155. Bergmeier W, Oh-Hora M, McCarl CA, Roden RC, Bray PF, Feske S. R93W mutation in Orai1 causes impaired calcium influx in platelets. *Blood*. 2009;113:675-678.
156. Authi KS. Orai1: a channel to safer antithrombotic therapy. *Blood*. 2009;113:1872-1873.
157. Pleines I, Eckly A, Elvers M, Hagedorn I, Eliautou S, Bender M, Wu X, Lanza F, Gachet C, Brakebusch C, Nieswandt B. Multiple alterations of platelet functions dominated by increased secretion in mice lacking Cdc42 in platelets. *Blood*. 2010;115:3364-3373.
158. Ridley AJ, Hall A. The small GTP-binding protein rho regulates the assembly of focal adhesions and actin stress fibers in response to growth factors. *Cell*. 1992;70:389-399.
159. Pellegrin S, Mellor H. Actin stress fibres. *J Cell Sci*. 2007;120:3491-3499.
160. Burridge K, Chrzanowska-Wodnicka M, Zhong C. Focal adhesion assembly. *Trends Cell Biol*. 1997;7:342-347.
161. Pleines I, Hagedorn I, Gupta S, May F, Chakarova L, van Hengel J, Offermanns S, Krohne G, Kleinschnitz C, Brakebusch C, Nieswandt B. Megakaryocyte-specific RhoA deficiency causes macrothrombocytopenia and defective platelet activation in hemostasis and thrombosis. *Blood*. 2012;119:1054-1063.
162. Bender M, Eckly A, Hartwig JH, Elvers M, Pleines I, Gupta S, Krohne G, Jeanclos E, Gohla A, Gurniak C, Gachet C, Witke W, Nieswandt B. ADF/n-cofilin-dependent actin turnover determines platelet formation and sizing. *Blood*. 2010;116:1767-1775.
163. Kotaka M, Lau YM, Cheung KK, Lee SM, Li HY, Chan WY, Fung KP, Lee CY, Waye MM, Tsui SK. Elfin is expressed during early heart development. *J Cell Biochem*. 2001;83:463-472.
164. Vallenius T, Scharm B, Vesikansa A, Luukko K, Schafer R, Makela TP. The PDZ-LIM protein RIL modulates actin stress fiber turnover and enhances the association of alpha-actinin with F-actin. *Exp Cell Res*. 2004;293:117-128.
165. Zhou Q, Chu PH, Huang C, Cheng CF, Martone ME, Knoll G, Shelton GD, Evans S, Chen J. Ablation of Cypher, a PDZ-LIM domain Z-line protein, causes a severe form of congenital myopathy. *J Cell Biol*. 2001;155:605-612.
166. Rebecchi MJ, Pentyala SN. Structure, function, and control of phosphoinositide-specific phospholipase C. *Physiol Rev*. 2000;80:1291-1335.

167. Falati S, Patil S, Gross PL, Stapleton M, Merrill-Skoloff G, Barrett NE, Pixton KL, Weiler H, Cooley B, Newman DK, Newman PJ, Furie BC, Furie B, Gibbins JM. Platelet PECAM-1 inhibits thrombus formation in vivo. *Blood*. 2006;107:535-541.

168. Thomas DH, Getz TM, Newman TN, Dangelmaier CA, Carpino N, Kunapuli SP, Tsygankov AY, Daniel JL. A novel histidine tyrosine phosphatase, TULA-2, associates with Syk and negatively regulates GPVI signaling in platelets. *Blood*. 2010;116:2570-2578.

169. Wong C, Liu Y, Yip J, Chand R, Wee JL, Oates L, Nieswandt B, Reheman A, Ni H, Beauchemin N, Jackson DE. CEACAM1 negatively regulates platelet-collagen interactions and thrombus growth in vitro and in vivo. *Blood*. 2009;113:1818-1828.

170. Schulte V, Reusch HP, Pozgajova M, Varga-Szabo D, Gachet C, Nieswandt B. Two-phase antithrombotic protection after anti-glycoprotein VI treatment in mice. *Arterioscler Thromb Vasc Biol*. 2006;26:1640-1647.

171. Gruner S, Prostredna M, Aktas B, Moers A, Schulte V, Krieg T, Offermanns S, Eckes B, Nieswandt B. Anti-glycoprotein VI treatment severely compromises hemostasis in mice with reduced alpha2beta1 levels or concomitant aspirin therapy. *Circulation*. 2004;110:2946-2951.

172. Weissmann N, Sydykov A, Kalwa H, Storch U, Fuchs B, Mederos y Schnitzler M, Brandes RP, Grimminger F, Meissner M, Freichel M, Offermanns S, Veit F, Pak O, Krause KH, Schermuly RT, Brewer AC, Schmidt HH, Seeger W, Shah AM, Gudermann T, Ghofrani HA, Dietrich A. Activation of TRPC6 channels is essential for lung ischaemia-reperfusion induced oedema in mice. *Nat Commun*. 2012;3:649.

7 APPENDIX

7.1 Abbreviations

α	alpha
β	beta
γ	gamma
µ	micro
AA	Amino acid
ACD	Acid-citrate-dextrose
ADAM	A disintegrin and metalloproteinase
ADF	Actin depolymerizing factor
ADP	Adenosine diphosphate
ATP	Adenosine triphosphate
BMC	Bone marrow chimeric
BSA	Bovine serum albumin
BTK	Bruton's tyrosine kinase
Ca^{2+}	Calcium
^{o}C	Degree Celsius
$[Ca^{2+}]_i$	intracellular calcium concentration
CLEC-2	C-type lectin receptor 2
CLP36	C-terminal LIM domain protein of 36 kDa
CRACM	Calcium release activated calcium modulator
CRP	Collagen-related peptide
CVX	Convulxin
DAG	Diacylglycerol
ECM	Extracellular matrix
ELISA	enzyme-linked immunosorbent assay
et al.	et alteri
F-actin	filamentous actin

FACS	Fluorescence-activated cell sorting
FcR	Fc receptor
$FeCl_3$	Ferric(III)chloride
FITC	Fluorescein isothiocyanate
FSC	Forward scatter
g	gram
GP	Glycoprotein
GPCR	G protein-coupled receptors
GTP	guanosine triphosphate
h	hour(s)
H_2O	water
HEPES	4-(2-hydroxyethyl)-1-piperazineethanesulfonic acid
IFN	Interferon
Ig	Immunoglobulin
IFI	integrated fluorescence intensity
IP	Immunoprecipitation
IP_3	Inositol-1,4,5-trisphosphate
IP_3R	IP_3 receptor
ITAM	Immunoreceptor tyrosine-based activating motif
l	liter
LAT	Linker of activated T cells
M	molar
MFI	Mean fluorescence intensity
min	minute(s)
MRI	Magnetic resonance imaging
MK	megakaryocyte
mL	milliliter
mm^2	square millimeter

NaCl	sodium chloride
o/n	overnight
OAG	1-oleoyl-2-acetyl-sn-glycerol
PA	Phosphatidic acid
PAGE	Polyacrylamide gel electrophoresis
PC	Phosphatidylcholine
PE	Phycoerythrin
PGI_2	Prostacyclin
PH	Pleckstrin homology
PI3K	Phosphoinositide-3-kinase
PIP_2	Phosphatidylinositol-4,5-bisphosphate
PIP_3	Phosphatidylinositol-3,4,5-triphosphate
PKC	Protein kinase C
PL	Phospholipase
PM	plasma membrane
prp	Platelet-rich plasma
PS	Phosphatidylserine
Rho	Ras homolog gene family
RT	Room temperature; in case of RT-PCR, RT indicates reverse transcription
s	second(s)
SD	standard deviation
SDS	Sodium dodecyl sulfate
SDS-PAGE	Sodium dodecyl sulfate polyacrylamide gel electrophoresis
SERCA	Sarco/endoplasmic reticulum Ca^{2+}-ATPase
SFK	Src family kinases
SH2	Src homology domain 2
SLP-76	SH2 domain containing leukocyte protein of 76 kDa
SOCE	Store-operated calcium entry

SSC	Sideward scatter
STIM	Stromal interaction molecule
TAE	TRIS acetate EDTA buffer
TBS	TRIS-buffered saline
TE	TRIS EDTA buffer
TF	Tissue factor
TG	Thapsigargin
TM	Transmembrane
tMCAO	Transient middle cerebral artery occlusion
TP	Thromboxane A_2 receptor
TRIS	Tris(hydroxymethyl)aminomethane
TRPC	Transient receptor potential channel
TTC	2,3,5-triphenyltetrazolium chloride
TxA_2	Thromboxane A_2
U	units
vWF	Von Willebrand factor
Wt	Wildtype

7.2.1 Publications

Gupta S, Braun A, Morowski M, Premsler T, Bender M, Nagy. Z, Sickmann A, Bösl M, Nieswandt B. CLP36 is a negative regulator of GPVI signaling in platelets. Submitted

Ramanathan G*, **Gupta S***, Thielmann I, Pleines I, Varga-Szabo D, May F, Mannhalter C, Dietrich A, Nieswandt B, Braun A. Defective Diacylglycerol-Induced Ca^{2+} Entry but Normal Agonist-Induced Activation Responses in TRPC6-Deficient Mouse Platelets. J Thromb Haemost. 2011 Dec 18. [Epub ahead of print]
* *both authors contributed equally*

Pleines I, Hagedorn I, **Gupta S**, May F, Chakarova L, van Hengel J, Offermanns S, Krohne G, Kleinschnitz C, Brakebusch C, Nieswandt B. Megakaryocyte-specific RhoA deficiency causes macrothrombocytopenia and defective platelet activation in hemostasis and thrombosis. Blood. 2011 Nov 1. [Epub ahead of print]

Bender M, Eckly A, Hartwig JH, Elvers M, Pleines I, **Gupta S**, Krohne G, Jeanclos E, Gohla A, Gurniak C, Gachet C, Witke W, Nieswandt B. ADF/n-cofilin-dependent actin turnover determines platelet formation and sizing. Blood. 2010 Sep 9;116(10):1767-75.

7.2.2 Oral Presentations

CLP36 is the negative regulator of GPVI signaling in mouse platelets. XXIIIrd Congress of the International Society on Thrombosis and Hemostasis, July 2011, Kyoto (Japan).
Winner of the **Young Investigator´s Award** (prize money: 500 US$).

LIM domain of CLP36 is the negative regulator of GPVI signaling. 55th Gesellschaft für Thrombose- und Hämostaseforschung e.V. (GTH congress), February 2011, Wiesbaden. (Germany)

7.2.3 Poster Presentations

CLP36 is a negative regulator of GPVI signaling in mouse platelets. Bio Bang, VIth International Symposium. The Graduate School of Life Sciences, University of Würzburg. October 2011, Würzburg (Germany)

Dynamism of cytoskeleton in mouse platelets. Vth International Symposium. The Graduate School of Life Sciences, University of Würzburg. October 2010, Würzburg. (Germany)

7.3 Acknowledgements

The writing of a dissertation can be an exciting or an isolating experience; yet it is obviously not possible without the personal & practical support of numerous people. Any attempt to list the people and opportunities with which my life has been richly blessed would be like trying to count stars in the heaven. Yet among these stand some individuals whose profound impact deserves special acknowledgement.

Prime most I thank Almighty God for his immeasurable love and mercy. His soul grace was my strength in all my knowledge and wisdom.

I take this opportunity to thank my supervisor and mentor Prof. Bernhard Nieswandt for his constant support, encouragement and invaluable guidance. His positive attitude and keen interest for research is highly motivating. I have always been inspired by his focused, scientific and meticulous approach towards work. His constructive criticism and discussions inspired me to go ahead in difficult times and deal with every problem during my PhD.

I extend my profound gratitude to Prof. Georg Krohne my immediate supervisor, for his enriching guidance and support. My heartfelt thanks to Prof. Johan Heemskerk for his critical feedback and suggestions on my PhD work.

I thank the Graduate School of Life Sciences (GSLS), Würzburg for funding my PhD project.

I am extremely thankful to Dr. Attila Braun for being a great senior and guiding me in every possible way which has helped me in bringing my PhD project to fruition. I have benefitted enormously with the discussions I had with him.

I would like to thank all the past and present lab members who have supported me and made this journey easier for me. I know it wouldn't have been possible to achieve this goal without them. I feel immense pleasure to thank David Stegner, Markus Bender, Alejandro Berna Erro and Irina Pleines who have always encouraged me in the lab and helped me to finally achieve my goal. My life in the lab would not have been pleasant without my colleagues and friends Lidija, Timo, Sebastian Hofmann, Ina Hagedorn, Martina, Judith, Deya, Ina Thielmann and all other lab members. I gratefully acknowledge their help during my PhD work. Special thanks to Frauke for extending an ear to listen to me at all times and giving me the right advice on the professional

and personal fronts of life. I am also thankful to all the technical assistants especially Sylvia Hengst for all her great help whenever needed.

Some people are always grumbling because roses have thorns. I am thankful that thorns have roses! This is what I feel when I remember Megha, Reshmi, Anu, Nandini, Ankita, Rajeev and Jyoti. Their compassionate company made my stay in Germany homely and memorable.

Friends are angels who lift us to our feet, when our wings have trouble remembering how to fly. I am extremely lucky to have by my side, my best of friends, Chitra, Bhavna, Neha, and Ruhel at all the times. They have always looked out for me and been there whenever I needed them. Thanks guys!! I am also thankful to Pradeep for the wonderful time spent with him during my time at JNU.

My special appreciation goes to my enlightened teachers, because of whom our own genuine compassion could be born, flourish & gave rise to the power to benefit others.

The main credit of my thesis goes to my parents who have provided me with their constant support, encouragement and unending love. They have always put up with my mood swings, backed me during my ups and downs, and gave me strength and courage to move forward. Words would never be sufficient to express my gratitude to them. Thank you Mummy and Papa for everything!! If I am anything today, it is because of you!! When I start counting blessings my whole life turns around. This is still not enough when I think of my grandparents. I express my heartiest gratitude to them for being a source of inexhaustible encouragement, unconditional love and inspiration to build up my educational career. Their influence is all over these pages and all over my life.

To my loving and caring sisters Shalu di, Ranu di and their loving families, who have always been there by my side. Their unconditional love and support always made me forget the lab issues and brought a smile to my face!! Special thanks to my younger sis Shruti for being the best sister in this world!!

Finally I owe great obligations for all those innocent mice that donated their lives for my doctoral thesis.

Shuchi

7.4 Affidavit

I hereby confirm that my thesis entitled

“The role of the *Canonical transient receptor potential* 6 (TRPC6) channel and the *C-terminal LIM domain protein of 36 kDa* (CLP36) for platelet function” is the result of my own work. I did not receive any help or support from commercial consultants. All sources and/or materials applied are listed and specified in the thesis.

Furthermore, I confirm that this thesis has not yet been submitted as part of another examination process neither in identical nor in similar form.

Würzburg ……

Date Signature

Eidesstattliche Erklärung

Hiermit erkläre ich an Eides statt, die Dissertation

„Die Rolle des *Canonical transient receptor potential 6* (TRPC6) Kanals und des *36 kDa C-terminalen LIM Domänenproteins* (CLP36) in der Thrombozytenfunktion“ eigenständig, d.h. insbesondere selbständig und ohne Hilfe eines kommerziellen Promotionsberaters, angefertigt und keine anderen als die von mir angegebenen Quellen und Hilfsmittel verwendet zu haben.

Ich erkläre außerdem, dass die Dissertation weder in gleicher noch in ähnlicher Form bereits in einem anderen Prüfungsverfahren vorgelegen hat.

Würzburg ……

Datum Unterschrift